

# The evolutionary history of the mammalian synaptonemal complex

**Dissertation**

zur Erlangung des naturwissenschaftlichen Doktorgrades der Julius-  
Maximilians-Universität Würzburg

vorgelegt von

**Johanna Fraune**

aus Höxter

Würzburg, 2014



Eingereicht am: .....

Mitglieder der Promotionskommission:

Vorsitzender: .....

Gutachter : .....

Gutachter: .....

Tag des Promotionskolloquiums: .....

Doktorurkunde ausgehändigt am: .....

## Index

<b>Index .....</b>	<b>3</b>
<b>1 List of figures .....</b>	<b>6</b>
<b>2 List of tables.....</b>	<b>7</b>
<b>3 Summary .....</b>	<b>8</b>
<b>4 Zusammenfassung .....</b>	<b>9</b>
<b>5 General Introduction.....</b>	<b>11</b>
<b>5.1 Meiosis.....</b>	<b>11</b>
5.1.1 Meiosis I .....	11
5.1.2 Meiosis II .....	14
<b>5.2 The synaptonemal complex (SC) .....</b>	<b>15</b>
5.2.1 The SC components of metazoan model organisms.....	16
5.2.2 The function of SC components and their assembly to a mature SC.....	20
<b>6 Aims of this study.....</b>	<b>25</b>
<b>7 Chapter I: The evolution of the two <i>bona fide</i> structural SC components of the mouse</b>	<b>27</b>
<b>Introduction.....</b>	<b>27</b>
<b>Results .....</b>	<b>28</b>
Sequence and structure of HySYCP1 and HySYCP3.....	29
Expression of HySYCP1 and HySYCP3 in <i>Hydra vulgaris AEP</i> .....	32
<b>Discussion.....</b>	<b>37</b>
<b>8 Chapter II: The evolution of the central element components of the murine SC .....</b>	<b>40</b>
<b>Introduction.....</b>	<b>40</b>
<b>Results.....</b>	<b>40</b>
Phylogeny of SYCE1, SYCE2, SYCE3 and Tex12.....	40
Expression of HySYCE2 and HyTex12 in <i>Hydra vulgaris AEP</i> .....	43
Interaction of HySYCE2 and HyTex12 <i>ex vivo</i> .....	47
<b>Discussion.....</b>	<b>47</b>

---

<b>9</b>	<b>Chapter III: The evolution of the mammalian lateral element protein SYCP2 .....</b>	<b>50</b>
	<b>Introduction.....</b>	<b>50</b>
	<b>Results.....</b>	<b>51</b>
	Phylogeny of SYCP2.....	51
	Sequence and expression of the SYCP2 orthologue in <i>Hydra vulgaris</i> AEP.....	53
	<b>Discussion.....</b>	<b>55</b>
<b>10</b>	<b>General Discussion .....</b>	<b>57</b>
	<b>10.1 The dynamic evolution of the SC.....</b>	<b>57</b>
	<b>10.2 The cnidarian SC: <i>Hydra</i> as model system for meiosis research? .....</b>	<b>60</b>
<b>11</b>	<b>Perspectives .....</b>	<b>67</b>
<b>12</b>	<b>Material .....</b>	<b>68</b>
	<b>12.1 Biological material.....</b>	<b>68</b>
	12.1.1 <i>Hydra</i> lineage: <i>Hydra vulgaris</i> AEP.....	68
	12.1.2 Bacteria .....	68
	12.1.3 Cell lines .....	69
	12.1.4 Antibodies .....	69
	<b>12.2 Molecular material .....</b>	<b>70</b>
	12.2.1 Plasmids .....	70
	12.2.2 Oligonucleotides .....	71
	12.2.3 Recombinant DNA constructs.....	73
	<b>12.3 Chemicals .....</b>	<b>74</b>
	<b>12.4 Computer software and Online Tools.....</b>	<b>75</b>
	<b>12.5 Equipment.....</b>	<b>75</b>
<b>13</b>	<b>Methods.....</b>	<b>77</b>
	<b>13.1 Microbiological methods .....</b>	<b>77</b>
	13.1.1 Culturing of bacteria .....	77
	13.1.2 Production of competent bacteria.....	78
	13.1.3 Transformation of <i>E. coli</i> bacteria with plasmid DNA.....	78
	<b>13.2 Molecular methods .....</b>	<b>79</b>
	13.2.1 RNA extraction .....	79
	13.2.2 Purification of plasmid DNA .....	79
	13.2.3 Polymerase chain reaction (PCR) .....	79
	13.2.4 DNA sequencing.....	81
	13.2.5 DNA gel electrophoresis.....	81

---

13.2.6	Preparative DNA gel electrophoresis and gel extraction .....	82
13.2.7	DNA cloning.....	83
<b>13.3</b>	<b>Biochemical methods .....</b>	<b>84</b>
13.3.1	Protein gel electrophoresis .....	84
13.3.2	Coomassie staining.....	86
13.3.3	Western Blot analysis.....	86
13.3.4	Expression and purification of HIS-tagged fusion proteins.....	88
13.3.5	Concentration and purification of proteins from aqueous solutions .....	90
13.3.6	Synthesis of specific antibodies .....	91
<b>13.4</b>	<b>Cell culture .....</b>	<b>94</b>
13.4.1	Culturing COS-7 cells .....	94
13.4.2	Transfection of COS-7 cells .....	94
<b>13.5</b>	<b>Histochemistry .....</b>	<b>95</b>
13.5.1	Hybridization histochemistry: Whole mount <i>in situ</i> hybridization .....	95
13.5.2	Immunohistochemistry .....	98
13.5.3	Immunocytochemistry .....	100
<b>13.6</b>	<b>Phylogenetic analysis.....</b>	<b>103</b>
13.6.1	Dataset assembly .....	103
13.6.2	Multiple sequence alignment .....	104
13.6.3	Phylogenetic tree construction.....	105
<b>14</b>	<b>References .....</b>	<b>107</b>
<b>15</b>	<b>Supplements .....</b>	<b>115</b>
15.1	Supplementary Figures .....	115
15.2	Supplementary Tables .....	129
	<b>Erklärung.....</b>	<b>146</b>
	<b>Lebenslauf.....</b>	<b>147</b>
	<b>List of scientific publications.....</b>	<b>148</b>
	Peer-reviewed articles .....	148
	Published abstracts.....	148
	<b>Danksagung.....</b>	<b>149</b>

## 1 List of figures

<b>Figure 5-1:</b> Prophase of meiosis I – the interplay of cohesion, SC assembly and homologous recombination.....	13
<b>Figure 5-2:</b> The inventory of mouse SC proteins..	16
<b>Figure 5-3:</b> Schematic diagram of the organization of the murine SC.....	18
<b>Figure 5-4:</b> Schematic diagram of the organization of the SC in <i>Drosophila melanogaster</i> .....	19
<b>Figure 5-5:</b> Schematic diagram of the organization of the SC in <i>Caenorhabditis elegans</i> .....	20
<b>Figure 5-6:</b> Assembly steps of the murine SC. ....	23
<b>Figure 6-1:</b> Phylogenetic tree of metazoan evolution. ....	26
<b>Figure 7-1:</b> The molecular phylogeny of SYCP1 and SYCP3. ....	28
<b>Figure 7-2:</b> Multiple alignments of the conserved domains of SYCP1 and SYCP3.....	30
<b>Figure 7-3:</b> Comparison of the rat and the Hydra SYCP1 and SYCP3.....	31
<b>Figure 7-4:</b> Testis-specific expression of <i>HySycp1</i> and <i>HySycp3</i> on the mRNA level. ....	32
<b>Figure 7-5:</b> <i>HySycp1</i> and <i>HySycp3</i> mRNAs are specifically synthesized in the basal testis layer.....	33
<b>Figure 7-6:</b> Testis-specific expression of HySYCP1 and HySYCP3 on the protein level. ....	34
<b>Figure 7-7:</b> Immunostaining of HySYCP1 and HySYCP3 on testis cryosections. ....	35
<b>Figure 7-8:</b> Immunostaining of HySYCP1 and HySYCP3 on chromosome spread preparations. ....	36
<b>Figure 7-9:</b> <i>Ex vivo</i> co-assembly of HySYCP3 and rat SYCP3. ....	38
<b>Figure 8-1:</b> Phylogeny of SYCE2, Tex12, SYCE1 and SYCE3. ....	42
<b>Figure 8-2:</b> Testis-specific expression of <i>HySyce2</i> and <i>HyTex12</i> on the mRNA level. ....	44
<b>Figure 8-3:</b> Testis-specific expression of HySYCE2 on the protein level. ....	45
<b>Figure 8-4:</b> Immunostaining of HySYCE2 and HyTex12 on chromosome spread preparations..	46
<b>Figure 8-5:</b> Co-assembly of HySYCE2 and HyTex12 in the heterologous system.....	47
<b>Figure 9-1:</b> Multiple alignment of SYCP2 orthologues.....	51
<b>Figure 9-2:</b> Phylogeny of SYCP2. ....	52
<b>Figure 9-3:</b> Testis-specific expression of <i>HySycp2</i> mRNA. ....	54
<b>Figure 10-1:</b> The dynamic evolution of the SC in <i>Metazoa</i> .....	57
<b>Figure 10-2:</b> The inventory of <i>Hydra</i> SC proteins.....	61
<b>Figure 10-3:</b> Schematic diagram of the organization of the <i>Hydra</i> SC.....	61
<b>Figure 10-4:</b> A longitudinal section through the <i>Hydra</i> testis.....	63
<b>Figure 10-5:</b> Electron microscopical image of the <i>Hydra</i> SC.....	64
<b>Figure 10-6:</b> dSTORM microscopy on Hydra chromosome spreads. ....	64
<b>Figure 10-7:</b> HyRPA localizes in several foci along the <i>Hydra</i> SC in pachytene spermatocytes..	65
<b>Figure 13-1:</b> Schematic illustration of the semidry Western blot set-up. ....	87

## 2 List of tables

<b>Table 12-1:</b> Primary antibodies used in this study.....	69
<b>Table 12-2:</b> Secondary antibodies used in this study. ....	70
<b>Table 12-3:</b> Oligonucleotides used in this study. ....	71
<b>Table 12-4:</b> Computer software and Online tools used in this study. ....	75
<b>Table 12-5:</b> Special equipment used in this study. ....	75
<b>Table 13-1:</b> Antibiotic solutions used in this study. ....	77
<b>Table 13-2:</b> Pipetting schemes for separating gels of different polyacrylamid content and for the stacking gel.....	85

### 3 Summary

The synaptonemal complex (SC) is a highly conserved structure in sexually reproducing organism. It has a tripartite, ladder-like organization and mediates the stable pairing, called synapsis, of the homologous chromosomes during prophase of meiosis I. Failure in homolog synapsis result in aneuploidy and/or apoptosis of the developing germ cells.

Since 1956, the SC is subject of intense research and its presence was described in various species from yeast to human. Its structure was maintained during millions of years of evolution consisting of two parallel lateral elements (LEs), joined by numerous transverse filaments (TFs) which run perpendicular to the LEs and an electron dense central element (CE) in the middle of the SC. Individual protein components, however, were characterized only in few available model organisms, as for example *Saccharomyces cerevisiae*, *Arabidopsis thaliana*, *Drosophila melanogaster*, *Ceanorhabditis elegans* and *Mus musculus*. Rather unexpectedly, these characterizations failed to detect an evolutionary homology between the protein components of the different SCs. This fact challenged the general idea of a single origin of the SC in the evolution of meiosis and sexual reproduction.

This thesis now addressed itself to the task to unravel the discrepancy between the high conservation of the SC structure and its diverse and apparently non-homologous protein composition, focusing on the animal kingdom. It is the first study dealing with the evolution of the SC in *Metazoa* and demonstrates the monophyly of the mammalian SC components in metazoan species. The thesis demonstrates that at least four out of seven murine SC proteins emerged in *Eumetazoa* at the latest and have been likewise part of an ancient SC as it can be found in the present-day cnidarian species *Hydra*. This SC displays the common organization and already possesses the minimal protein kit corresponding to the three different structural domains: LEs, TFs and the CE. Additionally, the individual phylogenies of the murine SC proteins revealed the dynamic evolutionary history of the ancient SC. Further components were added during the diversification of *Bilateria* and vertebrates while ancestral proteins likely duplicated in the vertebrate lineage and diversified or got lost in the branch leading to ecdysozoan species. It is hypothesized that the apparently non-homologous SC proteins in *D. melanogaster* and *C. elegans* actually do derive from the ancient SC proteins but diversified beyond recognition during the fast evolution of *Arthropoda* and *Nematoda*.

The study proposes *Hydra* as an alternative invertebrate model system for meiosis and SC research to the standard organisms *D. melanogaster* and *C. elegans*. Recent results about the cnidarian SC as well as the possible application of standard methods is discussed and summarized in the concluding section.



## 4 Zusammenfassung

Der Synaptonemalkomplex (SC) ist eine hochkonservierte Proteinstruktur. Er weist eine dreiteilige, leiterähnliche Organisation auf und ist für die stabile Paarung der homologen Chromosomen während der Prophase der ersten meiotischen Teilung verantwortlich, die auch als Synpase bezeichnet wird. Fehler während der Synpase führen zu Aneuploidie oder Apoptose der sich entwickelnden Keimzellen.

Seit 1956 ist der SC Gegenstand intensiver Forschung. Seine Existenz wurde in zahlreichen Organismen von der Hefe bis zum Menschen beschrieben. Seine Struktur aus zwei parallel verlaufenden Lateralelementen (LE), die durch eine Vielzahl von sogenannten Transversalfilamenten (TF) verbunden werden und dem Zentralen Element (CE) in der Mitte des SC ist dabei offensichtlich über die Millionen von Jahren der Evolution erhalten geblieben. Einzelne Proteinkomponenten des SC wurden jedoch nur in wenigen Modelorganismen charakterisiert, darunter *Saccharomyces cerevisiae*, *Arabidopsis thaliana*, *Drosophila melanogaster*, *Ceanorhabditis elegans* und *Mus musculus*. Unerwarteter Weise gelang es bei dieser Charakterisierung nicht, eine evolutionäre Verwandtschaft, d.h. eine Homologie zwischen den Proteinsequenzen der verschiedenen SCs nachzuweisen. Diese Tatsache sprach gegen die grundsätzliche Annahme, dass der SC in der Evolution nur einmal entstanden sei.

Diese Arbeit hat sich nun der Aufgabe gewidmet, die Diskrepanz zwischen der hochkonservierten Struktur des SC und seiner augenscheinlich nicht-homologen Proteinzusammensetzung zu lösen. Dabei beschränkt sie sich auf die Analyse des Tierreichs. Es ist die erste Studie zur Evolution des SC in *Metazoa* und demonstriert die Monophylie der Säuger SC Proteinkomponenten im Tierreich. Die Arbeit zeigt, dass mindestens vier von sieben SC Proteinen der Maus spätestens im letzten gemeinsamen Vorfahren der Gewebetiere (*Eumetazoa*) entstanden sind und auch damals Teil eines ursprünglichen SC waren, wie er heute in dem Nesseltier *Hydra* zu finden ist. Dieser SC weist die typische Struktur auf und besitzt bereits alle notwendigen Komponenten, um die drei Domänen – LE, TF und CE – zu assemblieren. Darüber hinaus ergaben die einzelnen Phylogenien der verschiedenen SC Proteine der Maus, dass der SC eine sehr dynamische Evolutionsgeschichte durchlaufen hat. Zusätzliche Proteine wurden während der Entstehung der *Bilateria* und der Wirbeltiere in den SC integriert, während andere ursprüngliche Komponenten möglicherweise Gen-Duplikationen erfuhren bzw. besonders in der Linie der Häutungstiere verloren gingen oder sich stark veränderten. Es wird die These aufgestellt, dass die auf den ersten Blick nicht-homologen SC Proteine der Fruchtfliege und des Fadenwurms tatsächlich doch von den ursprünglichen Proteinkomponenten abstammen, sich aber aufgrund der rasanten Evolution der Arthropoden und der Nematoden bis zu deren Unkenntlichkeit diversifizierten.

Zusätzlich stellt die Arbeit *Hydra* als alternatives wirbelloses Modellsystem für die Meiose- und SC-Forschung zu den üblichen Modellen *D. melanogaster* und *C. elegans* vor. Die kürzlich ge-

---

wonnenen Erkenntnisse über den *Hydra* SC sowie der Einsatz der Standard-Methoden in diesem Organismus werden in dem abschließenden Kapitel zusammengefasst und diskutiert.

## 5 General Introduction

### 5.1 Meiosis

Meiosis is the vital process of sexual reproduction and designates a special type of cell division that produces haploid daughter cells from diploid precursor cells. During meiosis, which takes place in the gonads, the chromosome set of the stem cell derived gonia (diploid) is divided in half to the haploid state of the mature germ cells. A male sperm and a female egg finally fuse during fertilization and reconstitute the diploid state of the resultant zygote. The zygote will develop into a new organism and is genetically unique. This is due to the random combination of maternal and paternal chromosomes on the one hand and the chromosomal rearrangement between homologous chromosomes - a process which is called homologous recombination - on the other hand which both happen in the developing gamete during meiosis.

The meiotic process is divided into two successively occurring divisions following only one round of DNA replication in premeiotic S-phase. During meiosis I (first division), the homologous chromosomes - called homologs - of the gonias<sup>1</sup> are separated and distributed to the daughter cells<sup>2</sup>. This reductional division is exceptional and makes up the meiotic process as meiosis II (second division) resembles the common equational division of mitosis. Sister chromatids are separated to the daughter cells during this second division finally producing haploid spermatids and eggs<sup>3</sup>.

#### 5.1.1 Meiosis I

In analogy to mitosis, meiosis I is divided into five phases that are characterized by comparable but also unique cellular events:

- a) **Prophase:** chromosome condensation, sister chromatid cohesion and meiosis-specific pairing of homologs
- b) **Prometaphase:** disassembly of the nuclear envelope and formation of the meiotic spindle
- c) **Metaphase:** meiosis-specific syntelic attachment of the spindle microtubules to the chromosome kinetochores and arrangement of the bivalents in the metaphase plate
- d) **Anaphase:** separation of the homologs to opposing cell poles by the release of cohesion
- e) **Telophase:** reassembly of the nuclear envelopes around the separated chromosomes

---

<sup>1</sup> The gonias are named spermatogonia in males and oogonia in females. They are diploid (2n) with two sister chromatid chromosomes (2C).

<sup>2</sup> These cells are called primary spermatocytes and oocytes. They are haploid (1n) with two sister chromatid chromosomes (2C).

<sup>3</sup> Sperms and eggs are haploid (1n) with one chromatid chromosomes (1C).

Assuming meiosis having evolved from mitosis only once, this first meiotic division, however, also harbors most evolutionary novelties and essential adaptations of the meiotic chromosome architecture that allow the reduction of the chromosome set and make the differences to the mitotic division (Petronczki *et al.* 2003; Wilkins and Holliday 2009). These specific features of meiotic chromosomes will be described in the following section.

**Meiotic cohesin complexes** assemble along the chromosomes early during prophase I forming a chromosomal cohesin core and mediating the connection between the sister chromatids which is called sister chromatid cohesion. In contrast to mitotic cohesins, these meiotic complexes will only be cleaved along the chromosome arms but stay intact at the centromeres in anaphase I. Their centromeric protection will assure that only the homologs will be separated in the first meiotic division while the sister chromatids stay attached at the centromeres until meiosis II (Revenkova and Jessberger 2005).

Also early in prophase I, the proteins of the **meiotic recombination** machinery assemble at the chromosomes. DNA double strand breaks (DSBs) are initially introduced in the recipient chromosome and become repaired step-by-step by different protein complexes which use the homologous donor chromosome as a repair template and manifest themselves as molecular identifiable and distinguishable recombination nodules at or between the chromosome axes. Different models<sup>4</sup> explain the possible ways of repair that lead to either reciprocal exchange of chromosome fragments, called cross-over, or non-cross-over<sup>5</sup> (De Massy 2003; Moens *et al.* 2007).

Cross-over events between homologs, which can physically be seen as chiasmata in late prophase I, are important for the generation of genetic variation but are also essential for the connection of the homologs during metaphase I. The chiasmata between the homologs and the cohesion between the sister chromatids mediate the force that holds the homologs together and opposes the pulling force from the meiosis-specific syntelic association of the spindle microtubules to only one of the two sister kinetochores of each chromosome during metaphase I. When in anaphase I the sister chromatid cohesion is released along the chromosome arms, the chiasmata are resolved and the homologs can be separated. The sister chromatids, however, remain connected and together they are pulled to one pole of the cell by the spindle microtubules as a consequence of the protected centromeric cohesion (Page and Hawley 2003; Revenkova and Jessberger 2005).

A third characteristic of meiotic prophase I chromosomes is the formation of the **synaptonemal complex** (SC). It assembles and likewise disassembles in the progress of prophase I and mediates the connection of the homologs, which is called synapsis, prior to the formation of chiasmata. Its assembly is strongly interdependent on the processes of meiotic cohesion and

---

<sup>4</sup> The double strand break repair model, DSBR, leads to cross-over via the formation of double Holliday junctions. The DSBR can also lead to non-cross-over products. The synthesis depending strand annealing model, SDSA, leads to non-cross-over.

<sup>5</sup> Non-cross-over can still come along with gene conversion, as can cross-over, by mismatch repair of the heteroduplex DNA in the intermediate chromosomal structures.

homologous recombination (Page and Hawley 2003; Page and Hawley 2004) as will be described in the following paragraphs.

As becoming obvious, prophase I certainly is the most crucial phase of this first division in which meiotic cohesion is established, homologous recombination takes place and the SC assembles (**Figure 5-1**). In accordance to this, the developing gametes remain in prophase for the longest time compared to the other phases of meiosis I. Prophase I itself is subdivided into five stages correspondingly to the morphological changes of the chromosome architecture (for review see e.g. Zickler and Kleckner 1998; Page and Hawley 2003).

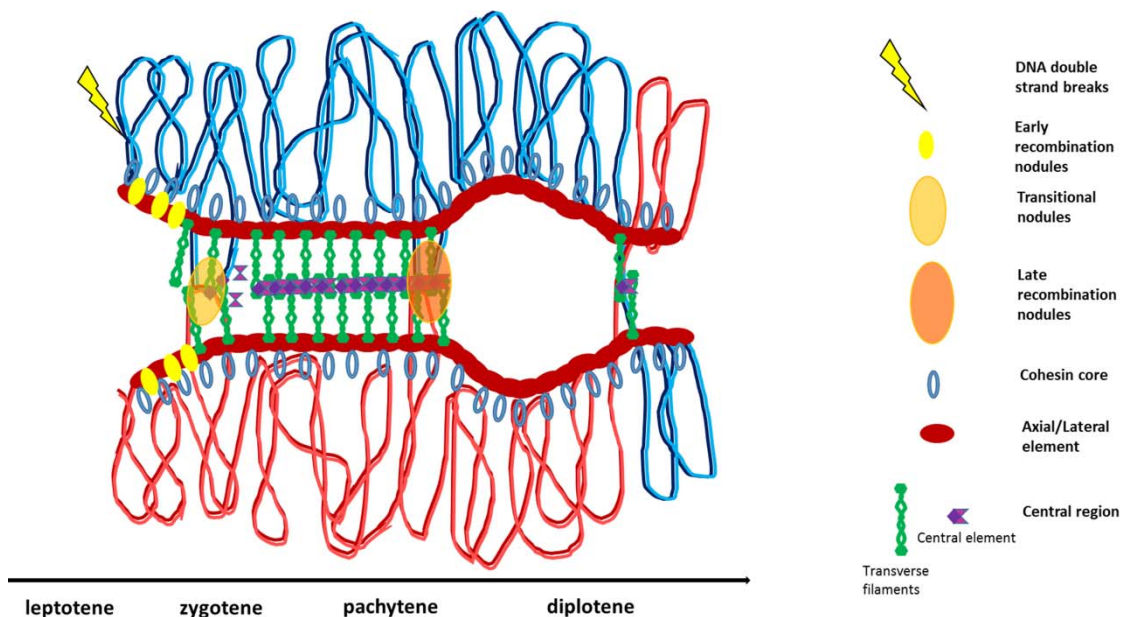


**Figure 5-1: Prophase of meiosis I – the interplay of cohesion, SC assembly and homologous recombination.** The model is based on data from mice. During leptotene, chromosomal axes are formed by the cohesin core and the proteins of the axial element. The homologous chromosomes (blue and red), each consisting of two sister chromatids (light and dark), start to condense. They are organized in loops which are attached to the axes. DNA double strand breaks are introduced into the DNA and will be processed by proteins of the early recombination nodules which form along the axes in high numbers. In zygotene, synapsis is initiated by the transverse filaments which initially bind to the axes. These are now called lateral elements. Proteins of the central element are recruited to transverse filaments stabilizing their interaction in the center of the SC. Approximately 60% of the early recombination nodules are transformed into transitional recombination nodules. In pachytene, the synapsis has progressed along the entire length of the chromosomes. In this phase, the synapsed chromosomes are called bivalents. In a late stage of pachytene, only one or two recombination nodules per bivalent are left which are in close association with the central element. These late recombination nodules mark the future sites of chiasmata in diplotene where reciprocal exchange between the homologous chromosomes has occurred. The SC disassembles by dissociation of the transverse filaments from the axes in diplotene and the homologs stay attached to each other only by the chiasmata.

In **leptotene** (leptos, greek thin), the chromosomes are fully replicated and consist of two sister chromatids. They are connected by the meiotic cohesin complexes which form the primary chromosomal core. The chromosomes become visible in the light microscope as thin threads as the chromatin starts to condense. The kinetochores assemble at their centromeres and the first components of the SC are recruited to the chromosome axes to form the so called axial elements (AE). Multiple early recombination nodules (ENs) can be detected as electron

dense foci which are associated with these AEs. They contain the RecA recombinase homologues RAD51 and DMC1 and mark the sites of initial DNA-DNA interactions between the homologs after DSB induction (Moens *et al.* 2002). Simultaneously with AE formation, the telomeres of the chromosomes become attached to the inner nuclear membrane. In mammals, this attachment is achieved via specialized conical thickenings of the chromosomal axes (Liebe *et al.* 2004). The telomeres move and cluster in the nuclear membrane close to the cytoplasmic centriole during the transition of leptotene to **zygotene** (zygos, greek paired). This very transient conformation is called bouquet stage and it is suggested that the telomere clustering supports the homology search and the alignment of the homologs as it coincides with synapsis initiation in many species (Scherthan *et al.* 1996). Synapsis is characterized by the assembly of the central region of the SC. During this stage, it progressively joins the two chromosome axes of a homologous chromosome pair like a zipper. The axes, which were formerly named AEs, are now renamed to lateral elements (LEs) in the context of the CR. At the same time, the ENs are processed into a decreasing number of recombination nodules which are defined as transitional nodules (TNs) in mammals. TNs now localize between the LEs and contain proteins, such as RPA, MSH4, BLM helicase and topoisomerase, which are implicated in the resolution of most of the early DNA-DNA interactions (Moens *et al.* 2002). Results from mice (Tarsounas *et al.* 1999; Baudat *et al.* 2000; Bolcun-Filas *et al.* 2009) and from yeast (Storlazzi *et al.* 1996; Agarwal and Roeder 2000) research further suggest that some recombination nodules at this stage may function as initiation sites for synapsis. At these sites, the assembly of the CR starts and spreads into both directions to connect the homologs over their entire length. In **pachytene** (pakhos, greek thick) finally, the SC is fully assembled along each chromosome pair. It now consists of the two LEs from the homologs and the elongated central region which bridges the gap between the LEs and mediates their synapsis. The chromatin is highly condensed and organized in loops that are associated with the LEs. The synapsed chromosomes, which are also called bivalents at this stage, can be seen as thick threads in the light microscope. Furthermore, the telomeres are released from the bouquet stage and few recombination nodules are converted into late nodules (LN). These LNs were originally discovered and described as recombination nodules in 1975 (Carpenter 1975) and indicate the actual sites where crossing-over events have occurred. Usually, only one or two of initially several hundreds of DSBs per bivalent are processed into crossing-overs. The rest of them have been repaired without a reciprocal exchange of chromosome fragments (Moens *et al.* 2002). Subsequently in **diplotene** (diploos, greek double), the SC disassembles but the homologs remain attached via their few chiasmata. The final stage, called **diakinesis** (kinesis, greek movement), is a transition phase to prometaphase during which the chromosomes reach their highest degree of condensation.

### 5.1.2 Meiosis II

As denoted above, meiosis II is an equational division which is very similar to the mitotic division of somatic cells. However, there is no S-phase with DNA replication before the meiocytes enter prophase of meiosis II. In prophase II, the chromosomes condense and will be aligned in

the metaphase plate during metaphase II by the amphytelic association of the spindle microtubules to the sister kinetochores. In anaphase II, the previously protected sister chromatid cohesion is split at the centromeres, finally, to allow the separation of the chromatids. During telophase II, the chromatin decondenses and four new nuclear envelopes assemble around the separated single chromatid chromosomes to form four haploid nuclei.

## 5.2 The synaptonemal complex (SC)

The SC is an evolutionarily well conserved feature of meiosis I whose structure strongly resembles ladder (see also **Figure 5-1**). There are the two lateral elements (LEs) which assemble along the homologous chromosomes and form the proteinaceous chromosomal axis in combination with the cohesin core. These LEs become firmly connected by the central region (CR). It consists of multiple layers of transverse filaments (TFs) and a central element (CE) which can be seen as electron dense region in the center of the SC in electron micrographs. The CE runs parallel to the LEs (Schmekel and Daneholt 1995). The TFs, which run perpendicular to the LEs and the CE, bind to the LEs and interact head-to-head with the TFs from the opposing axis. Their interaction is stabilized longitudinally and between the layers by the proteins of the CE. In 1956, Moses and Fawcett described the SC for the first time as a common central core structure in the chromosomes of spermatocytes from various species (Fawcett 1956; Moses 1956). Since then, the SC is accepted as ubiquitous structure in nearly all sexually reproducing organisms (Gillies 1975; von Wettstein *et al.* 1984).<sup>6</sup>

But individual protein components of the SC have been characterized in only few model systems, mainly in *Saccharomyces cerevisiae* and *Arabidopsis thaliana* and the three standard metazoan model organism *Mus musculus* (and *Rattus norvegicus*), *Drosophila melanogaster* and *Caenorhabditis elegans*. However, only the three organisms from the animal kingdom were considered in this study.

Comparing the SCs from mouse, *Drosophila* and *C.elegans*, the structural tripartite organization is very similar including a width of approximately 100 - 200 nm. However, the different protein components of the respective domains (LEs, TFs and CE) exhibit great primary amino acid sequence diversities (e.g. Page and Hawley 2004; Anderson *et al.* 2005; Bogdanov *et al.* 2007; Bolcun-Filas and Schimenti 2012). This lack of sequence identity<sup>7</sup> is surprising considering a single origin of meiosis in general and, in particular, the structural conservation of the SC. It leaves confusion about the evolutionary relationship and origin of the different SC components.

---

<sup>6</sup> Exceptions are for example *Schizosaccharomyces pombe* and *Drosophila melanogaster* males which lack a SC.

<sup>7</sup> The sequence identity/similarity, which is given by the number of identical or similar residues in the primary amino acid sequences, is an indicator for the homology of different proteins. Homologous proteins are evolutionary descends of a common ancestor.

### 5.2.1 The SC components of metazoan model organisms

#### *Mus musculus* and *Rattus norvegicus*

So far, seven SC components have been characterized in the mouse/rat model system (**Figure 5-2**).

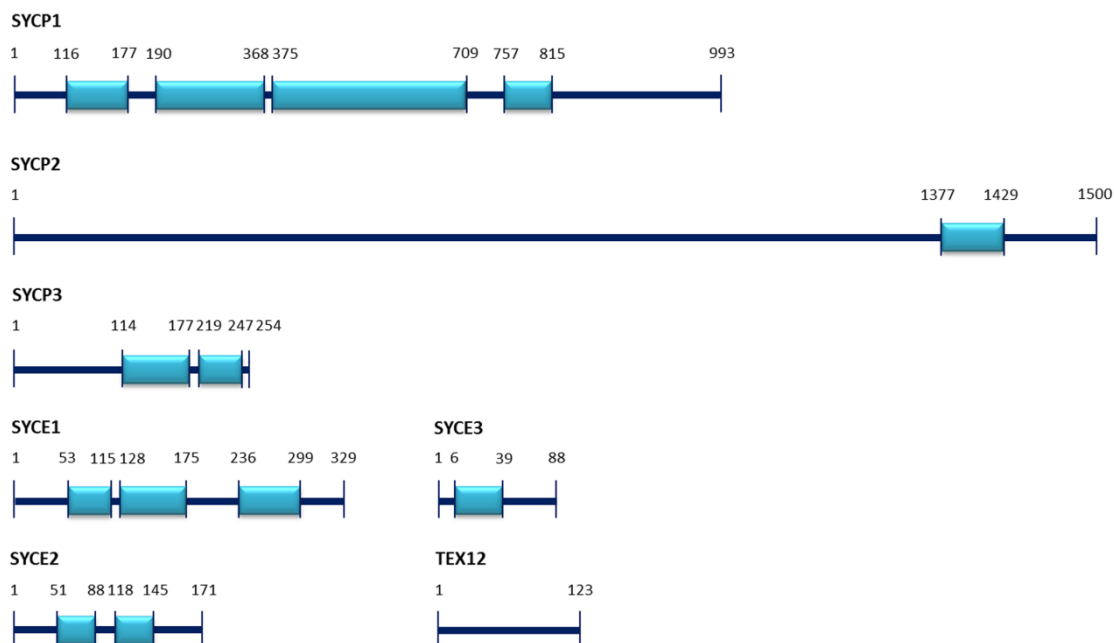


**Figure 5-2: The inventory of mouse SC proteins.** The length of the proteins is indicated in numbers of amino acids. The extension and position of coiled coil domains, which were predicted by the Lupas algorithm, are represented by the light blue boxes. The diagram is adopted from Fraune *et al.* 2012a.

SYCP2 and SYCP3 are the major constituents of the LEs (Lammers *et al.* 1994; Offenberg *et al.* 1998). Both proteins assemble along the chromosome axes in leptotene and remain localized in the AEs/LEs until diplotene (Schalk *et al.* 1998). After SC disassembly, the proteins can be further detected in the centromeric region until metaphase I (Dobson *et al.* 1994; Offenberg *et al.* 1998). The murine SYCP3 is 254 amino acids (aa) long.<sup>8</sup> In the mouse and the rat, the protein appears in two different isoforms of 30 kDa and 33 kDa, resulting from two alternative transcription start points (Botelho *et al.* 2001; Alsheimer *et al.* 2010). SYCP3 is organized in an  $\alpha$ -helical central domain<sup>9</sup> and non-helical termini. Especially the central domain and two previously identified flanking motifs - CM1 and CM2<sup>10</sup> - exhibit a high degree of sequence conservation in a comparison of vertebrate protein sequences (Baier *et al.* 2007b). Ectopic expression of SYCP3 revealed that the protein is able to assemble to higher order filaments and networks in the heterologous system of somatic COS-7 cells which resemble the basic fibrils of the AEs/LEs (Yuan *et al.* 1998; Baier *et al.* 2007b). The conserved region was thereby found to be necessary and sufficient for this polymerization process (Baier *et al.* 2007b). Beside its homo-

<sup>8</sup> The rat SYCP3 is 257 aa long.

<sup>9</sup> The coiled coil regions in the mouse range from aa 114-247, in the rat the rod domain is predicted from aa 116-250.

<sup>10</sup> In the rat, CM1 ranges from aa 87-106 and CM2 ranges from aa 252-257.



typic interaction, SYCP3 can also bind to SYCP2 which is the second LE component. It is a large protein of 1,500 aa in the mouse and has a single putative coiled coil domain at its C-terminal end. This domain is essential for its interaction with SYCP3 but also for its binding capacity to SYCP1 (Yang *et al.* 2006; Winkel *et al.* 2009).

SYCP1 is the protein component of the TFs (Meuwissen *et al.* 1992). In the mouse, it is 993 aa long and shows a characteristic central coiled coil region<sup>11</sup> which is flanked by globular termini as well. This central rod domain is essential for homotypic interactions similar to SYCP3. In the heterologous system, e.g. in somatic COS-7 cells, SYCP1 is also able to form higher order structures which are called polycomplexes. These polycomplexes resemble stacks of SCs showing alternating layers of different electron density as it is characteristic for the LE and the CE in the electron microscope (Öllinger *et al.* 2005). Polymerization analysis with different *Sycp1* mutants encoding longer or shorter coiled coil domains revealed that the TF protein is the main determinant for the SC width (Öllinger *et al.* 2005). Beyond, the C-terminus was found to be necessary for polycomplex formation, too (Öllinger *et al.* 2005) and its interaction with SYCP2 (Winkel *et al.* 2009). SYCP1 molecules most likely form parallel dimers within the SC. These dimers reach in the direction of the LEs with their C-termini and overlap/interact in the CE with their N-termini (Liu *et al.* 1996; Schmekel *et al.* 1996; Schücker *et al.* 2014).

Additionally, there are four proteins that specifically localize to the CE: SYCE1, SYCE2 (Costa *et al.* 2005), SYCE3 (Schramm *et al.* 2011) and Tex12 (Hamer *et al.* 2006). Most of them are rather small with molecular masses of 19 kDa (SYCE2), 14 kDa (Tex12) and 12kDa (SYCE3). SYCE1 is the largest known CE protein with 38 kDa. These proteins do not contain any additional structural characteristics besides the predicted coiled coil motifs for SYCE1, SYCE2 and SYCE3. Binding and polymerization studies, however, revealed a complex interaction network of the proteins with each other and the TF component SYCP1. SYCE1, SYCE2 and SYCE3 are diffusely distributed in COS-7 cells when transfected individually but are recruited into the polycomplexes when co-transfected with SYCP1 (Costa *et al.* 2005; Schramm 2011). This indication to an *in vitro* binding capacity of these proteins to SYCP1 could be strengthened by co-immunoprecipitation experiments. SYCE1 and SYCE2 interact with the N-terminus of SYCP1, with each other and with themselves under these experimental conditions (Costa *et al.* 2005). Furthermore, SYCE3 was shown to bind to SYCE1 and SYCE2 (Schramm *et al.* 2011). An interaction of Tex12, however, could only be detected with SYCE2 (Hamer *et al.* 2006). According to a structural analysis of the human SYCE2-Tex12 interaction, these proteins form very stable hetero-octamers. SYCE2 molecules tetramerize in an antiparallel manner via their central and C-terminal coiled coil motifs in this model. The N-terminal domains of the tetramers interact with the C-termini of Tex12 dimers which form via their central dimerization sites. Electron microscopic analysis of these building units showed their ability to assemble into filament-like structures whose dimensions correlate with the dimensions of the CE (Davies *et al.* 2012).

---

<sup>11</sup> In the rat, SYCP1 is 997 aa long and has a molecular mass of 125 kDa. The coiled coil domains range from aa 116-815 in the mouse and from aa 120-818 in the rat.

The following model for the SC organization in the mouse emerged from these data (**Figure 5-3**).

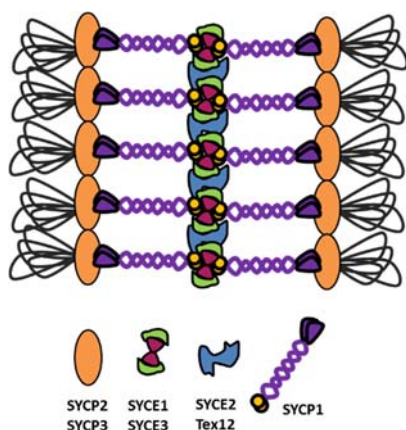


**Figure 5-3: Schematic diagram of the organization of the murine SC.** Two lateral elements, which are associated with the homologous chromosomes and consist of SYCP2 and SYCP3, are synapsed by the formation of the central region. The central region is formed by SYCP1 dimers which make the transverse filaments and the proteins of the central element - SYCE1, SYCE2, SYCE3 and Tex12. The central element components stabilize the head-to-head interaction of the opposing transverse filaments in the middle of the SC. The diagram is adapted from Schramm 2011 and Fraune *et al.* 2012a.

In this model, SYCP1 and SYCP3 are considered as the *bona fide* structural SC proteins among all components. Their prominent ability to self-assemble to higher order structures in the absence of any additional meiotic protein and the fact that these structures resemble subregions of the SC argue for the idea that SYCP1 and SYCP3 act as a structural framework, recruiting and integrating additional components into the complex (Fraune *et al.* 2012a).

### ***Drosophila melanogaster* female**

In the 1920<sup>th</sup>, the analysis of *Drosophila* meiosis started with the isolation of the first meiotic mutant *c(3)G* (Lake and Hawley 2012). *C(3)G* was finally characterized as a major component of the *Drosophila* SC quite recently. It was shown to be the constituent of the TFs revealing a similar domain organization to the mammalian SYCP1. *C(3)G* is 744 aa long and has a predicted central rod domain from aa 158 to aa 646 which is flanked by globular termini (Page and Hawley 2001). Within the SC, the protein spans the distance between the LEs and the CE and exhibits the same orientation with its N-terminus in the center of the SC and the C-terminus in the LEs (Anderson *et al.* 2005). The N-terminus was found to be essential for polymerization of *C(3)G* molecules to dimers and tetramers in the CR and also for polycomplex formation in oocytes. The C-terminus, however, is dispensable for molecule polymerization as C-terminal deletion proteins still form cylindrical polycomplexes in *Drosophila* oocytes (Jeffress *et al.* 2007). This is converse to the situation of mammalian SYCP1 which compellingly requires the C-terminal domain for its polymerization but not the N-terminus. Additionally, polymerization of *C(3)G* depends on another protein which was described in 2008 as sole potential CE protein, Corona (Cona). It does not contain any coiled coil region but localizes to the outer edge of the electron dense region of the CE (Page *et al.* 2008; Lake and Hawley 2012).

*C(2)M* is localized at the inner side of the AEs/LEs of the SC close to the C-termini of *C(3)G* during prophase I (Anderson *et al.* 2005). The proteins show the same localization pattern in immunofluorescence analyses and *C(2)M* is proposed to function as linker between the TFs and the LEs (Manheim and Mckim 2003; Anderson *et al.* 2005). Besides *C(2)M*, the LEs are composed by several proteins including cohesins, the ORD protein and Nipped-B (Bickel *et al.* 1996;

Webber *et al.* 2004; Gause *et al.* 2010; Lake and Hawley 2012). In summary, the following model of the *Drosophila* SC was developed (Figure 5-4).

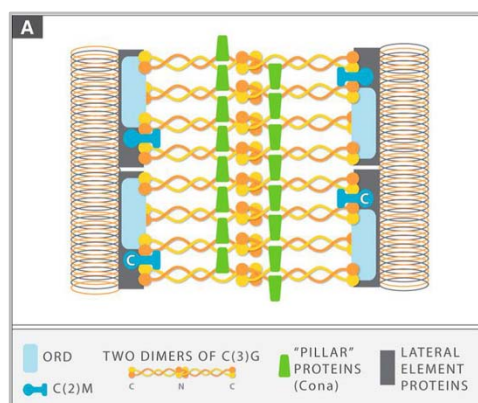


**Figure 5-4: Schematic diagram of the organization of the SC in *Drosophila melanogaster*.** Lateral elements are composed of the ORD protein and C(2)M, amongst others. Dimers of C(3)G molecules form the transverse filaments. Two of them bridge the distance between the lateral elements by a head-to-head interaction in the central element. CONA is located at the outer edge of the central element. The diagram is adopted from Hawley 2011.

### *Caenorhabditis elegans*

In *C. elegans*, HIM-3 was identified as first component of the SC being an essential component of the AEs. The study was one of the first functional descriptions of a SC component in animals. HIM-3 is 291 aa long and shares some homology to the yeast SC protein Hop1p. Both belong to the HORMA-domain containing proteins (Zetka *et al.* 1999). Additionally, three paralogs of HIM-3 were found, HTP-1, HTP-2 (Couteau and Zetka 2005) and HTP-3 (Goodyer *et al.* 2008), which are constituents of the AEs as well. Each of the proteins seems to fulfill specialized functions. HIM-3 is a major constituent of the AEs and essential for SC assembly and chiasmata formation (Zetka *et al.* 1999). Besides an essential function in AE formation, HTP-3 is required for recombination initiation (Goodyer *et al.* 2008; Severson *et al.* 2009) while HTP-1/2 seems to coordinate homolog pairing and SC formation to prevent non-homologous synapsis (Couteau and Zetka 2005).

In recent years then, further SC components were characterized outside the HIM-3 family which all localize in the CR of the SC (Macqueen *et al.* 2002; Colaiacovo *et al.* 2003; Smolikov *et al.* 2007; Smolikov *et al.* 2009). But a distinction between TF and CE proteins as in mammals or *Drosophila* is virtually infeasible. All four proteins, SYP-1, SYP-2, SYP-3 and SYP-4, co-localize in immunofluorescence analyses and the localization of each is dependent on the other three proteins. They form small foci during leptotene/zygotene and localize along the chromosome axes continuously in pachytene. In 2011, their interactions and contributions to SC organization were nicely analyzed by Schild-Prüfert (Schild-Prüfert *et al.* 2011). By yeast-two-hybrid analysis, co-immunoprecipitations and immunoelectron microscopy, they unraveled a complex interaction network of SYP-1, SYP-2, SYP-3 and SYP-4 that is suggested to be responsible for the connection of the two LEs of the SC. SYP-1 is 490 aa long and has a central coiled coil domain which allows homotypic interactions and dimerization similar to SYCP1 and C(3)G. The C-terminus is essential for this polymerization property. Within the SC, the N-termini of the SYP-1 dimers lie in the center. Therewith, SYP-1 resembles TF proteins of other organisms except that it is not able to span the entire CR of the *C. elegans* SC on its own. The other CR proteins are required instead. Via its coiled coil domain, SYP-1 can bind to the C-terminus of SYP-2, a

213 aa long coiled coil protein. This reaches into the center of the SC with its own C-terminus. Additionally, the C-terminus of SYP-1 can interact with the N-terminus of SYP-3. SYP-3 is a 225 aa long protein whose C-terminus is localized close to the LEs. It seems to act as a linker to the last SYP protein, SYP-4, which is the largest CR protein with 605 aa. It can bind to the N-terminus of SYP-3. Its own N-terminus is localized in the center of the SC. The data suggested the following model (**Figure 5-5**) to explain the organization of the *C. elegans* SC in which SYP-3 and SYP-4 might mediate the connection to the LEs while SYP-1 and SYP-2 fulfill a TF-like function.

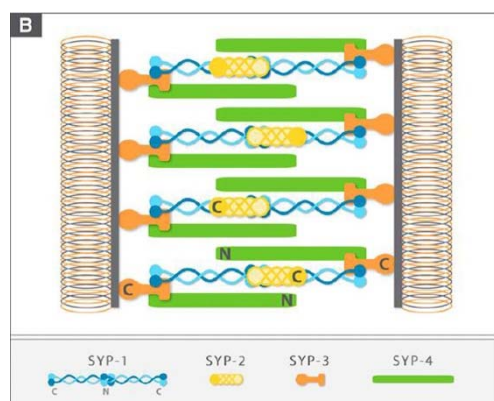


**Figure 5-5: Schematic diagram of the organization of the SC in *Caenorhabditis elegans*.** Lateral elements are composed of proteins from the HIM-3 family (not shown). A complex interplay of the SYP proteins, which all localize in the central region, bridge the distance between the lateral elements. SYP-1 and SYP-2 fulfill a transverse filament-like function. A complex of SYP-3 and SYP-4 is supposed to mediate the linkage to the lateral elements. The diagram is adopted from Hawley 2011.

In summary, the SCs of the mouse, *Drosophila* and *C. elegans* share the common ladder-like organization of two LEs and a CR spanning the distance between them. Moreover, the TF proteins from the different species or TF-like proteins in the case of *C. elegans* show structural similarities. All of them are composed of a central rod-domain which can mediate homotypic dimerization/polymerization and globular termini. But despite these similarities, nearly all investigators stumbled across the fact that the proteins lack any detectable sequence homology and therefore any evolutionary relationship amongst the different taxa (e.g. Page and Hawley 2004; Anderson *et al.* 2005; Bogdanov *et al.* 2007; Bolcun-Filas and Schimenti 2012). Maybe coming along with this, the principles regulating the formation of synapsis are also quite different in mouse, flies and nematodes.

### 5.2.2 The function of SC components and their assembly to a mature SC

The assembly of the SC and its interdependencies on meiotic cohesion and the process of homologous recombination becomes more comprehensive by looking at the mouse model system. Similarities or differences to flies or nematodes will be considered at each step if corresponding data are available (Page and Hawley 2004; Fraune *et al.* 2012a).

#### First step: The assembly of the chromosomal axes and the axial elements

The SC assembly begins with the formation of the chromosome axes during leptotene in all three species. The formation of the AEs is related to meiotic cohesin protein components in any case. In mouse meiocytes, SYCP3 is essential for AE assembly. The AE formation is abolished in the absence of SYCP3 (Liebe *et al.* 2004) and the second axial component SYCP2 cannot be recruited to the chromosomes anymore (Yuan *et al.* 2000). Expression of a C-terminally

truncated SYCP2 leads to a failure of AE formation in mouse spermatocytes as well (Yang *et al.* 2006). Though a chromosomal cohesin core is established in the absence of an intact AE in *Sycp3*<sup>-/-</sup> spermatocytes, the respective proteins, e.g. SMC1, SMC3, STAG3, localize more discontinuously and the chromosomal axes appear significantly longer than in wild-type (Yuan *et al.* 2000; Pelttari *et al.* 2001; Liebe *et al.* 2004). Conversely, depletion of meiotic cohesin subunits, e.g. SMC1 $\beta$  (Revenkova *et al.* 2004) or REC8 (Bannister *et al.* 2004), affects AE morphology and assembly. It even completely abolishes the AE formation if the two meiotic kleisin subunits REC8 and RAD21L are depleted in a double knock-out (Llano *et al.* 2012). This suggests that the cohesin core is necessary for the assembly of a defined AE. A third organizational axes layer is made by the HORMA-domain proteins HORMAD1 and HORMAD2. They preferentially bind to unsynapsed chromosome axes and become displaced from the AEs by synapsis formation in a TRIP13-dependent manner (Wojtasz *et al.* 2009). A *Hormad1*<sup>-/-</sup> mutant mouse model suggests that the HORMADs function in a meiotic “synapsis” checkpoint. This activates, maybe indirectly via BRCA1, the ATR kinase which in turn regulates the transcriptional silencing of unsynapsed chromosomes, called the meiotic silencing of unsynapsed chromosomes - MSUC (Daniel *et al.* 2011). The gene silencing could result in the abruption of the meiotic process (Turner *et al.* 2005). It becomes obvious from this that the chromosomal axes consist of several layers - the cohesin core, the HORMADs and the AEs - which can assemble independently but yet need each other to form full-length and stable chromosomal axes.

On similar dependencies between the AEs and cohesins were also reported in *C. elegans* and *Drosophila*. In *C. elegans* prophase I nuclei, the localizations of HIM-3, HTP-1, HTP-2 and HTP-3 depend on the presence of the meiotic kleisin subunits on the one hand. On the other hand, the AE component HTP-3 is likely to be essential for normal loading of the cohesin subunits REC-8 and SMC-1 to the chromosomes. Furthermore, HTP-3 is necessary for the association of HIM-3 and HTP-1/2 to the chromosomal axes (Severson *et al.* 2009). HTP-3, therefore, seems to function as a key regulator for the assembly of the AEs recruiting cohesin and non-cohesin proteins to the chromosome axes. In *Drosophila*, the ORD protein is essential for wild-type SC morphology but also for the stable association of cohesins with the chromosomes (Page and Hawley 2004; Webber *et al.* 2004).

In contrast to its relation to meiotic cohesins, the AE formation occurs independently on recombination initiation (Romanienko and Camerini-Otero 2000) and vice versa (Yuan *et al.* 2000) in the mouse although this takes place during leptotene as well. The induction of DSBs occurs prior/or simultaneously to the formation of the chromosome axes and is catalyzed by the evolutionarily highly conserved topoisomerase Spo11 in mouse as in the other organisms (Cole *et al.* 2010). Conversely to the situation in mammals, the *htp-3* mutant of *C. elegans* suggests that an AE component might be critical in early recombination initiation in this organism (Goodyer *et al.* 2008). Yet some previous genetic studies in mice proposed that, even though not necessary for DSB formation, AEs function in recombination pathway choice and direct recombination proteins to favor interhomolog rather than intersister recombination repair of DSBs in meiosis (Kouznetsova *et al.* 2011; Li *et al.* 2011). Definitely, DSB formation is required

for further steps of homolog pairing and synapsis in mammals but not in *C. elegans* and *Drosophila* where synapsis is DSB-independent (Page and Hawley 2003).

### **Second step: The assembly of the central region**

Synapsis starts during zygotene with the assembly of the CR and a failure in DSB formation results in the almost complete absence of synapsed homologs in murine pachytene cells as apparent in the *Spo11*<sup>-/-</sup> knock-out mouse. Only 5-10% of meiotic nuclei showed some degree of synapsis as indicated by the presence of SYCP1, SYCE1 and SYCE2 in this study. The synapsis, however, occurred mainly between non-homologous chromosomes (Baudat *et al.* 2000; Romanienko and Camerini-Otero 2000; Bolcun-Filas *et al.* 2009). Besides, different studies have reported about interactions between early proteins of the recombination machinery and SC components. In the first study, binding abilities of the recombinases RAD51 and DMC1 with SYCP3 and between RAD51 and SYCP1 could be detected in a yeast two-hybrid system (Tarsounas *et al.* 1999). Furthermore, *Syce1*<sup>-/-</sup> spermatocytes revealed a co-localization of RAD51 and SYCE2. A biochemical interaction between these proteins was verified by co-immunoprecipitation experiments (Bolcun-Filas *et al.* 2009). Based on this, it was speculated that these interactions might mediate the assembly of the CR from sites of homologous recombination ensuring synapsis between homologs.

The further steps of SC assembly in mouse spermatocytes could be modeled by comparing the fate of the different CR proteins in the various knock-out backgrounds (Fraune *et al.* 2012a; **Figure 5-6**). If DSB induction has occurred normally, SYCP1 initially associates with the AEs via its C-terminus in zygotene. The formation of the AEs in leptotene is independent on SYCP1 and the CE-specific proteins (De Vries *et al.* 2005; Bolcun-Filas *et al.* 2007; Hamer *et al.* 2008; Bolcun-Filas *et al.* 2009; Schramm *et al.* 2011). But even though it occurs beforehand, a defined AE is no absolute requirement for the recruitment of SYCP1 to the chromosomes. In *Sycp3*<sup>-/-</sup> spermatocytes, which do not form AEs, SYCP1 can still bind to the chromosomal axes and form stretches of the CR although these are much shorter than in wild-type (Liebe *et al.* 2004). It is possible that, in this case, the cohesin core is sufficient to allow the binding of the TFs (Peltari *et al.* 2001). Disruption of the AEs and major parts of the cohesin core, as it is found in the kleisin double mutant *Rec8*<sup>-/-</sup> *Rad21*<sup>-/-</sup>, however, finally leads to a failure in SYCP1 association as well (Llano *et al.* 2012). In the wild-type situation, SYCE3 is recruited to SYCP1 in the next step followed by SYCE1. Their knock-out phenotypes (*Syce1*<sup>-/-</sup> and *Syce3*<sup>-/-</sup>) suggest that these two proteins are essential for synapsis initiation because SYCP1 can indeed bind to the chromosome axes but fails to mediate synapsis. Neither do *Syce1*<sup>-/-</sup> nor *Syce3*<sup>-/-</sup> spermatocytes reveal any CE-like structure at a pachytene-like stage in the electron microscope (Bolcun-Filas *et al.* 2009; Schramm *et al.* 2011). After binding of this initiation complex, SYCE2 and Tex12 are loaded in the last step of the SC assembly process. Differently to SYCE1 and SYCE3, these two proteins are dispensable for synapsis initiation. Small foci of CR-like structures containing SYCP1, SYCE1 and SYCE3 could be identified between the aligned AEs in electron micrographs of *Syce2*<sup>-/-</sup> and *Tex12*<sup>-/-</sup> spermatocytes. Because synapsis is initiated but

not extended, SYCE2 and Tex12 were hypothesized to act as an elongation complex promoting expansion of the CR over the entire length of the chromosomes (Bolcun-Filas *et al.* 2007; Hamer *et al.* 2008; Bolcun-Filas *et al.* 2009). The important role of SYCP1 in the CR assembly becomes obvious in the *Sycp1*<sup>-/-</sup> phenotype: AEs assemble and align in these knock-out meocytes, but none of the CE-specific proteins can be recruited to these axes and synapsis cannot be established (De Vries *et al.* 2005; Hamer *et al.* 2006; Schramm *et al.* 2011). This further supports the idea of SYCP1 as a framework providing component for the setup of the CR.

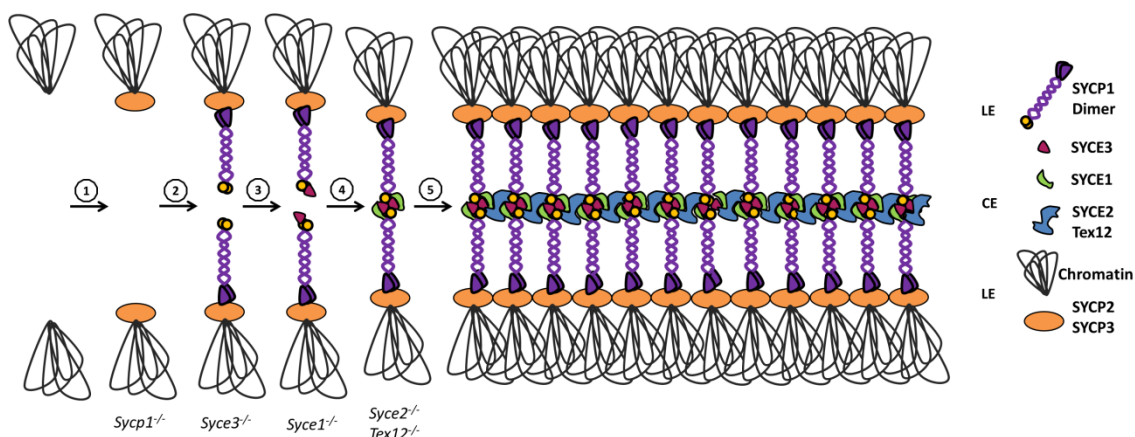


**Figure 5-6: Assembly steps of the murine SC.** The different steps of the assembly process were modeled on the basis of immunocytological and electronmicroscopical data of available knock-out mice which lack individual SC proteins. 1: SYCP2 and SYCP3 assemble along the chromosomes to form the lateral elements. This still occurs in the absence of SYCP1. 2: SYCP1 dimers are recruited to the axes. Its association is independent on the proteins of the central element. 3: SYCE3 initially associates with the SYCP1 dimers, even in the absence of SYCE1 or SYCE2. 4: SYCE1 binds to SYCE3. Together they mediate the head-to-head interaction of the transverse filaments. With this, synapsis is initiated and this initiation is independent on SYCE2 and Tex12. 5: SYCE2 and Tex12 interact with SYCE1 and SYCE3 thereby ‘zippering’ the TFs longitudinally to allow final synapsis elongation. The diagram is adopted from Fraune *et al.* 2012a and was primarily designed by Sabine Schramm (Schramm 2011).

Not as much is known about the individual steps of CR assembly in *Drosophila* or *C. elegans*. The *Drosophila ord* mutant suggests that in flies as in mice defined AEs are dispensable for the polymerization of the C(3)G molecules (Webber *et al.* 2004). Additionally, Page and colleagues proposed for the Corona protein that it might function in a similar way to SYCE2/Tex12 as it is essential for “zippering” of the TFs (Page *et al.* 2008). In *C. elegans*, the localization of one CR component is dependent on the presence of the other CR proteins as well as on the AE proteins HTP-3, HIM-3 and, at least in an *htp-1* mutant background, HTP-2 (Zetka *et al.* 1999; Couteau and Zetka 2005; Goodyer *et al.* 2008).

### Third step: The mature SC

Remarkably and despite the diversity of SC assembly modes, the processing of recombination intermediates<sup>12</sup>, which form shortly after DSB induction, is highly dependent on the CR and a mature SC in all species. Especially the final transition to LNs, which indicate the formation of

<sup>12</sup> Recombination intermediates are single end invasion strand exchange intermediates and double Holliday junctions with heteroduplex DNA.

chiasmata, is defective in the absence of an intact CR (Page and Hawley 2001; Macqueen *et al.* 2002; Colaiacovo *et al.* 2003; De Vries *et al.* 2005; Bolcun-Filas *et al.* 2007; Smolikov *et al.* 2007; Hamer *et al.* 2008; Page *et al.* 2008; Bolcun-Filas *et al.* 2009; Smolikov *et al.* 2009; Schramm *et al.* 2011). The function of the mature SC during the final processing of homologous recombination thereby might be of a dual character: 1) The LNs are generally characterized by the localization of DNA mismatch repair proteins which are homologous to the bacterial MutS and MutL. In mice, these are the MutL homologues MLH1 and MLH3. They are essential for formation of class I cross-over which display positive interference<sup>13</sup> (Baker *et al.* 1996; Moens *et al.* 2002; Kolas and Cohen 2004; Moens *et al.* 2007). It is possible that the CR can act as a platform for the recruitment of proteins of the homologous recombination machinery close to the DNA. This hypothesis is based on observations made in the electron microscope where LNs were seen in close contact to the CE of beetle spermatocytes (Schmekel and Daneholt 1998). Furthermore, the above described interactions between proteins of the homologous recombination machinery and SC components (Tarsounas *et al.* 1999; Bolcun-Filas *et al.* 2009) provide initial indications for a complex interaction network between the elements of these two meiotic features which might explain their tight interdependency. 2) Besides the reciprocal recombination of the DNA, the chromosomal axes also need to be exchanged to produce chiasmata. Borner *et al.* suggested a mechanical function of the mature SC because the final structural conformation from recombination intermediates to chiasmata occurs in the context of an elongated SC in pachytene. The model proposes that the mature SC constrains mechanical stress along the chromosome axes which is transduced into forces by associated recombination complexes to perform interchanges of the axes and the DNA. The model also considers SC twisting, which has been observed in meiotic cells since decades (Zickler and Kleckner 1999), to be the essential motion to bring the axes into close vicinity and to allow axes/DNA exchange between the homologs (Borner *et al.* 2004).

In summary, the SC and its canonical components are not solely responsible for the establishment of the chromosomal axes nor are they essential for DSB induction and formation of early recombination intermediates. Definitely, however, a mature SC is necessary for a stable synapsis and the final class I, MLH1-dependent cross-over formation in mouse as well as in flies and nematodes. These major functions of the SC were additionally emphasized in a double knock-out mouse of *Sycp1*<sup>-/-</sup> and *Sycp3*<sup>-/-</sup> which completely lacks a SC structure and displays defects in chromosome integrity, synapsis and formation of MLH1-dependent cross-over (Kouznetsova *et al.* 2011).

Generally, failures in SC formation lead to checkpoint activation, abruption of meiosis and often apoptosis of the respective meiocytes to avoid aneuploid germ cells. This finally results in the infertility of the organism or the production of mutated offspring.

---

<sup>13</sup> Positive interference means the inhibition of further cross-over events in close proximity to an initial cross-over. As consequence, there are only one or two cross-over events per bivalent.



## 6 Aims of this study

The apparent lack of sequence homology between the respective protein components is rather puzzling considering the information about the SC and its functions gained from the different metazoan model organisms. On the one hand, there is a highly conserved structural SC organization of LEs and a CR in *Drosophila*, *C. elegans* and mouse. The major functions of this structure seem likewise conserved being essential for a stable synapsis of homologs and the formation of chiasmata. Both would indicate that the SC is ancient in metazoan and has been conserved in evolution. On the other hand, the various SC components do not share any sequences similarity challenging this idea of a single origin of the SC in animals.

The major aim of this study was to unravel this evolutionary puzzle about the metazoan SC. As the primary interest applies to the mammalian complex, this was the starting point for the analysis.

Following questions were asked:

- Did the SC arise only once in metazoan evolution or did it evolve independently in different taxa?
- When did the mammalian SC components emerge?
- How did the SC evolve during animal diversification?

To answer these questions, a broad phylogenetic approach ought to be used to identify potential homologous proteins - called homologues - of the mammalian SC components. Cytological and biochemical methods were planned to be applied for the determination of an accordant localization and function of the detected homologues in a basal metazoan, e.g. *Hydra*. *Hydra* is a fresh water polyp which belongs to the very old phylum of *Cnidaria*. This phylum separated from the *Bilateria* over 500 million years ago. *Hydra* is a classical biological model organism in many respects. Despite its simple body plan, it has a differentiated germ line and can reproduce sexually. The phylogenetic tree in **Figure 6-1** illustrates the ancient character of *Hydra* and displays the evolutionary relationship of the different model organisms. It will function as a reference tree for the comparison with the phylogenies of the analyzed proteins.

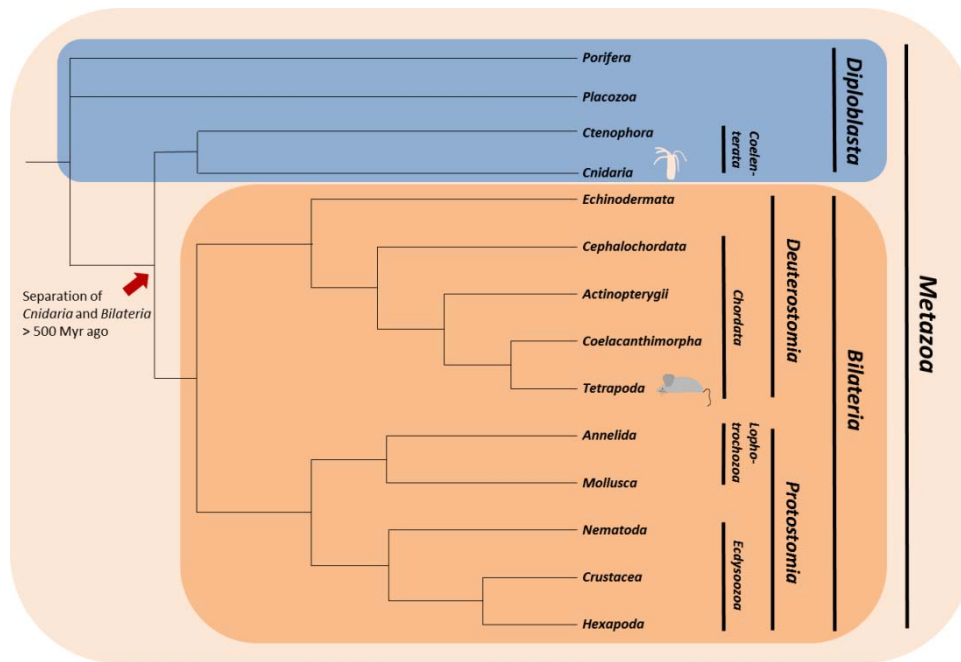


**Figure 6-1: Phylogenetic tree of metazoan evolution.** Over 500 million years (Myr) ago, the common ancestor of *Hydra* (*Cnidaria*) and mouse (*Tetrapoda*) diverged into the different lineages of *Coelenterata* and *Bilateria*. The *Bilateria* then separated into the *Deuterostomia* and *Protostomia*. The other metazoan model organisms *Caenorhabditis elegans* (*Nematoda*) and *Drosophila melanogaster* (*Hexapoda*) belong to the protostomian clade of *Ecdysozoa*. The figure is adopted from Fraune *et al.* 2014.

Together, the obtained data should allow to compile a model about the evolutionary history of the mammalian SC in respect to the evolution of *Metazoa* and to consider *Hydra* as a complementary invertebrate model system for meiosis research.

## 7 Chapter I: The evolution of the two *bona fide* structural SC components of the mouse

According to Fraune *et al.* 2012b

### Introduction

The study began with the examination of SYCP1 and SYCP3 as the two *bona fide* structural components of the murine SC. It is the major subject of this chapter.

Both proteins are polymerizing proteins containing typical coiled coil domains. This very common domain motif particularly challenged the search for true homologues in metazoan species during the phylogenetic analysis. Many false positive homologues appeared in the database search especially outside the vertebrate lineage when using the complete protein sequences. Therefore, the search had to be conducted more specifically using only sequence domains as seeds that are highly characteristic for the respective protein. In the case of SYCP3, these domains were characterized by Baier *et al.* in 2007 (Baier *et al.* 2007b). They aligned SYCP3 sequences of different vertebrate species amongst which were the previously characterized meSYCP3 of medaka fish (Iwai *et al.* 2006). The alignment revealed a conserved general domain organization of the SYCP3 proteins and, more interestingly, two sequence domains which exhibited an increased fraction of identical residues between the species and which were named conserved motif 1 and conserved motif 2.<sup>14</sup> The motifs were found around the central rod-domain, being 19 and 6 aa long, respectively. Although the predicted length of the flanked coiled coil domains in the different species varied a lot, the distance of 146 aa between CM1 and CM2 seemed to be surprisingly fixed in vertebrate evolution. Accordingly, these 146 residues of the mouse/rat were used for a deeper BLAST analysis on the NCBI database (Fraune *et al.* 2012b). A similar approach was applied to SYCP1. Besides meSYCP3, Iwai and colleagues characterized the SYCP1 homologue in medaka (meSYCP1) as well (Iwai *et al.* 2006). A comparison of the rat SYCP1 and the meSYCP1 again displayed two motifs in the N-terminal coiled coil region (CM1) and the last third of the protein (CM2) which showed the highest degree of sequence conservation (Winkel 2009). CM1 is 83 aa long<sup>15</sup> and shows 65% sequence identity between rat and fish. CM2 comprises 31 aa<sup>16</sup> of which 74% are identical between rat and fish (Fraune *et al.* 2012b). In the outcome of this sequence comparison, the CM1 was decided to be useful for the deeper BLAST analysis to identify further SYCP1 homologues outside the vertebrate lineage.

---

<sup>14</sup> These are CM1 with 78% sequence identity and CM2 with 100% sequence identity between rat and fish SYCP3. See also the introduction on p. 16.

<sup>15</sup> In the rat, CM1 ranges from aa 106 to aa 188.

<sup>16</sup> In the rat, CM2 ranges from aa 724 to aa 754.

Using these conserved sequence domains of SYCP1 and SYCP3, Jean-Nicolas Wolff<sup>17</sup> and Manfred Alsheimer<sup>18</sup> succeeded to identify various orthologues<sup>19</sup> for each component in vertebrate but also invertebrate species (see also **Supplementary Table 1** and **Supplementary Table 2**). Among these were also sequences from the very basal cnidarian species *Hydra*. Phylogenetic trees, reconstructed on the basis of these domain sequences, confirmed a common origin of the SYCP1 and SYCP3 orthologues in *Metazoa* (Fraune *et al.* 2012b; see **Figure 7-1**).

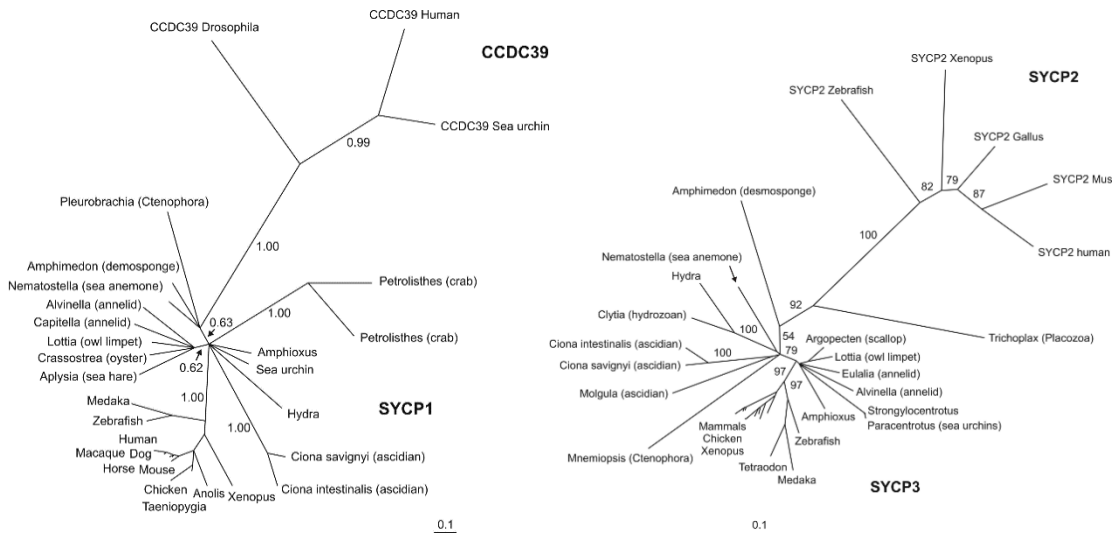


**Figure 7-1: The molecular phylogeny of SYCP1 (left) and SYCP3 (right).** The trees were calculated from alignments of the most conserved regions which are 83 amino acids of SYCP1 CM1 and 171 amino acids from CM1 to CM2 in the case of SYCP3. The phylogeny of SYCP1 was calculated by Bayesian Inference. CCDC39 sequences were used as outgroup. The tree robustness is indicated by posterior probabilities. The phylogeny of SYCP3 was calculated by the neighbor joining method. Bootstrap values are given as indication for branch robustness. SYCP2 sequences were used as outgroup in this case. The phylogenies of SYCP1 and SYCP3 display the common origin of the orthologues in *Metazoa* in both cases. The figure is adopted from Fraune *et al.* 2012b and was built by Jean-Nicolas Wolff.

## Results

Based on these data the putative *Hydra* SYCP3 (HySYCP3) and SYCP1 (HySYCP1) should be characterized regarding their sequence and structure as well as their expression pattern to explore a potential function during meiosis and a contribution to SC formation in a basal metazoan species. If this characterization showed a similarity of the cnidarian and mammalian proteins regarding all three features, this would be a precise indicator for the true orthology and the common evolutionary origin of the SYCP1 and SYCP3 homologues. The characterization was carried out using the strain *Hydra vulgaris* AEP (Martin *et al.* 1997; Hemmrich *et al.* 2007). It was morphologically described as strain of the *vulgaris* group once (Martin *et al.* 1997) but recent molecular data revealed that the strain AEP is closer related to *Hydra carnea* (Hemmrich *et al.* 2007).

<sup>17</sup> Université Lyon 1, Ecole Normale Supérieure, France.

<sup>18</sup> Cell and Developmental Biology, Biocenter, University of Würzburg.

<sup>19</sup> Orthologues are homologues which are found in different species.

It produces a higher amount of gonads than other *Hydra* species (Hemmrich *et al.* 2007) which is useful for the analysis of putative meiotic proteins. A culture of *Hydra vulgaris* AEP<sup>20</sup> was established in the laboratory with animals donated from Thomas Bosch<sup>21</sup>.

### Sequence and structure of HySYCP1 and HySYCP3

Based on the genomic data from *Hydra magnipapillata*, which are available on the public NCBI database (Chapman *et al.* 2010), primers were initially designed to clone and sequence the full-length cDNAs of *HySycp1* and *HySycp3* of *Hydra vulgaris*.<sup>22</sup> These sequences were used in the study to query the up to this former date non-public Compagen database which contains transcriptomic data from *Hydra vulgaris* AEP (Hemmrich *et al.* 2012). There was only little sequence divergence between *Hydra vulgaris* and *Hydra vulgaris* AEP according to the database information.<sup>23</sup> So the same primers could be used to clone and sequence the corresponding cDNA sequences from *Hydra vulgaris* AEP.<sup>24</sup> These were then used as references throughout the rest of the study. mRNA was extracted from 5-10 sexual animals and converted into complete cDNA by reverse transcription. The cDNA served as template for the amplification of the specific cDNA sequences of *HySycp1* and *HySycp3* by a *Phusion*-PCR.<sup>25</sup>

Analyzing the translated sequences of the putative HySYCP1 and HySYCP3 revealed that both proteins possess a rather high sequence identity in the respective conserved domains, namely CM1 for HySYCP1 and CM1 to CM2 for HySYCP3, in an alignment with several representative metazoan species from the prior phylogenetic analysis (**Figure 7-2**).

---

<sup>20</sup> For culturing conditions of *Hydra* see on page 68.

<sup>21</sup> Institute of Zoology, University of Kiel.

<sup>22</sup> *HymSycp1* and *HymSycp3* primer sequences are given in **Table 12-3**. The cloning was performed by Karoline Winkel and Manfred Alsheimer. The animals were retrieved from Georg Krohne, Biocenter, University of Würzburg. The GenBank accession No. of *HySycp1* and *HySycp3* of *H. vulgaris* are JQ906934 and JQ906932, respectively.

<sup>23</sup> 99% identity for HySYCP3 and 96% identity for HySYCP1 were calculated by BLAST.

<sup>24</sup> The GenBank accession No. of *HySycp1* and *HySycp3* of *H. vulgaris* AEP are JQ906935 and JQ906933.

<sup>25</sup> For the protocol of mRNA extraction and RT-PCR see on pages 79 f.

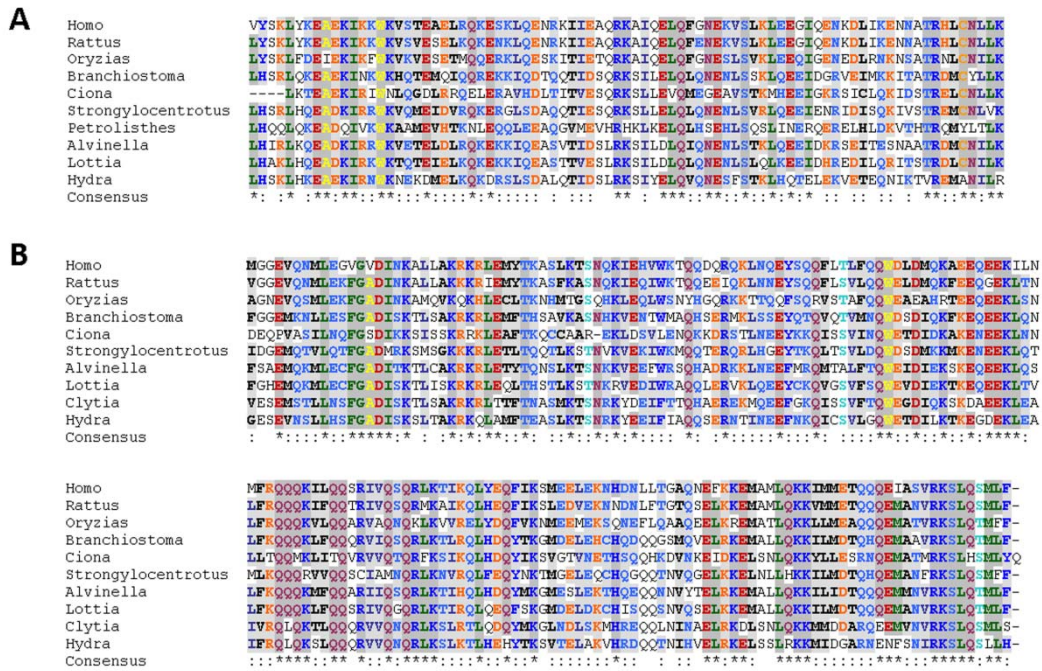


**Figure 7-2: Multiple alignments of the conserved domains of SYCP1 (A) and SYCP3 (B).** A: Alignment of the 83 amino acids of SYCP1 CM1 from various representative metazoan species. B: Alignment of the 171 amino acids from CM1 to CM2 in SYCP3 sequences from various representative metazoan species. The alignments were created by ClustalO and annotated with CHROMA. Identical residues are marked with a star in the consensus line while colons indicate residues with similar features. The threshold for grouping of the residues was set to 80%. Even the most basal species *Hydra (AEP)* still reveals a significant fraction of identical/similar residues compared to other metazoan species in both alignments. The figure is adapted from Fraune *et al.* 2012b.

Furthermore, a prediction of the secondary structure<sup>26</sup> proposed central coiled coil domains and globular termini for both cnidarian proteins suggesting a conservation in domain structure as well. The structural similarity between the mammalian and the cnidarian SYCP1 and SYCP3 becomes most obvious in the following comparisons (**Figure 7-3**).

<sup>26</sup> Prediction of secondary structures occurred in accordance to the Lupas algorithm. See **Table 12-4** for a list of the used online services.

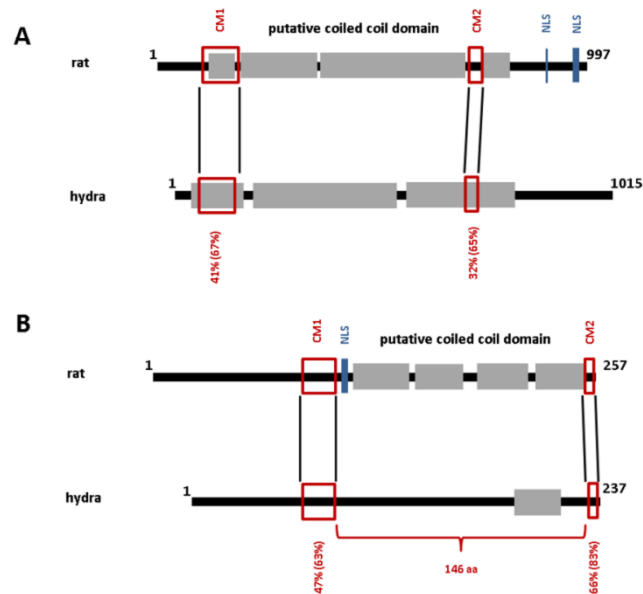


**Figure 7-3: Comparison of the rat and the Hydra SYCP1 (A) and SYCP3 (B).** Protein length is given in amino acids. The gray boxes represent putative coiled coil domains which were predicted by the Lupas algorithm. Position and dimension of the conserved motifs (CM) are denoted by the red boxes. Their sequence identity and similarity (in parentheses) are given in percentages (%). A: SYCP1 proteins from rat and *Hydra* reveal a great structural similarity regarding the extended central coiled coil regions. CM1 and CM2 exhibit a sequence identity of 41% and 32%, respectively. B: SYCP3 proteins of rat and *Hydra* differ in the extension of the predicted central rod domain. However, the distance between CM1 and CM2 is constant (146 amino acids). The motifs themselves show a sequence identity of 47% and 66%. The diagram is adapted from Fraune *et al.* 2012b and the initial design was made by Karoline Winkel in the case of SYCP1 (Winkel 2009).

HySYCP1 (**Figure 7-3, A**) is 1,015 aa long and has predicted coiled coil domains from approximately aa 36-157, aa 180-515 and aa 534-788.<sup>27</sup> The CM1 and CM2 can be found from aa 55-137 and aa 673-703. These domains exhibit a sequence identity of 41% and 32%, respectively, with an overall sequence identity from the full-length protein of about 20% in a comparison with the rat SYCP1 calculated from alignments with ClustalO.

HySYCP3 (**Figure 7-3, B**) consists of 237 aa. A coiled coil domain is predicted in the C-terminal region from aa 187-214. The CM1 and CM2<sup>28</sup> show sequence identities of 47% and 66% to CM1 and CM2 of the rat protein, respectively, while the full-length protein identity is approximately 36%. Interestingly, even the constant distance of 146 aa between CM1 and CM2 is maintained in the *Hydra* orthologue.

Thus the putative SYCP1 and SYCP3 orthologues in *Hydra* exhibit considerably high sequence identities in the particular conserved regions of CM1 and CM2 in an alignment with the rat proteins (**Figure 7-3**), as well as in multiple alignments with several metazoan orthologues (**Figure 7-2**). Furthermore, the predicted secondary structures of the HySYCP1 and HySYCP3

<sup>27</sup> Depending on the algorithm, these domains can be split into different coiled coil domains ranging from about aa 36-157, aa 180-276 and aa 280-515 as well as from aa 534-679 and aa 690-788.

<sup>28</sup> CM1 and CM2 in HySYCP3 range from aa 64-82 and from aa 230-235.

with central rod domains and globular termini support the assumption of a true orthology of the mammalian and the cnidarian proteins (**Figure 7-3**).

### Expression of HySYCP1 and HySYCP3 in *Hydra vulgris* AEP

Having shown a significant similarity between the mammalian SYCP1/SYCP3 and the cnidarian HySYCP1/HySYCP3 in sequence and structure, the expression pattern of both candidates needed to be analyzed on the mRNA and the protein level.

RT-PCR<sup>29</sup> was applied to examine if the mRNAs might be expressed in meiotic tissue specifically as expected. Therefore, about 60-80 animals were separated in four fractions containing heads, mid-pieces, feet and testes. mRNA was then extracted from these body tissue fractions and was reversely transcribed into tissue specific cDNAs. Equal volumes of these cDNA probes were taken as templates in parallel *Phusion*-PCR approaches to finally amplify, first, the full-length cDNA of *HySycp3* and secondly, the 5' region of *HySycp1* from bp 1-1,012 with the aid of sequence specific primers<sup>30</sup>. The *Hydra* actin was amplified from the same probes and used as internal control to demonstrate an equal cDNA concentration in each tissue fraction (**Figure 7-4**).

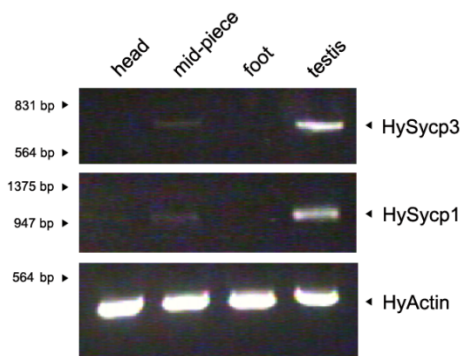


**Figure 7-4: Testis-specific expression of *HySycp1* and *HySycp3* on the mRNA level.** In RT-PCR, amplification of *HySycp3* (714 bp) and *HySycp1* (1,012 bp) specifically occurs in the testis fraction but not in the other fractions indicating their tissue specific expression. Slight signals can be detected in the mid-piece fraction. These result from left-overs of the testes which were previously associated with the body column. Amplification of *HyActin* demonstrates the equal concentration of mRNA in the different fractions.

Obviously, the mRNA of *HySycp3* and *HySycp1* is most prominent in the testes as it is demanded for a role in meiosis. Slight signals can also be detected in the mid-piece fractions where left-overs of the previously associated testes contaminated the probes.

Another method to detect mRNA expression in a specific tissue is the *in situ* hybridization<sup>31</sup> was performed on whole animals to precisely localize the mRNA of *HySycp1* and *HySycp3* along the body axis. Antisense RNA probes, labeled with digoxigenin, were generated against the full-length *HySycp3* mRNA and again the 5' region of the *HySycp1* mRNA from bp 1-1,012. The probes were hybridized to the prepared animals and afterwards detected by the  $\alpha$ -Dig antibody<sup>32</sup> which is coupled to an alkaline phosphatase (AP).

<sup>29</sup> For the protocol of the RT-PCR see on pages 79 f.

<sup>30</sup> The respective primer sequences are given in **Table 12-3**.

<sup>31</sup> For the protocol of the ISH see on page 95.

<sup>32</sup> For dilution of the primary anti-Dig antibody see **Table 12-1**.



The AP catalyzes an enzymatic reaction which, given the right substrate, results in a dark purple precipitate. This precipitate indicates the expression site of the targeted mRNA.

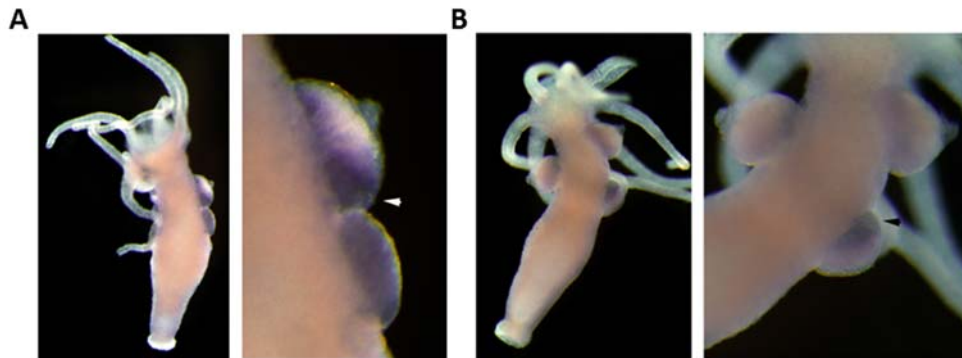


**Figure 7-5: *HySycp1* (A) and *HySycp3* (B) mRNAs are specifically synthesized in the basal testis layer.** In whole mount *in situ* hybridization with Dig-labeled RNA probes against *HySycp1* (1-1,012 bp) and *HySycp3* (714 bp), the basal layer of the testes is stained specifically (see arrowheads). The figure is adapted from Fraune *et al.* 2012b.

In **Figure 7-5**, one can clearly see the purple staining of the basal layer of the testes where the mRNAs of *HySycp1* (A) and *HySycp3* (B) are expressed. Because spermatocytes, which undergo the first meiotic division, are located in this region of the testis (Kuznetsov *et al.* 2001), a potential function of the proteins in early meiosis and the formation of the SC became more likely after this experiment.

To analyze the expression of HySYCP1 and HySYCP3 on the protein level, antibodies<sup>33</sup> had to be raised which would recognize the proteins in Western blot and immunofluorescence analysis. Different antigenic polypeptides from HySYCP1 and HySYCP3 were expressed from beforehand cloned pET21a plasmids<sup>34</sup> and purified via an attached HIS-tag<sup>35</sup>. The purified protein samples were used for immunization of a rabbit and/or a guinea-pig whose final bleedings were affinity-purified before use.

In a first attempt, the specificity of the antibodies and the expression of the HySYCP1 and HySYCP3 were analyzed in a Western blot<sup>36</sup>. Again, heads, mid-pieces, feet and testes of approximately 60 animals were prepared and collected in four different tubes. Excess *Hydra* medium was discarded and the tissues were dissolved in about 50-60  $\mu$ l 2x SDS sample buffer each. Equal amounts of the proteins in every tissue fraction were then separated in an 8% SDS-Page for the detection of HySYCP1 or a 12% SDS-Page for the detection of HySYCP3 and afterwards transferred to the nitrocellulose membrane by blotting for 1 h. The membranes were saturated with 10% milk and incubated with the primary antibodies. Antibody detection occurred via

<sup>33</sup> For a list of the generated polyclonal antibodies see **Table 12-1** and for the protocol of generating specific antibodies see on page 91.

<sup>34</sup> For the protocol of DNA cloning, see on page 83. A list of all recombinant DNA constructs, which were cloned for this matter, is supplied in on page 73.

<sup>35</sup> For the protocol of protein expression and purification see on page 88.

<sup>36</sup> For the protocol of the Western blot analysis see on page 86.

peroxidase (HRP)-coupled secondary antibodies<sup>37</sup> and a chemiluminescent light reaction. Subsequently, the blot was stripped<sup>38</sup> to prepare it for another immunoreaction with an  $\alpha$ -actin antibody. Detection of actin was performed to confirm the loading of the protein samples in each lane of the protein gel.

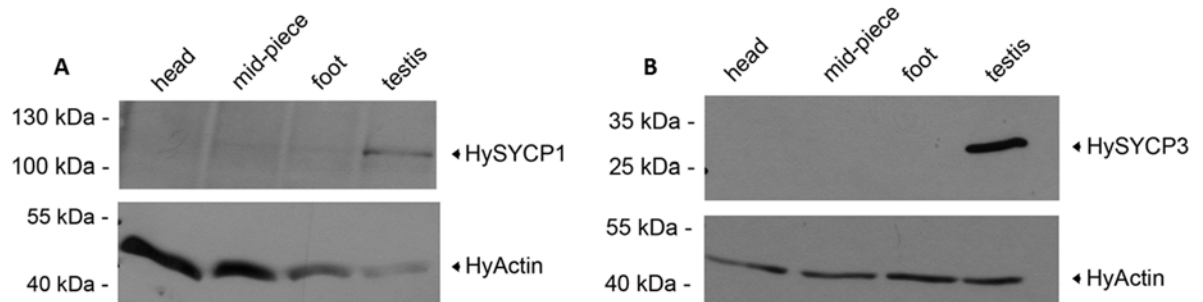


**Figure 7-6: Testis-specific expression of HySYCP1 (A) and HySYCP3 (B) on the protein level.** In Western blot analysis, the rabbit  $\alpha$ -HySYCP1 (C-Term) antibody (1:10,000) and the guinea-pig  $\alpha$ -HymSYCP3 (1:1,000) recognize their target proteins in the testis lane, exclusively. The respective protein bands of HySYCP1 and HySYCP3 reveal the expected molecular mass of 118 kDa and 27 kDa, respectively. No signal can be detected in the head, the mid-piece or the foot. The detection of HyActin is used as loading control for each lane of the protein gel.

According to the Western blot analysis (**Figure 7-6**), not only the mRNAs but also the proteins HySYCP1 (A) and HySYCP3 (B) are present in the testis tissue. Distinct signals with the predicted molecular mass of 118 kDa (HySYCP1) and 27 kDa (HySYCP3) can be seen in the testis lane exclusively in blot A and B indicating specific antibody reactions.

Additionally, the antibodies were tested in immunofluorescence analysis to also examine the localization of their target proteins on a cellular level. Cryosections of *Hydra* mid-pieces were prepared and incubated with the  $\alpha$ -HySYCP1 and  $\alpha$ -HymSYCP3 antibodies<sup>39</sup> according to the protocol on page 99.

<sup>37</sup> For dilution of the primary antibodies in Western Blot analysis see **Table 12-1**. For dilution of the secondary antibodies see **Table 12-2**.

<sup>38</sup> For the protocol of stripping the nitrocellulose membranes see on page 88.

<sup>39</sup> For the dilution of the primary antibodies in immunofluorescence analysis see **Table 12-1**.

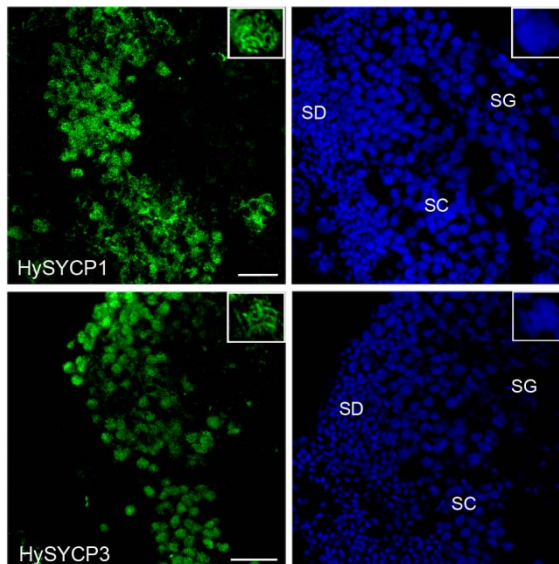


**Figure 7-7: Immunostaining of HySYCP1 and HySYCP3 on testis cryosections.** On cryosections of *Hydra* testes the rabbit  $\alpha$ -HySYCP1 (C-Term) antibody (1:600) and the guinea-pig  $\alpha$ -HymSYCP3 (1:150) stain thread-like structures in spermatocytes (SC) but not in spermatogonia (SG) or spermatids (SD). In higher magnification (Insets), the threads can be identified as synaptonemal complexes. The figure is adopted from Fraune *et al.* 2012a.

In the confocal laser scanning microscope, one can see that the antibodies stain thread-like structures in the nuclei of *Hydra* spermatocytes (**Figure 7-7**). Neither spermatogonia nor spermatids show similar fluorescently labeled protein structures which is again an indication for the specificity of the antibodies. Beyond, the immunohistochemistry on cryosections shows that indeed the target proteins HySYCP1 and HySYCP3 are components of a chromosomal structure which highly resembles the SC and which assembles at the expected stage of meiosis in spermatocytes. This strongly suggests that HySYCP1 and HySYCP3 are part of a cnidarian SC, maybe fulfilling similar functions to the mammalian SYCP1 and SYCP3.

In order to verify the idea of HySYCP1 and HySYCP3 being likewise *bona fide* structural components of the *Hydra* SC, chromosome spreads ought to be prepared in which the SCs are highly accessible for the antibodies. Therefore, a protocol for dry-down spread preparations of mouse spermatocytes was adapted to the *Hydra* tissue. Immunofluorescence analysis on these chromosome spreads<sup>40</sup> was intended for the higher resolution of the cnidarian SC structure and the localization of HySYCP1 and HySYCP3 within the SC (**Figure 7-8**).

<sup>40</sup> For the protocol of *Hydra* chromosome spread preparations and the following immunofluorescence analysis see on page 100. For the dilution of the primary antibody in immunofluorescence analysis see **Table 12-1**.

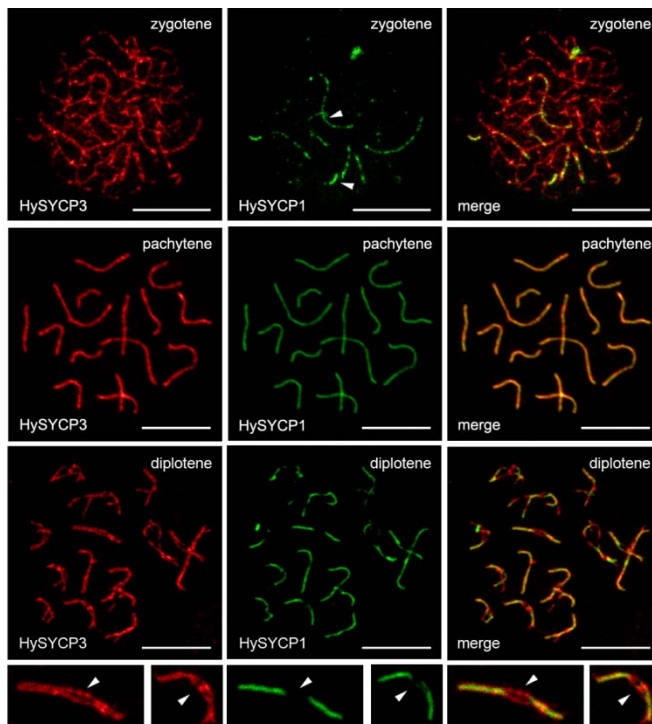


**Figure 7-8: Immunostaining of HySYCP1 and HySYCP3 on chromosome spread preparations.** On chromosome spreads of *Hydra* testes the rabbit  $\alpha$ -HySYCP1 (C-Term) antibody (1:900) and the guinea-pig  $\alpha$ -HymSYCP3 (1:150) antibody stain the 15 SCs of pachytene spermatocytes. In accordance to their mammalian orthologues, HySYCP3 localizes to the chromosome axes while HySYCP1 is restricted to the few sites of synapsis in zygotene. In diplotene, the axes, marked by HySYCP3, begin to separate and HySYCP1 dissociates from these sites. In a higher magnification, HySYCP1 can be seen to localize between the parallel running axes of the bivalents (HySYCP3). Scale bar, 10  $\mu$ m. The figure is adopted from Fraune *et al.* 2012a.

In a co-localization experiment with antibodies against HySYCP3 and HySYCP1 (**Figure 7-8**), it can be seen that both proteins are part of thread-like SCs in *Hydra* pachytene spermatocytes. The counted number of 15 SCs in the nucleus correlates with the information that *Hydra* has 30 chromosomes and therefore 15 synapsed bivalents in meiosis (Zacharias *et al.* 2004; Anokhin *et al.* 2010). Moreover, comparing the localization of HySYCP3 and HySYCP1 in other stages of prophase I, such as zygotene and diplotene, with information about the localization of mammalian SYCP3 and SYCP1 one can detect a highly similar pattern. As presented in the introduction in more detail, the SC assembly begins in leptotene with the polymerization of SYCP3 to form defined AEs. In zygotene, these AEs/LEs are consecutively connected by SYCP1 dimers which build the TFs. In pachytene, the chromosomes are fully synapsed and both proteins, SYCP1 and SYCP3, seem to completely co-localize in the confocal laser scanning microscope. Finally in diplotene, the SC disassembles and SYCP1 more and more dissociates from the LEs. The same dynamic localization pattern of HySYCP1 and HySYCP3 can be seen in the spread spermatocytes of *Hydra* in **Figure 7-8**. In zygotene, HySYCP3 is present along the chromosomal axes which are already synapsed by TFs at some sites. These sites are denoted by HySYCP1 which apparently co-localizes with few HySYCP3 signals (see arrowheads in the top row). In pachytene, the localization of the proteins overlaps completely while in diplotene HySYCP1 is lost where the LEs are disconnected and start to separate again into two distinct axes (see arrowheads in bottom row). The magnifications of certain SCs during diplotene in the bottom row of **Figure 7-8** illustrate the localization of the remaining HySYCP1 between the two parallel running axes (HySYCP3) of the respective bivalent.

## Discussion

The phylogenetic analysis, which was performed to find homologues of the mammalian SYCP1 and SYCP3, resulted in the identification of various putative orthologous sequences from several vertebrate but also invertebrate species (see also **Supplementary Table 1** and **Supplementary Table 2**). Thus, species variety in the phylogenetic trees ranges from human to sponges (**Figure 7-1**). Orthologues of SYCP1 could be detected in all vertebrate classes, in *Tunicata* (ascidian) and *Brachiostoma floridae* (Amphioxus) as a representative of the *Cephalochordata*, as well as in species from *Echinodermata* (sea urchin), *Annelida* (*Alvinella*, *Capitella*), *Mollusca* (oyster), *Cnidaria/Ctenophora* (*Hydra*, *Nematostella/Pleurobrachia*) and *Porifera* (*Amphimedon*). Furthermore, two sequences were found originating from crabs (belonging to *Crustacea*) as sole representative of *Ecdysozoa*. These, however, show an exceptionally large evolutionary distance as it is indicated by their long branches. Apart from this, the proteins cluster together in the phylogenetic tree which roughly recovers metazoan phylogeny (Philippe *et al.* 2009; see also reference tree in **Figure 6-1**). This points to their potential common origin. Likewise, SYCP3 orthologues were found in *Chordata* (vertebrates, *Tunicata* and *Cephalochordata*), *Echinodermata* (sea urchin), *Annelida* (*Alvinella*, *Eulalia*), *Mollusca* (limpet), *Cnidaria/Ctenophora* (*Hydra*, *Nematostella/Mnemiopsis*), *Porifera* (*Amphimedon*) and also *Trichoplax* (*Placozoa*). The resultant phylogenetic tree displays the supposed common origin of these proteins as well. However in this case, no orthologues were identified in the clade of *Ecdysozoa*, such as *Nematoda*, and *Insecta* and *Crustacea* (two subphyla of *Arthropoda*) which mainly compose this clade (Aguinaldo *et al.* 1997). This is interesting because sequences were gathered from the earliest branching metazoan clades (*Porifera*, *Placozoa*, *Cnidaria* and *Ctenophora*), a fact that actually points to an origin of SYCP1 and SYCP3 at the time of metazoan emergence. Against this background, the lack of SYCP3 orthologues in *Ecdysozoa* could be interpreted by two different hypotheses. Either the protein got lost during the divergence of the ecdysozoan lineage or the protein diversified beyond recognition because of a very fast evolutionary rate in the ecdysozoan phyla. Considering the existence of very distantly related SYCP1 sequences in ancient arthropods, the second hypothesis seems to be more likely.

In conclusion, this means that SYCP1 and SYCP3 form monophyletic groups sharing common origins at the point of metazoan divergence over 500 million years ago. Interestingly however, an evolutionary relation to proteins from the large phyla of *Nematoda* and *Insecta* is not recognizable. If one assumes that SYCP1 and SYCP3 were functional parts of the SC *ab initio* and therewith that the SC arose only once in metazoan evolution, a potential scenario would be that these proteins have massively diversified in these phyla and therewith in *Drosophila* and *C. elegans* but still are components of the respective SCs.

Though, this way of interpreting the phylogeny of SYCP1 and SYCP3 is founded on the assumption that the SC protein composition is ancient in *Metazoa* as well. The opposing hypothesis would be that the SC emerged independently in different taxa by recruiting other ancient and preexisting proteins. To distinguish between these two possibilities, the experimental charac-

terization of HySYCP1 and HySYCP3 from *Hydra vulgaris AEP* - one of the most basal metazoan species - was performed. This characterization demonstrates the meiosis-specific expression of the proteins (**Figure 7-4**, **Figure 7-5**, and **Figure 7-6**) and their involvement in the formation of a cnidarian SC. Additionally, the immunofluorescence analysis on chromosome spreads (**Figure 7-8**) illustrates the probable homologous functions of HySYCP3 and HySYCP1 within the complex compared to their mammalian counterparts. HySYCP3 is, equally to the mouse SYCP3, a component of the LEs shaping the chromosomal axes from zygotene until diplotene. HySYCP1 is most likely the protein component of the TFs because a) its localization is restricted to synapsed regions in zygotene and diplotene, b) it localizes in the CR between the parallel axes of the bivalents in diplotene and c) it resembles the prototypic TF protein in size and secondary domain organization by being a large protein with a central, extended coiled coil region.

Polymerization studies in the heterologous system, which were performed in the context of a master thesis by Miriam Wiesner (Wiesner 2013), also support the hypothesis of a functional homology between the mammalian and the cnidarian SC proteins. Especially for HySYCP3, she could verify its ability to interact with rat SYCP3. Co-transfected into COS-7 cells, HySYCP3 is recruited into the filamentous network of the mammalian protein (**Figure 7-9**, C).

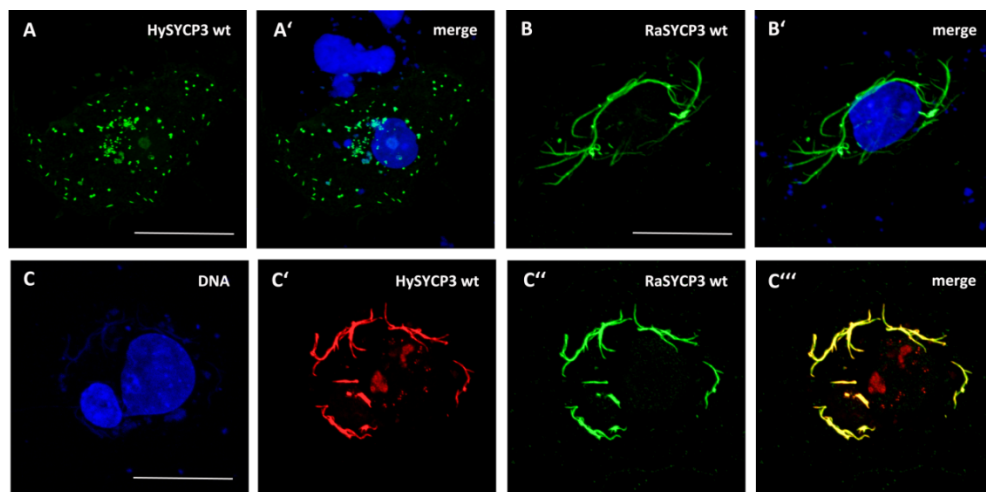


**Figure 7-9: Ex vivo co-assembly of HySYCP3 and rat SYCP3.** Transfected into COS-7 cells, HySYCP3 forms small aggregates (A), while rat SYCP3 can assemble into a cytoplasmic network of higher order filaments (B). However in the case of a co-expression of HySYCP3 and rat SYCP3, HySYCP3 is recruited into the network formed by the rat protein (C). Scale bar, 20  $\mu$ m. The figures is adopted from Wiesner 2013 and Fraune *et al.* 2014.

This co-assembly points to similar structural properties between the SYCP3 orthologues which have been conserved despite of a time period of more than 500 million years since their divergence. This was already reported for medaka SYCP3 and rat SYCP3 (Baier *et al.* 2007a). Most likely, the central region of 146 aa containing CM1, CM2 and the coiled coil region, is the functional mediator of this SYCP3 polymerization and therefore was preserved in evolution (Baier *et al.* 2007b).

Thus, this is the first study illustrating the monophyly of SC components in *Metazoa*. It shows that not only the proteins SYCP1 and SYCP3 themselves but also their involvement in the SC

---

composition is ancient in animals because the SC in *Hydra* contains at least two proteins which are orthologous to these murine SC proteins.

## 8 Chapter II: The evolution of the central element components of the murine SC

According to Fraune *et al.* 2013

### Introduction

In the previous work of chapter I, it could be shown that the murine SYCP1 and SYCP3 are ancient in *Metazoa*. Their emergence was traced to the earliest branching metazoans *Porifera*, *Placozoa* and *Coelenterata* (*Cnidaria* and *Ctenophora*) suggesting that the proteins are as old as metazoans themselves (Fraune *et al.* 2012b). Furthermore, it was concluded that their involvement in the SC protein composition is ancient in animals as well. However, only two out of seven characterized components were analyzed - a fact that does not allow further conclusions, especially regarding the questions a) how did the SC evolve during metazoan diversification as a whole? and b) what was its ancestral structure and function? Therefore, the other mouse SC components had to be examined in order to answer these questions.

Thus this chapter focuses on the evolution of the CE components and their expression in the early branching cnidarian *Hydra*, if present. Together with SYCP3 and SYCP1, all major SC domains - LEs, TFs and CE - would then be considered.

### Results

The second part of the study was organized in analogy to the first part in chapter I. Again, homologues of each murine CE component, which are SYCE1, SYCE2, SYCE3 and Tex12, had to be identified in a broad phylogenetic search. Their potential role in SC formation should be confirmed in a basal metazoan species, e.g. *Hydra*, by an expression analysis on the mRNA and protein level.

### Phylogeny of SYCE1, SYCE2, SYCE3 and Tex12

Using BLASTp and tBLASTn to query several different databases, starting with the full-length mouse CE proteins SYCE1, SYCE2, SYCE3 and Tex12 and ending with specific HMM profiles<sup>41</sup>, revealed that SYCE1, SYCE2 and Tex12 are ancient in animals. SYCE3, instead, was found to be restricted to the vertebrate lineage.

---

<sup>41</sup> For a list of the used databases see **Table 12-4** and for the protocol of the dataset assembly see on page 103. The RefSeq No. on NCBI of SYCE1, SYCE2, SYCE3 and Tex12 are NP\_001137237, NP\_082230, NP\_001156352 and NP\_079963.



In more detail, orthologues of SYCE1, SYCE2 and Tex12 could be identified in nearly all bilaterian lineages which include the invertebrate phyla *Lophotrochozoa* (*Annelida* and *Mollusca*, belonging to *Protostomia*) and *Echinodermata* (belonging to *Deuterostomia*) as well as *Chordata* which encompasses *Cephalochordata* and vertebrates. It is worth mentioning that an orthologue of SYCE1 could not be detected in any bird species. A simple explanation could be the lack of sufficient sequence data for birds. However, as orthologues of the other three CE components were found in birds, it could be the result of a true loss or massive divergence of SYCE1 in this class as well. Notably, also cnidarian sequences from *Nematostella* and/or *Hydra* showed up in the analysis which displayed considerable homologies to SYCE2 and Tex12. An orthologue of SYCE1 could not be detected in any *Cnidaria* species. The database query with SYCE3 did not produce significant hits in invertebrate species at all but only in vertebrate species (see also **Supplementary Table 3**, **Supplementary Table 4**, **Supplementary Table 5**, and **Supplementary Table 6**).

The multiple alignments of the murine CE proteins and their respective orthologues identified the central regions to be the most conserved parts. This is from aa 59-153 of the mouse protein for SYCE2<sup>42</sup> and from aa 61-121 for Tex12<sup>43</sup>. SYCE1 includes a large conserved region which comprises most of the coiled coil region from aa 58-268 in the mouse. The SYCE3 orthologues, as SYCE3 is very small, exhibit conservation across nearly 100% of the protein which is from aa 1 to aa 86 in the mouse (see also **Supplementary Figure 1**, **Supplementary Figure 2**, **Supplementary Figure 3**, and **Supplementary Figure 4**).

Phylogenetic trees were reconstructed for each component based on these conserved domains (**Figure 8-1**) using Maximum likelihood and Bayesian Inference.<sup>44</sup>

---

<sup>42</sup> In human SYCE2, the conserved region is from aa 67 to aa 161.

<sup>43</sup> In human Tex12, the conserved region is from aa 61 to aa 123.

<sup>44</sup> For the protocol of generating multiple alignments see on page 104. For the protocol of phylogenetic tree reconstruction see on page 105. And for a list of the respective computer programs and online services see **Table 12-4**.

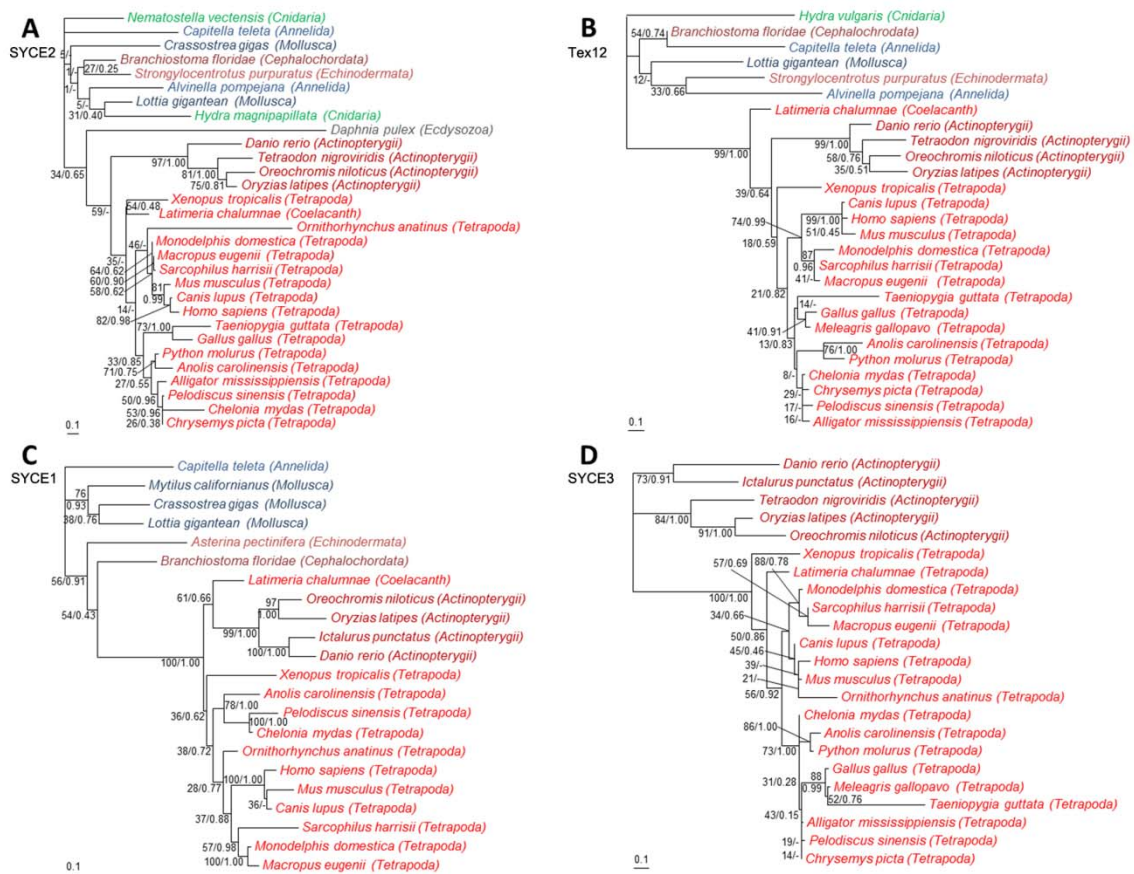


**Figure 8-1: Phylogeny of SYCE2 (A), Tex12 (B), SYCE1 (C) and SYCE3 (D).** Unrooted maximum likelihood trees were calculated from the multiple alignments of (A) 30 sequences and 75 kept amino acid positions for SYCE2, **Supplementary Figure 1**, (B) 27 sequences and 59 kept amino acid positions for Tex12, **Supplementary Figure 2**, (C) 22 sequences and 150 kept amino acid positions for SYCE1, **Supplementary Figure 3**, and (D) 23 sequences and 81 kept amino acid positions for SYCE3, **Supplementary Figure 4**. Branch robustness is indicated by bootstrap values (given in percentage) and posterior probabilities (given in fractions) calculated with PhyML and MrBayes (e.g. 50/0.5). A dash indicates that the respective branch of the maximum likelihood tree is not recovered in the consensus Bayesian tree (e.g. 50/-). The bars display the average number of substitutions per site. Color code of species: *Cnidaria* are shown in green, *Lophotrochozoa* are shown in blue, *Ecdysozoa* are shown in gray, *Deuterostomia* are shown in red. Different shades of the respective colors are used to distinguish between different sublineages. The dataset assembly and the computational tree calculation was supported and confirmed by Céline Brochier-Armanet. The figure is adopted from Fraune *et al.* 2013.

In a more general view, the phylogenies of SYCE2 (A), Tex12 (B) and SYCE1 (C) recover the phylogeny of metazoan species (Philippe *et al.* 2009; see also reference tree in **Figure 6-1**). In detail, however, the deepest nodes of the SYCE2 and Tex12 trees (**Figure 8-1**, A and B), which lead to the invertebrate species, are not resolved very well. This is documented by low bootstrap values (BV) and low Bayesian posterior probabilities (PP) of mostly less than (BV) 50 or (PP) 0.5. Probably, the low statistical support is due to the relatively small number of sites that were kept for the phylogenetic analyses<sup>45</sup> and large evolutionary distances between some orthologues, as indicated by the long branches that are associated with few invertebrate species, e.g. *Alvinella* and *Capitella* in **Figure 8-1**, B. Yet the global separation of invertebrates and

<sup>45</sup> Sites from the alignments which were kept for tree reconstruction are indicated in red in the supplementary figures.

vertebrates (**Figure 8-1**, A: BV = 59; B: BV = 99) as well as the resolution within the vertebrates is confirmed by sufficient statistical support in the majority of the nodes. The phylogeny of SYCE1 (**Figure 8-1**, C), instead, remains consistent with the phylogeny of animals even in a closer examination. In this case, more positions could be kept for the analysis, resulting in a robust resolution and nodes with higher statistical support. The phylogeny of SYCE3 is broadly consistent with the phylogeny of vertebrates pointing to the more recent and lineage specific origin of this protein (**Figure 8-1**, D).

Interestingly, and in agreement with the previous study (see chapter I), the almost absolute absence of any ecdysozoan species in the phylogeny of SYCE1, SYCE2, SYCE3 and Tex12 is striking. Again, only one sequence was found in a crustacean species - *Daphnia pulex* - that reveals some homology to SYCE2. However, in the phylogeny it appears to be associated with a very long branch which again is very similar to the situation of the crab SYCP1 sequence and points to a high evolutionary rate and a large sequence divergence during diversification of *Arthropoda*.

For the sake of completeness, the search of homologues was repeated using the only alternative characterized CE/CR proteins of *Drosophila* and *C. elegans* as seeds as well to query the available databases. Neither CONA of *Drosophila melanogaster*<sup>46</sup> nor *C. elegans* SYP-2, SYP-3 and SYP-4<sup>47</sup> yielded orthologues outside their respective genus of *Drosophila* or *Caenorhabditis*. So again, it failed to reveal a homology between SC proteins of mammals, flies and nematodes.

### **Expression of HySYCE2 and HyTex12 in *Hydra vulgaris* AEP**

Orthologues of SYCE2 and Tex12, as of SYCP1 and SYCP3 in chapter I, could be identified in the basal metazoan *Hydra*. Yet their function in the formation of a cnidarian SC had to be demonstrated.

Thus, the found database sequences of *Hydra Syce2* and *Hydra Tex12*<sup>48</sup> were used to query the *Hydra vulgaris* AEP transcriptome data on the Compagen server (Hemrich *et al.* 2012). The respective proteins of *Hydra vulgaris* AEP match with 98% (HySYCE2) and 99% (HyTex12) sequence identity. According to this mRNA information, primers were designed to clone and sequence the complete cDNA of *HySyce2* and *HyTex12* from *Hydra vulgaris* AEP.<sup>49</sup> The obtained sequences matched 100% with the information from the Compagen database and were submitted to GenBank on NCBI.<sup>50</sup>

---

<sup>46</sup> The RefSeq of CONA on NCBI is NP\_650719.

<sup>47</sup> The RefSeq of the SYP proteins on NCBI are NP\_504462, NP\_492345 and NP\_491960.

<sup>48</sup> For accession numbers and further information on the detected orthologues see **Supplementary Table 3** and **Supplementary Table 4**.

<sup>49</sup> *HySyce2* and *HyTex12* primer sequences are given in **Table 12-3**. For the protocol of cDNA cloning and sequencing see on pages 81 and 83.

<sup>50</sup> The GenBank accession No. of *HySyce2* and *HyTex12* of *H. vulgaris* AEP are KC580661 and KC580662.

On the mRNA level, the expression of *HySyce2* and *HyTex12* were tested via RT-PCR and *in situ* hybridization. For RT-PCR, again, mRNA of four different tissue fractions – head, mid-piece, foot, and testis – was reversely transcribed into cDNA, which in turn was used as template for the specific amplification of the full-length cDNA of *HySyce2* and *HyTex12* (Figure 8-2, A and B). For *in situ* hybridization, Dig-labeled RNA probes were generated against the full-length cDNA of *HySyce2* with 459 bp and *HyTex12* with 336 bp and hybridized to whole animals (Figure 8-2, C and D).<sup>51</sup>

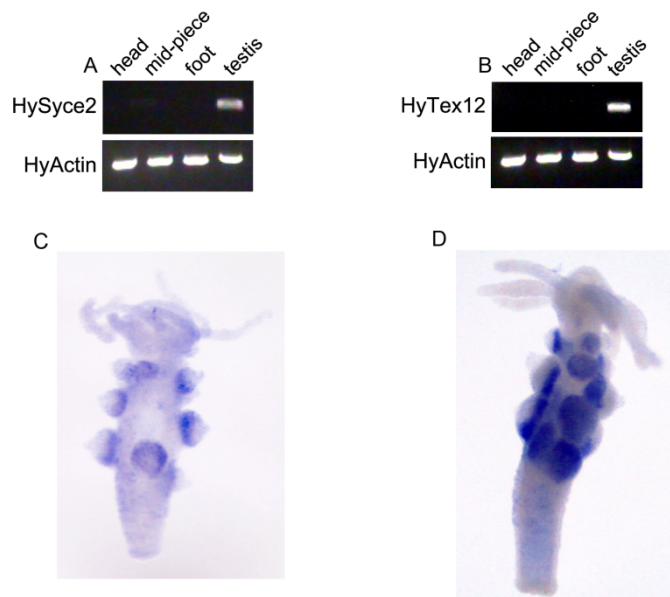


**Figure 8-2: Testis-specific expression of *HySyce2* (A, C) and *HyTex12* (B, D) on the mRNA level.** In RT-PCR, mRNAs of *HySyce2* (A) and *HyTex12* (B) are specifically amplified in the testis fraction. Faint signals in the mid-piece fraction result from contamination with left-overs of the previously associated testis tissue. Amplification of *HyActin* demonstrates the equal concentration of mRNA in the different fractions. By whole mount *in situ* hybridization with Dig-labeled RNA probes against full-length mRNA of *HySyce2* (C) and *HyTex12* (D), the synthesis of the respective mRNAs can be localized to the basal testis layer where spermatocytes are found by the dark purple staining. The figure is adopted from Fraune *et al.* 2013.

In Figure 8-2 A and B, one can see the testis specific synthesis of *HySyce2* and *HyTex12* mRNA. Faint bands can also be detected in the mid-piece fraction where left-overs of the previous associated testes remained at the body column. *HyActin* was amplified from the same cDNA probes to demonstrate the equal concentration of cDNA in all fractions. Image C and D of Figure 8-2 display the results from the *in situ* hybridization which point to an expression of both mRNAs in the testes of *Hydra*. Clearly, one can see the purple staining of the testis base which is where spermatocytes are localized (Kuznetsov *et al.* 2001).

In a next step, antibodies had to be generated against HySYCE2 and HyTex12.<sup>52</sup> Full-length cDNAs were cloned into pET21a plasmids.<sup>53</sup> These plasmids were used for expression of Hy-

<sup>51</sup> For protocol of the RT-PCR see on page 79. For the ISH protocol see on page 95. *HySyce2* and *HyTex12* primer sequences for RT-PCR and RNA probe synthesis are given in Table 12-3.

<sup>52</sup> For a list of the generated polyclonal antibodies see Table 12-1 and for the protocol of generating specific antibodies see on page 91.

SYCE2-6xHIS and HyTex12-6xHIS in *E. coli* Rosetta bacteria.<sup>54</sup> The purified proteins were sent out for immunization of a rabbit and guinea-pig. The final bleedings of the  $\alpha$ -HySYCE2 antibodies were affinity-purified before use while the final sera were functioning appropriately in the case of the  $\alpha$ -HyTex12 antibodies.

The antibodies were then tested in Western blot analysis<sup>55</sup>, initially. As for the RT-PCR, heads, mid-pieces, feet and testes of approximately 60 animals were collected in tubes and afterwards dissolved in ca. 50  $\mu$ l 2x SDS sample buffer. The probes were loaded onto 15 % SDS protein gels and transferred to nitrocellulose membranes by blotting for 40 min after electrophoresis. The membranes were saturated with 10% milk in TBST before incubation with the primary antibodies. Detection of the bound primary antibody occurred via a peroxidase-coupled secondary antibody and the chemiluminescent light reaction in the dark chamber.<sup>56</sup>

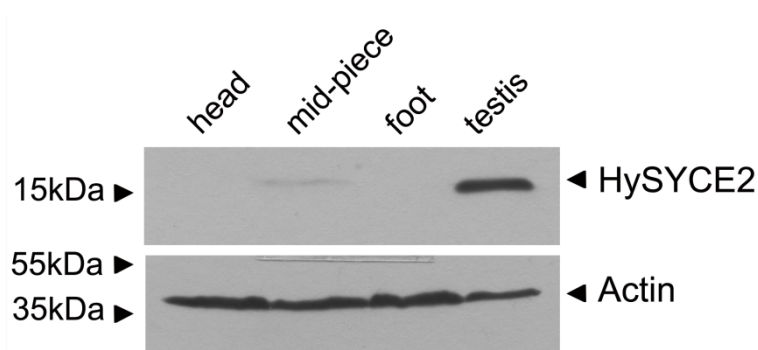


**Figure 8-3: Testis-specific expression of HySYCE2 on the protein level.** In Western blot analysis, the rabbit  $\alpha$ -HySYCE2 antibody (1:2,000) recognizes its target protein in the testis lane. The respective protein band of HySYCE2 reveals the expected molecular mass of 17.6 kDa. A faint signal can be detected in the mid-piece lane. The detection of HyActin is used as loading control for each lane of the protein gel. The figure is adopted from Fraune *et al.* 2013.

The  $\alpha$ -HySYCE2 antibody functioned in the blot analysis as expected. A distinct band can be seen in the testis fraction revealing the predicted molecular mass of HySYCE2 of approximately 17.6 kDa (**Figure 8-3**). The faint band in the mid-piece fraction results from testis contamination as in the RT-PCR analysis. Unexpectedly, the  $\alpha$ -HyTex12 antibody did not function in Western Blot analysis. No specific band of the expected molecular mass of 12.6 kDa, which would indicate the presence of HyTex12, could be detected in the testes. Instead, strong background signals and many probably unspecific bands were generated being most prominent in the head lane.

<sup>53</sup> For the protocol of DNA cloning see on page 83 and for list of recombinant DNA constructs see on page 73.

<sup>54</sup> For the protocol of the protein expression and purification see on page 88.

<sup>55</sup> For the protocol of the Western blot analysis see on page 86.

<sup>56</sup> For the dilution of the primary antibodies in Western blot analysis see **Table 12-1**. For the dilution of the secondary antibodies see **Table 12-2**.

Nevertheless, both antibodies were tested in immunofluorescence analysis<sup>57</sup> as well. On chromosome spreads, not only the  $\alpha$ -HySYCE2 antibody but also the  $\alpha$ -HyTex12 antibody recognized the 15 thread-like structures in the *Hydra* pachytene spermatocytes that are characteristic for SCs (**Figure 8-4**). Co-localization with HySYCP1 shows that HySYCE2 (A) and HyTex12 (C) overlap with the TF protein in pachytene. But they localize in a more punctate pattern compared to the rather continuous staining of HySYCP1. In contrast, a co-staining of HySYCE2 (B) and HyTex12 (D) with HySYCP3 in diplotene cells demonstrates that the proteins only co-localize at synapsed regions of the axes. At sites where the LEs dissociate from each other, neither HySYCE2 nor HyTex12 can be detected anymore (B and D, insets). The last panel of **Figure 8-4** (E) shows the double staining of HySYCE2 and HyTex12 in a pachytene spermatocyte. Their localizations match across large parts of the SCs and, once more, display a punctate rather than continuous pattern.

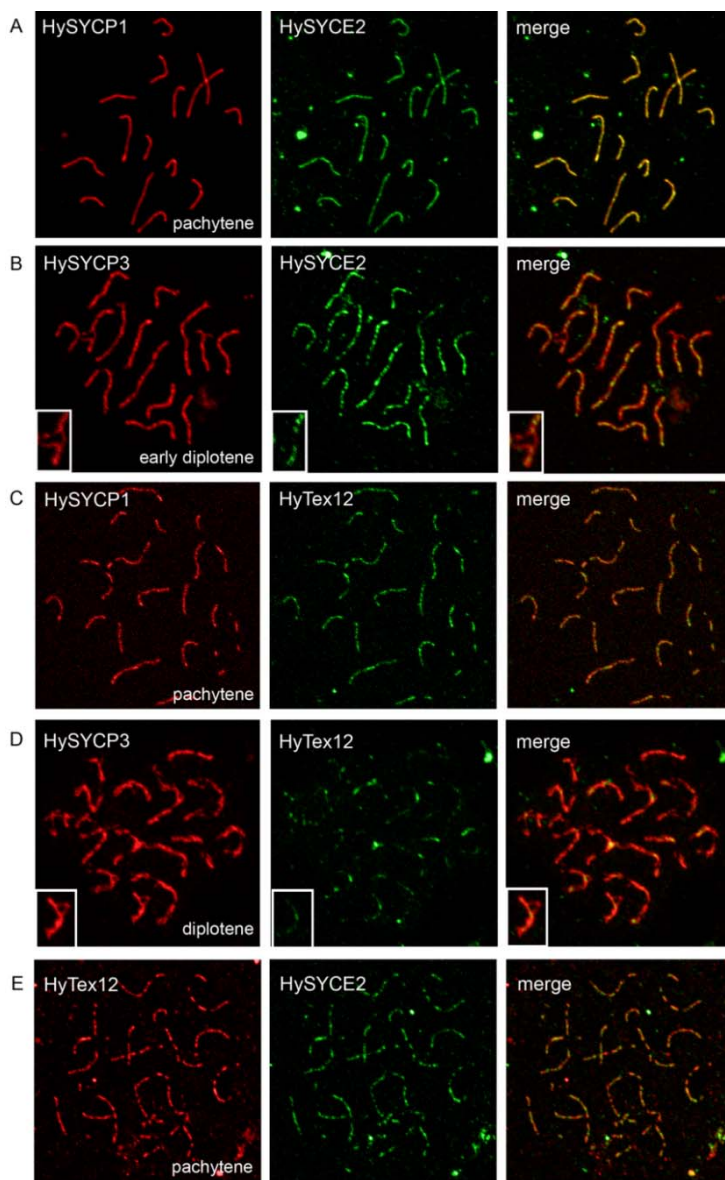


**Figure 8-4: Immunostaining of HySYCE2 and HyTex12 on chromosome spread preparations.** On chromosome spreads of *Hydra* testes the guinea-pig  $\alpha$ -HySYCE2 antibody (1:200) and the rabbit and guinea-pig  $\alpha$ -HyTex12 (1:300) antibodies stain the 15 SCs of pachytene spermatocytes. In a co-staining of (A) HySYCE2 (gp  $\alpha$ -HySYCE2) with HySYCP1 (rb  $\alpha$ -HySYCP1) and (C) HyTex12 (rb  $\alpha$ -HyTex12) with HySYCP1 (gp  $\alpha$ -HySYCP1), the proteins appear to have an overlapping localization with the TF protein in pachytene cells. In a co-staining of (B) HySYCE2 (gp  $\alpha$ -HySYCE2) with HySYCP3 (rb  $\alpha$ -HySYCP3) and (D) HyTex12 (gp  $\alpha$ -HyTex12) with HySYCP3 (rb  $\alpha$ -HySYCP3), however, co-localization of the proteins with the LEs is restricted to synapsed regions in diplotene spermatocytes. This can be seen clearly in the higher magnification of image (B) and (D). Co-staining of (E) HySYCE2 (gp  $\alpha$ -HySYCE2) and HyTex12 (rb  $\alpha$ -HyTex12) reveals the punctate pattern of both proteins. The figure is adopted from Fraune *et al.* 2013.

<sup>57</sup> For the protocol of immunofluorescence analysis on chromosome spreads see on page 100 and for appropriate dilution of the primary antibodies see **Table 12-1**.

### Interaction of HySYCE2 and HyTex12 *ex vivo*

Because an interaction of the murine SYCE2 and Tex12 was shown by Hamer *et al.* (2006), an ability to interact was likewise suspected for the cnidarian orthologues. The *ex vivo* expression of meiotic proteins in heterologous systems is a sophisticated way to get first indications regarding their potential polymerization and interaction properties. To test a co-assembly of HySYCE2 and HyTex12, their respective cDNAs were cloned into eukaryotic expression plasmids in a first step.<sup>58</sup> The plasmids were transfected into COS-7 cells and after 24 h, the cells were fixed and prepared for immunofluorescence analysis.<sup>59</sup> The wild-type HySYCE2 was detected by the rabbit  $\alpha$ -HySYCE2 antibody, while HyTex12 was expressed with an N-terminal myc tag and could be detected using an  $\alpha$ -myc antibody.<sup>60</sup>

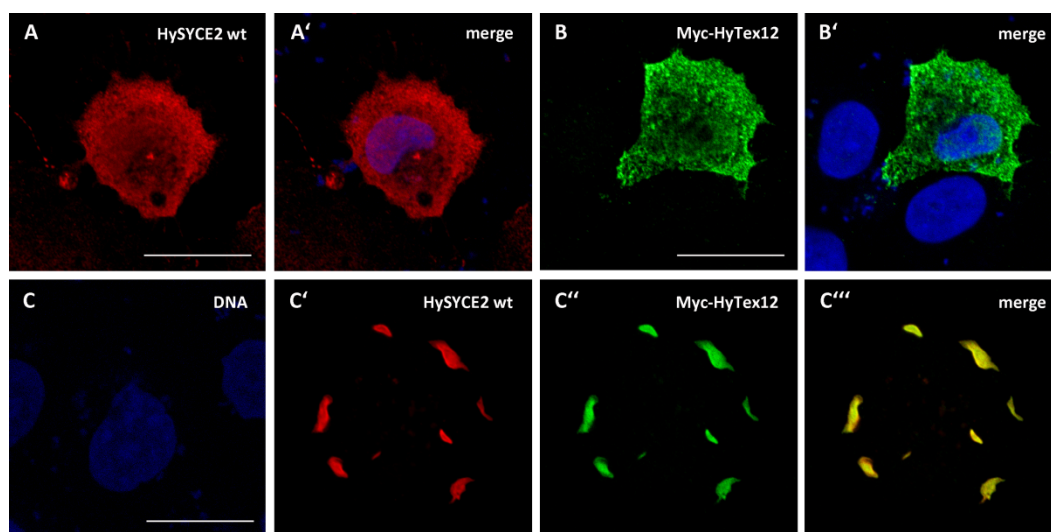


**Figure 8-5: Co-assembly of HySYCE2 and HyTex12 in the heterologous system.** Individually transfected into COS-7 cells, (A) wild-type HySYCE2 (B) myc-HyTex12 are evenly distributed in the cytoplasm. (C) Co-transfection, however, leads to aggregation of the proteins and a co-assembly to needle-like structures that indicate their ability to interact with each other. Scale bar, 20  $\mu$ m. The figure is adopted from Fraune *et al.* 2014.

In **Figure 8-5** one can see that, individually expressed, HySYCE2 (A) and HyTex12 (B) are evenly distributed in the cytoplasm of COS-7 cells. However, co-expression leads to the formation of elongated aggregates which include both proteins (C). This behavior suggests that HySYCE2 and HyTex12, indeed, possess the properties to interact with each other.

## Discussion

The picture that emerges from the phylogenetic analysis of the CE proteins SYCE1, SYCE2, SYCE3 and Tex12 is quite interesting. The collection of orthologues for SYCE1, SYCE2 and Tex12

<sup>58</sup> For a list of recombinant DNA constructs which were cloned for this purpose see on page 73 and for the protocol of DNA cloning see on page 83.

<sup>59</sup> For the protocol of cell transfection see on page 94. For the protocol of immunofluorescence analysis on cells see on page 102.

<sup>60</sup> For dilution of the respective primary antibodies in immunofluorescence analysis see **Table 12-1**.

(see also **Supplementary Table 3**, **Supplementary Table 4** and **Supplementary Table 5**) and the global recovery of metazoan phylogeny by their respective phylogenetic trees (**Figure 8-1**) suggest the following: SYCE1 emerged in the last common ancestor of *Bilateria* which encompasses *Protostomia* and *Deuterostomia* while SYCE2 and Tex12 emerged even earlier in the last common ancestor of *Eumetazoa* which comprises *Bilateria* and *Cnidaria*. A more ancient origin in the ancestor of *Metazoa*, as in the case of SYCP1 and SYCP3, cannot be predicted because no homologous sequences could be found in *Porifera* or *Placozoa*. Possibly, this is due to too little sequence information available for these basal branches. However, the phylogeny of SYCE3 reveals a much more recent origin of this latest CE component in the ancestor of vertebrates (**Supplementary Table 6**; **Figure 8-1**).

A likewise ancient role of SYCE2 and Tex12 in the formation of a SC was demonstrated in the basal metazoan *Hydra*. The characterization of HySYCE2 and HyTex12 revealed their meiotic role in the formation of a cnidarian SC (**Figure 8-2** and **Figure 8-3**). In accordance to the mouse SYCE2 and Tex12, HySYCE2 and HyTex12 seem to be specific for the CR, probably for the CE, of the SC which is indicated by their co-localization with HySYCP1 and their disappearance where the LEs desynapse in diplotene. Furthermore, both proteins exhibit the same punctate localization pattern as their mammalian orthologues which was described by Hamer *et al.* (2006) (**Figure 8-4**). The multiple alignments of the SYCE2 and Tex12 orthologues elucidated conserved regions in the center of the proteins (see also **Supplementary Figure 1** and **Supplementary Figure 2**). Most likely, these regions are of particular value for the function of the proteins. In mammals, SYCE2 and Tex12 are supposed to act in concert and to form an own complex. As they are both essential for the elongation of synapsis (Bolcun-Filas *et al.* 2007; Hamer *et al.* 2008), it is called the elongation complex. Just recently, Davies *et al.* could demonstrate the constitutive character of the human SYCE2-Tex12 complex and identified aa 57 to 165 of hSYCE2 and 49 to 123 of hTex12 to be essential for their polymerization to hetero-octamers (Davies *et al.* 2012). These regions are consistent with the conserved domains that were defined by the alignments (see also footnote 42 and 43). Therefore, these domains might also be essential for an association of HySYCE2 and HyTex12 to form an elongation complex in *Hydra* that is comparable to the mammalian interaction. In agreement with this, the proteins can assemble to aggregates when they are ectopically expressed in somatic COS-7 cells (**Figure 8-5**), a result which indicates their ability to interact.

All together, the phylogeny and the protein characterization of HySYCE2 and HyTex12 demonstrate the ancient character of SYCE2 and Tex12 and their original function in the assembly of the SC since their first emergence in the common ancestor of *Eumetazoa* or even earlier if orthologues of SYCE2 and Tex12 could be found in *Porifera* and/or *Placozoa* in the future.

Obviously, SYCE1 and SYCE3, however, were recruited to the already existing SC at later time points. SYCE1 appears to be ancient emerging in the common ancestor of *Bilateria*. It is possible that an orthologue exists in *Cnidaria* as well which was just not detected because of too little sequence data and which would indicate the same early origin together with SYCE2 and Tex12. However, database analysis was performed intensively and no orthologues were found



in species being more basal than *Annelida* and *Mollusca*. A true absence of SYCE1 in *Cnidaria*, therefore, is more likely. All information indicates that SYCE3, however, truly emerged in the ancestor of vertebrates much more recently.

The analysis has shown that the present-day murine CR/CE is an ancient structure of the SC which is composed by likewise ancient (SYCE1, SYCE2 and Tex12) but additionally more recent (SYCE3) components. Thus, the SC has undergone a rather dynamic evolution which was unexpected because its global structure is highly conserved in *Metazoa*.

However, the ecdysozoan species again display an exception as it already has been observed in the analysis of the previous chapter. Once more, there is only one identified homologue - a SYCE2 orthologue - in *Daphnia* as single exception of the broad absence of *Ecdysozoa* in the phylogenies of the CE proteins. As already proposed for SYCP1 and SYCP3, this one sequence argues that the CE/CR proteins in flies (*Drosophila*) and nematodes (*C. elegans*) are also derived from the ancient metazoan CE proteins but highly diverged beyond recognition during diversification of *Arthropoda* and *Nematoda*. But still it is possible that CONA of *Drosophila* and the SYP proteins of *C. elegans* emerged much more recently and genus-specifically. Then, they would have arisen independently of SYCE1, SYCE2 and Tex12 by convergent evolution to fulfill analogous functions within the SC. As there are no detectable homologues of CONA or any SYP protein outside the respective genus of *Drosophila* or *Caenorhabditis* either, it is not possible to make assure statements about the true origin of these alternative CE/CR proteins in flies and nematodes. However, as mentioned above, the first hypothesis assuming a high sequence divergence because of high evolutionary rates is favored due to this one detected homologous sequence of SYCE2 in *Daphnia*.

## 9 Chapter III: The evolution of the mammalian lateral element protein SYCP2

Unpublished data

### Introduction

As the evolution of six out of seven mammalian SC proteins was analyzed in the previous chapters, this third section now deals with the evolution of the last mammalian SC component, SYCP2. SYCP2 could be described as a “step child” of the SC proteins. It was only rarely major subject of investigations (Offenberg *et al.* 1998; Schalk *et al.* 1998; Yang *et al.* 2006; Winkel *et al.* 2009). SYCP2 is the largest murine SC component with 1,500 amino acids, a fact that makes it unwieldy for experimental work. It is part of the LEs together with SYCP3 and possesses only a small coiled coil domain in its C-terminal region (Yang *et al.* 2006). In the heterologous system, SYCP2 cannot polymerize (Pelttari *et al.* 2001; Winkel *et al.* 2009) as do the *bona fide* structural SC components SYCP1 and SYCP3. A true *Sycp2* knock-out mouse does not exist. Conclusions about its function were gained from a transgenic mouse expressing a mutated version of SYCP2 which lacks the coiled coil region from residue 1,346 - 1,476 and with this its interaction domain with SYCP3 (Yang *et al.* 2006) and SYCP1 (Winkel *et al.* 2009). In these *Sycp2* mutated spermatocytes, AE formation is disrupted and SYCP3 accumulates in large aggregates. It therefore was suggested that SYCP2 is the major determinant of AE formation. However, this interpretation is questionable regarding the incomplete depletion of the protein and contradictory results from the true *Sycp3*<sup>-/-</sup> knock-out mouse (Yuan *et al.* 2000; Pelttari *et al.* 2001).

Another feature of SYCP2 was described by Kneissel *et al.* (2001). They characterized the karyoskeletal protein NO145 of the frog *Xenopus laevis* which localizes in the nucleolar cortical skeleton of the oocytes. The analysis of the amino acid sequence revealed a strong homology to SYCP2 especially in an approximately 200 residue long domain in the N-terminal regions of the respective proteins.

The analysis of SYCP2 was performed separately in the end because this homology hampered the search for orthologues of the SC protein in non-mammalian species. Furthermore, the evolutionary relationship between NO145 and SYCP2 opened additional questions about a potential last common ancestor of both proteins and the point of their separation. It was of avail that the chicken SYCP2 was characterized as the only non-mammalian orthologue just a few years ago (Zheng *et al.* 2009).

## Results

Consistent with the proceeding of chapter I and II, homologues of SYCP2 had to be identified in a BLAST search. Their evolution was reconstructed in a phylogenetic tree. A hypothesized ancient function of the ancestral SYCP2 in SC formation ought to be confirmed by an expression analysis in the basal metazoan *Hydra*.

### Phylogeny of SYCP2

The BLASTp and tBLASTn algorithms on diverse databases were used to identify potential orthologues of the mammalian SYCP2.<sup>61</sup> These BLAST searches using several different queries revealed numerous sequences with significantly low e-values originating from vertebrate but also invertebrate species. A scan against specific HMM profiles confirmed or disproved the high probabilities of a true homology between the hits and the query. Doubtful sequences were removed. Redundant sequences and isoforms originating from the same species were identified and selected or removed from the dataset with the help of a preliminary phylogenetic tree. This led to a set of sequences, finally, which consists of two homologous sequences from most vertebrate species and one homologous sequence from one representative of the invertebrate clades of *Echinodermata*, *Mollusca*, *Annelida*, *Platyhelminthes*, *Ecdysozoa*, *Cnidaria* and *Placozoa* but not from *Porifera* (see also **Supplementary Table 7**). Many, especially non-mammalian sequences appear to be partial and are much shorter than 1,500 amino acids. Interestingly, the multiple alignment shows that the highest conservation between the detected sequences and a mammalian query, e.g. the mouse SYCP2 sequence<sup>62</sup> is predominantly confined to an N-terminal domain of SYCP2 which lies within its first 400 amino acids (**Figure 9-1**).

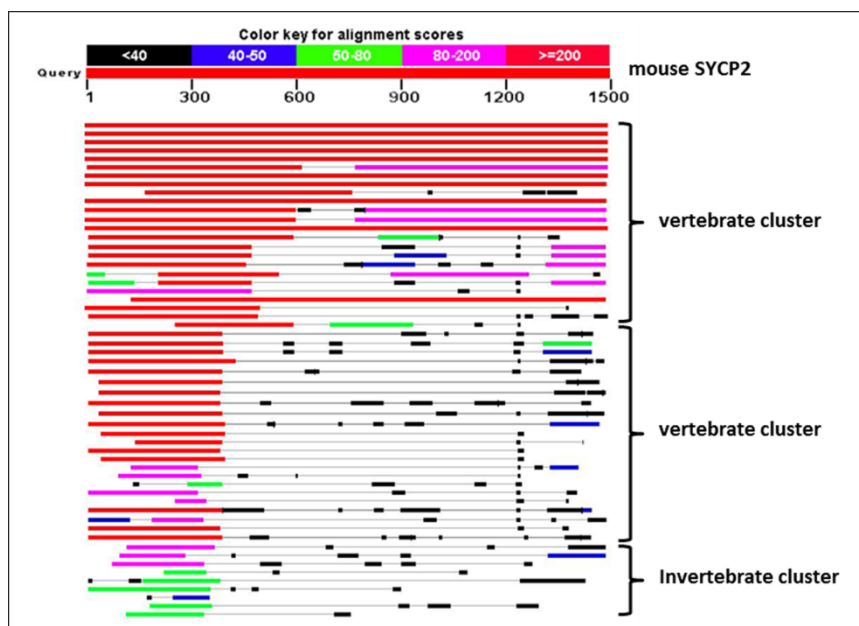


**Figure 9-1: Multiple alignment of SYCP2 orthologues.** The alignment displays the highest sequence conservation in the N-terminal domain of the mouse SYCP2 query. The (exemplary) illustrated homologous sequences can be separated into two different vertebrate clusters and one invertebrate cluster. For further details, see also the text below. The diagram is adopted from the NCBI BLAST.

<sup>61</sup> For a list of the used databases see **Table 12-4** and for the protocol of the dataset assembly see on page 103.

<sup>62</sup> The RefSeq No. on NCBI of the mouse SYCP2 is NP\_796165.2.

A phylogenetic tree was then carefully reconstructed on the basis of 279 conserved and aligned amino acids<sup>63</sup> originating from a taxonomically balanced subset of 36 sequences using Maximum likelihood and Bayesian Inference (**Figure 9-2**; for the multiple alignment see **Supplementary Figure 5**).<sup>64</sup>

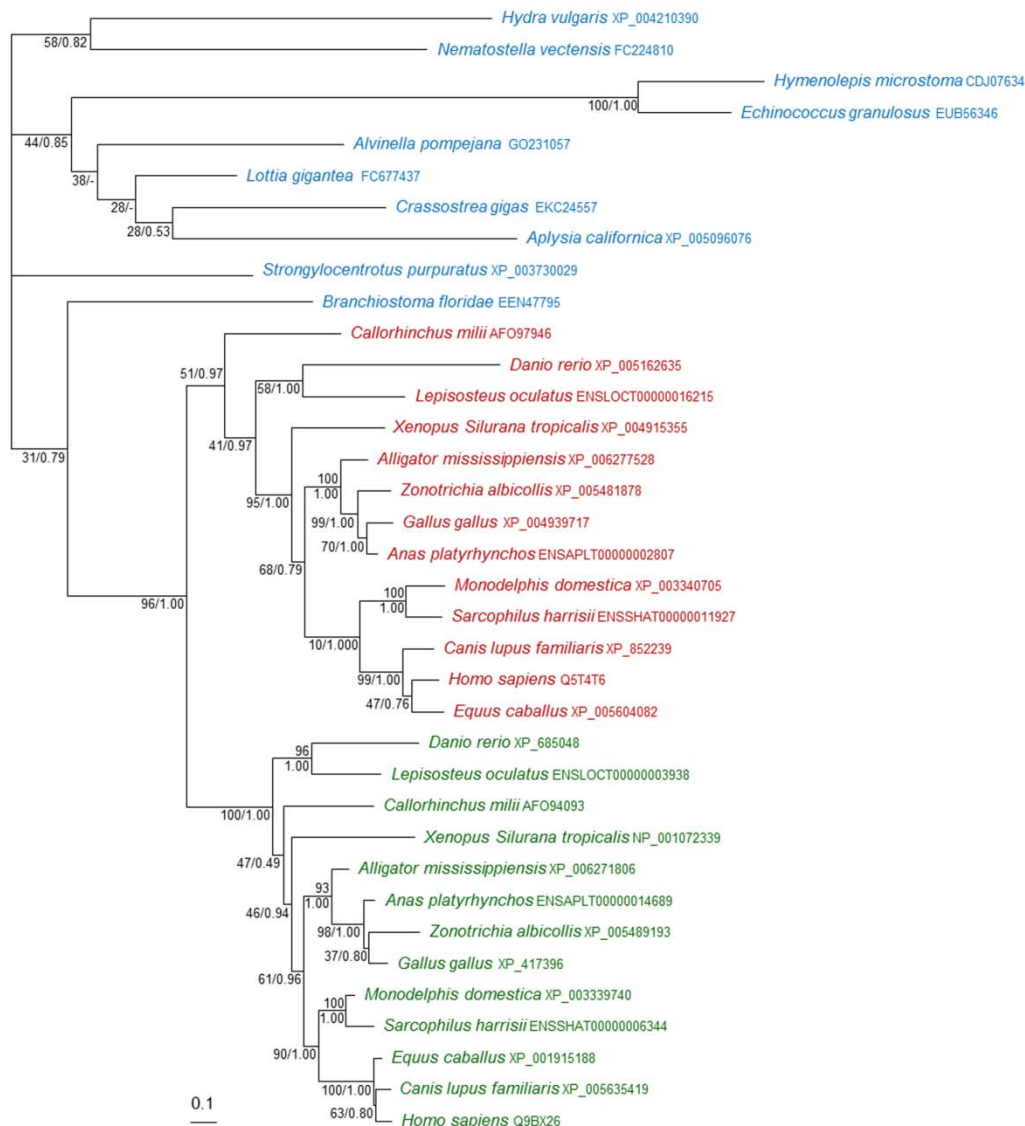


**Figure 9-2: Phylogeny of SYCP2.** Unrooted maximum likelihood tree was calculated from the multiple alignment of 36 sequences and 279 kept amino acid positions, see **Supplementary Figure 5**. Branch robustness is indicated by bootstrap values (given in percentage) and posterior probabilities (given in fractions) calculated with PhyML and MrBayes (e.g. 50/0.5). A dash indicates that the respective branch of the maximum likelihood tree is not recovered in the consensus Bayesian tree (e.g. 50/-). The bar displays the average number of substitutions per site. Color code of species: Invertebrate species are shown in blue, the predicted SYCP2 cluster is shown in green and the predicted NO145/SYCP2-like cluster is shown in red. The dataset assembly and the computational tree calculation was supported and confirmed by Céline Brochier-Armanet.

<sup>63</sup> The conserved residues which were kept for phylogenetic tree reconstruction range from aa 121-186, 189-319, 326-339, 342-346, 352-360, 366-388, 935-941, 946-957, 973-977, 1,014-1,019 and 1,359-1,363 of the human SYCP2 with the Accession No.Q9BX26.

<sup>64</sup> For the protocol of the phylogenetic tree reconstruction see on page 105 and for a list of the respective computer programs see **Table 12-4**.

A comparison with the phylogeny of *Metazoa* (Philippe *et al.* 2009; see also reference tree in **Figure 6-1**) reveals that the two respective sequences of the vertebrate species separate into two distinct clusters in this tree (green and red in **Figure 9-2**). Both are further separated from the invertebrate sequences (blue in **Figure 9-2**). These invertebrate sequences appear at the base of the tree and their displayed relations recover the general invertebrate evolution. The sequences of *Trichoplax adherens* (Placozoa) and the crustacean sequence of *Calanus finmarchicus* (Ecdysozoa)<sup>65</sup> were not included into the tree. The detected sequences were too short to be useful in the phylogenetic analysis. However, both sequences revealed a convincing degree of homology to the different queries in the BLAST search. According to the tree, the divergence of the two vertebrate clusters occurred after the separation of the branch leading to the *Cephalochordata*. An individual inspection of each vertebrate cluster shows that one contains the characterized SYCP2 orthologues of human and chicken<sup>66</sup>, beyond other predicted SYCP2 sequences (green cluster), while the second cluster (red cluster) contains the annotated human NO145 protein and a protein sequences of *Xenopus Silurana tropicalis* which is annotated as SYCP2-like and reveals are very high sequence identity (79%) to the characterized *Xenopus* NO145 protein sequence<sup>67</sup> over the entire protein length. Further sequences referred to as SYCP2-like proteins can be found in this cluster as well. Within itself, each cluster is well resolved and both recover the vertebrate phylogeny with a high statistical support as indicated by the high bootstrap values and high posterior probabilities at the corresponding branches. Therewith, the tree suggests a gene duplication event in the branch leading to vertebrates which would have given raise to the apparent paralogues<sup>68</sup> SYCP2 and NO145/SYCP2-like.

Although the identities of the vertebrate sequences seem to be obvious from this phylogeny, the identities of the basal invertebrate orthologues, however, remain unknown. Are they functional proteins of the ancient SC or components of the nucleolus? Which protein, SYCP2 or NO145, is the ancient one?

### Sequence and expression of the SYCP2 orthologue in *Hydra vulgaris* AEP

To answer the question about the identity of the invertebrate sequences which show homology to SYCP2, the sequence and the expression of the orthologous protein fragment in *Hydra* was analyzed. The detected sequence from NCBI originates from *Hydra magnipapillata* (Hym-SYCP2)<sup>69</sup> and is 212 amino acids long. Amino acids 1-122 of this sequence align to the amino acids 226-347 of the human and the mouse SYCP2. A BLAST search in the *Hydra vulgaris* AEP transcriptome of the Compagen server (Hemmrich *et al.* 2012) resulted in 134 aligned amino

---

<sup>65</sup> The Accession No. on NCBI of the homologous proteins of *Trichoplax* and *Calanus* are XP\_002113953.1/EDV23043.1 and FK041407.1. See also **Supplementary Table 7**.

<sup>66</sup> The Accession No. on NCBI of human and chicken SYCP2 are Q9BX26 and XP\_417396.4.

<sup>67</sup> The Accession No. on NCBI of human and *Xenopus leavis* NO145 are Q5T4T6 and AAI61717.1, respectively. See also **Supplementary Table 7**.

<sup>68</sup> Paralogues are homologous proteins, which emerged from a gene duplication event within the same genome. Paralogues do not necessarily keep the same function.

<sup>69</sup> The Accession No. on NCBI for the potential HymSYCP2 is XP\_004210390.1.

acids from two different contigs, the first containing the aligned amino acids 1-99 of HymSYCP2 with a sequence identity of 96%. These residues mainly correspond to the conserved region which was also kept for reconstruction of the phylogenetic tree.<sup>70</sup> Different cloning attempts revealed that only the predicted cDNA of this first contig encoding for amino acid 1-99 of *Hydra vulgaris* AEP SYCP2 (HySYCP2) was feasible to clone in one continuous sequence. Sequencing of this partial *HySycp2* cDNA yielded a 100% match with the Compagen database information.<sup>71</sup>

The corresponding cDNA of 297 bp was used to synthesize a Dig-labelled antisense RNA probe for *in situ* hybridization on whole animals.<sup>72</sup> In **Figure 9-3** one can see the purple staining of the testes. Within the testis, only the basal layer is stained which is where spermatocytes are located (Kuznetsov *et al.* 2001). It is a familiar staining pattern which was already observed in the analyses of chapter I and II and which suggested an actual role of the respective examined proteins in meiosis and SC formation. Given this similarity, the above result points to an expression of *HySycp2* in spermatocytes and maybe even to a localization of the HySYCP2 protein within the cnidarian SC. The alternative would be a nucleolar expression corresponding to a cnidarian *No145* mRNA. This, however, would be expected to yield another result in the *in situ* hybridization as this mRNA should not be expressed in spermatocytes (Kneissel *et al.* 2001).



**Figure 9-3: Testis-specific expression of *HySycp2* mRNA.** The *HySycp2* mRNA can be localized to the basal testis layer as indicated by the dark purple staining of the whole mount *in situ* hybridization with a Dig-labeled RNA probe against the partial (297bp) mRNA of *HySycp2*.

However, to finally show the localization of the protein HySYCP2 within the SC of *Hydra*, antibodies need to be generated for Western blot and immunofluorescence analysis. Therefore, the sequenced part of the *HySycp2* cDNA was cloned into the pET21a plasmid which was used for

<sup>70</sup> In the multiple alignment, amino acid 1-94, 101-114, 120-123, 129-137 and 143-166 of HymSYCP2 were kept for the phylogenetic tree reconstruction. The first part from amino acid 1-94 aligns to amino acid 1-94 of the *Hydra vulgaris* AEP sequence of contig HAEP\_T-CDS\_v02\_43970. The residues 105-134 correspond to residues from a second contig of the *Hydra vulgaris* AEP transcriptome, HAEP\_T-CDS\_v02\_36446.

<sup>71</sup> *HySycp2* primer sequences are given in **Table 12-3**. For the protocol of cDNA sequencing and cloning see on pages 81 and 83.

<sup>72</sup> For the protocol of the ISH see on page 95.

the expression of HySYCP2-6xHIS in *E. coli* Rosetta bacteria. The purified fusion protein was sent out for immunization and the serum should be available in the following months.<sup>73</sup>

## Discussion

The obtained results complement and extend the analysis of the SC evolution in *Metazoa* and represent another example for the dynamic evolutionary history of this structure.

Together the metazoan phylogeny (**Figure 9-2**) and the *in situ* hybridization on *Hydra* (**Figure 9-3**) suggest that SYCP2 is as old as metazoans themselves and maybe it is part of the ancient SC. One could further speculate that HySYCP2 is a component of the LEs of the SC - as its mammalian orthologue. But definitely a closer inspection of its expression in *Hydra* is necessary. As soon as an antibody is available, its specificity needs to be tested to analyze the localization of the protein. The possibility of a localization in the nucleoli of the oocytes, corresponding to NO145, needs to be considered during the experiments as well. But a localization within the LEs of the SC would support the indicated hypothesis that the ancestral protein indeed is the SC component SYCP2.

In any case, the protein seems to have emerged in the last common ancestor of *Metazoa* as potential orthologues could not only be detected in many invertebrates, e.g. *Cnidaria* but also in the even earlier branching *Placozoa Trichoplax adherens* (**Supplementary Table 7**). Another sequence was found in the crustacean species *Calanus finmarchicus*. Although it was not included into the phylogenetic tree, the sequence reveals a sufficient degree of homology to vertebrate SYCP2 protein sequences to be considered as a true orthologue. Having in mind the results of chapter I and II, the potential existence of an orthologue of the mammalian SYCP2 in an ecdysozoan species is very interesting and provides a further indication to the hypothesis that homologous proteins of the mammalian SC proteins do exist in the clade of *Ecdysozoa* but probably diversified exceptionally strongly. If the lack of proteins which are homologous to SYCP2 in sponges demonstrates a true absence in these species is hard to tell because only little genome data are available for this clade.

Interestingly, a closer inspection of the identified metazoan SYCP2 orthologues further revealed that their conservation is mainly based on a domain in the N-terminal region of the respective mouse protein (**Figure 9-1**). This corresponds to the information given by Kneissel who reported the highest sequence identity in the N-termini of rat SYCP2 and *Xenopus* NO145 (Kneissel *et al.* 2001). But it does not correlate with the C-terminal domain of SYCP2 which was described to be important for the interaction with SYCP1 and SYCP3 in the mouse (Yang *et al.* 2006; Winkel *et al.* 2009). So the question arises what is the functional importance of this N-terminal region which made it so important to conserve it during evolution? It is hardly possi-

---

<sup>73</sup> For the protocols of DNA cloning, protein expression and antibody generation see on pages 83, 88 and 91 and for list of recombinant DNA constructs see on page 73.

ble to answer this question about the potential function of this region. Specific annotated domains or motifs, which would point to a certain function, could not be detected.

The phylogenic tree (**Figure 9-2**), finally, indicates that the duplication event of the ancient gene occurred in the branch leading to the vertebrate lineage. This would have resulted into the paralogues SYCP2 and NO145. Although the proteins fulfill specific and distinct functions, both are large components of nuclear scaffold structures (Offenberg *et al.* 1998; Kneissel *et al.* 2001). This could be interpreted as another indication of their common origin from the same gene. Gene duplication events like this are not unusual during the evolution of vertebrates indeed and two rounds of whole genome duplications are assumed to have occurred in their ancestral species (Dehal and Boore 2005). Eventually, the gene duplication event of *Sycp2*, then, is another example for the dynamic evolution of the SC and its components in *Metazoa*.



## 10 General Discussion

### 10.1 The dynamic evolution of the SC

According to Fraune *et al.* 2012b and Fraune *et al.* 2013

The analyses from the preceding chapters were performed to answer the major questions of this study which were raised in section 6. They revealed the monophyly of the mammalian SC components and point to a single origin of the SC in *Metazoa*. This was in question considering the diverse SC protein sequences of mouse, *D. melanogaster* and *C. elegans*. Nevertheless, the SC has undergone a dynamic evolutionary history which is illustrated in **Figure 10-1**.

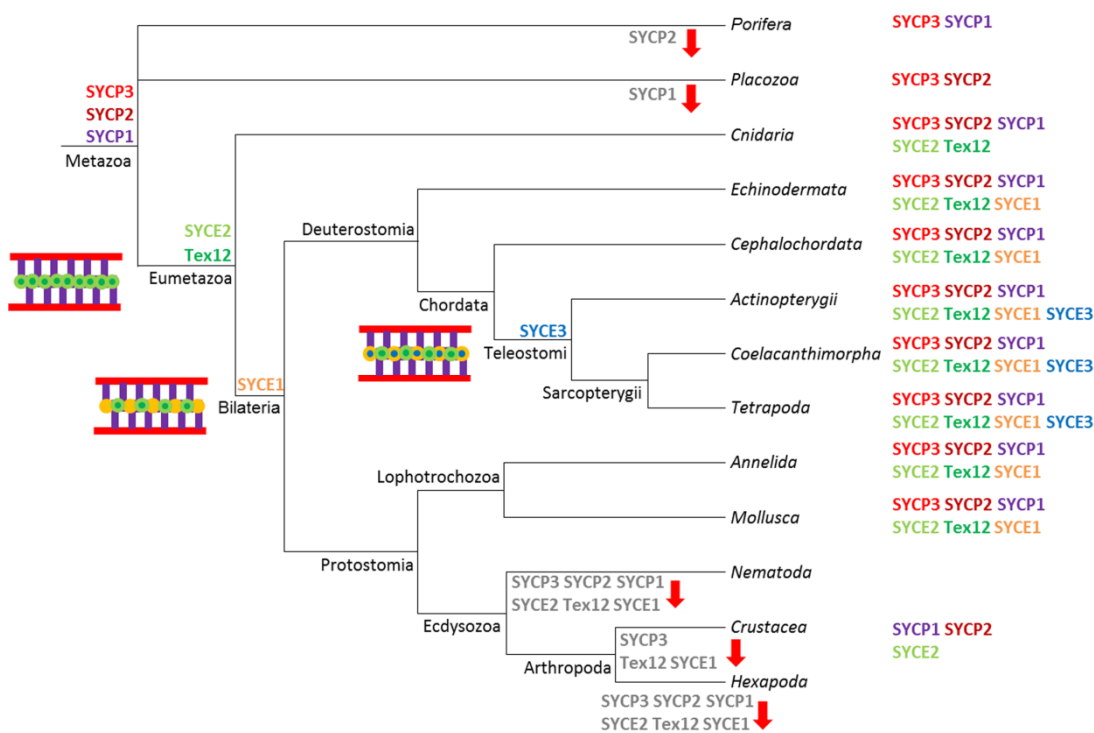


**Figure 10-1: The dynamic evolution of the SC in *Metazoa*.** An ancient SC made of SYCP1, SYCP3, possibly SYCP2, SYCE2 and Tex12 emerged in the last common ancestor of *Eumetazoa*. SYCE1 and SYCE3 evolved later in the ancestor of *Bilateria* and vertebrates, respectively. Schematic diagrams of the potential SC structures are given besides the branches. The orthologues, which were found in the present-day organisms of the different metazoan lineages, are shown behind their taxonomic names. Potential losses or strong divergence of individual components are indicated by their gray font and a red arrow at the corresponding branch. The figure is adapted from Fraune *et al.* 2013.

SYCP1 and SYCP3 together with SYCE2 and Tex12 emerged as early as eumetazoans themselves. In combination, the proteins are involved in the assembly of an SC in the basal organism *Hydra*. This indicates the primary and original function of the proteins in the formation of an ancient SC being composed of SYCP3 in the LEs, SYCP1 as component of the TFs and SYCE2 and Tex12 forming the CE in the ancestor of *Eumetazoa*. It is very likely that this ancestral SC

emerged even earlier in the ancestor of *Metazoa* because orthologues of SYCP1 and SYCP3 were found in *Porifera* and *Placozoa* as well. This, however, could not be demonstrated as orthologues of SYCE2 and Tex12 were not detected in any of these sister groups of *Eumetazoa*. Another component, SYCP2, primarily appears in the common ancestor of *Metazoa* as well. Its initial expression analysis suggests a similar function in SC assembly in *Hydra*, but yet this needs to be analyzed in more detail. In any case, further components seemed to have been added to this ancient SC structure in the ancestor of *Bilateria* (SYCE1) and vertebrates (SYCE3).

But not only addition of new components occurred. Also losses/replacements or strong divergences of proteins seemed to have happened especially in the branch leading to ecdysozoan species. The lack of any detectable homology between the flies, the nematodes and the ancient SC components of mammals or cnidarians can be interpreted in either ways. One explanation could be that the ancient protein components were lost and non-homologously replaced by other proteins in *Arthropoda* and *Nematoda*. Then the SCs of present-days animals would not all share a common origin. The SC would have emerged independently and much more recently in certain lineages by convergent evolution and in analogy to the ancient SC. In this case, only the general secondary structure of the proteins, especially of the TF components, would have been conserved. The second explanation is that the SC proteins in flies and nematodes, or ecdysozoan species in general, indeed derived from the ancient proteins. But they would have diversified to such a high degree that the homology cannot be detected anymore because of higher evolutionary rates. The second hypothesis seems to be most probable as very distantly related orthologues of SYCP1, SYCE2 and likely SYCP2 could be identified in the ecdysozoan phylum of *Crustacea*. Indeed, ecdysozoans have ostensibly lost many gene families which are otherwise conserved from *Hydra* to human (Galliot 2012). Thus, the SC components are not the first case in which *Drosophila* and *C. elegans* hold a rather exceptional role. Evolutionary analysis of the *lamin* gene(s) in *Metazoa* for example revealed that just *Drosophila* and *C. elegans* exhibit an unusual gene organization most likely due to a strong genetic drift (Peter and Stick 2012).

Additionally, a further example for the dynamic evolution of the SC components is provided by the case of SYCP2. Although not yet sufficiently demonstrated, its phylogeny proposes a gene duplication event of a SC component. Most likely, this happened during the strong diversification of the vertebrate lineage and led to the emergence of a SYCP2 paralogue in the new evolving species. This paralogue, NO145, still maintained its role as a protein from a nuclear scaffold structure although it is diversified in localization and function (Kneissel *et al.* 2001).

The evolution of the SC in metazoans now poses new questions, e.g. why did certain components evolve earlier than others? What is their functional difference and, therefore, functional significance in the formation of the SC?

It is evident from the various different SC mutants that a functional SC requires all three structural domains: LEs, TFs and CE. The LEs and the TFs are indispensable for the assembly of a SC with sufficient structural integrity to fulfill its function (for review about the mammalian SC,

see e.g. Bolcun-Filas and Schimenti 2012; Fraune *et al.* 2012a). The need of SYCP1 and SYCP3 as *bona fide* structural components of the LEs and TFs, therefore, seems to be undisputable and their emergence in the ancestor of metazoans is logically consistent. At least *in vitro*, the mammalian SYCP1 and SYCP3 do not require additional components to polymerize to higher order structures which already resemble the respective SC domains pointing to their significance in the assembly process (Yuan *et al.* 1998; Öllinger *et al.* 2005). *In vivo*, the proper localization of the mammalian SYCP3 is influenced by the presence of SYCP2 (Yang *et al.* 2006). But even this protein might be present in the common ancestor of the metazoan species. In any case, the situation is different for the CE. Although the CE is essential for the SC assembly *in vivo per se*, it is possible that originally only a minimal protein kit was needed to perform its ancient function.

Most of the relevant information about the function of the mammalian CE proteins SYCE1, SYCE2, SYCE3 and Tex12 resulted from studies of the knock-out mice. SYCE1 and SYCE3 likely act together and are essential for the initiation of synapsis in mammals. In the absence of either protein, SYCP1 can bind to the LE but fails to synapse the homologous chromosomes (Bolcun-Filas *et al.* 2009; Schramm *et al.* 2011). Derived from this function, the proteins were described to form a synapsis initiation complex. These two proteins are missing in cnidarians and therefore were probably not part of the ancestral SC. This implies that other mechanisms beside the mammalian initiation complex should exist to initiate synapsis. The crux of these mechanisms are unknown, however, theoretically it is possible that SYCP1 alone is sufficient to start synapsis in the absence of a specialized initiation complex in basal organisms because it is able to polymerize *in vitro*. The mammalian SYCE2 and Tex12 in contrast are not essential for initiation but for elongation of synapsis (Bolcun-Filas *et al.* 2007; Hamer *et al.* 2008). Correspondingly, they form the so-called elongation complex in mammals, a very stable protein complex (Davies *et al.* 2012). Precisely these two proteins are conserved from *Cnidaria* to human suggesting a greater functional relevance of SYCE2/Tex12 than of SYCE1/SYCE3 for the formation of the SC. The murine SYCE2 can bind to SYCP1 (Costa *et al.* 2005). Yet this is not shown for HySYCE2 and HySYCP1. But a comparable interaction of these two proteins in cnidarians would provide the missing linkage between the initiation and the elongation of synapsis. Thus, in a hypothesized model, HySYCP1 could mediate synapsis initiation while HySYCE2 and HyTex12 are recruited to the TFs to mediate the elongation along the entire chromosomes. Additionally, the importance of the elongation complex might also be related to the process of homologous recombination. Indeed, SYCE2, SYCP1 and SYCP3 are the only components of the murine SC so far for which a direct interaction with the homologous recombination machinery - with RAD51 and DMC1 - was described (Tarsounas *et al.* 1999; Bolcun-Filas *et al.* 2009). RAD51 is highly conserved from mouse (RefSeq: NP\_035364.1) to *Hydra* (RefSeq: XP\_002169171.1) exhibiting a sequence identity of 82% in an alignment with BLAST. Thus, an interaction between HyRAD51 and HySYCE2 or/and HySYCP1/HySYCP3 would be conceivable and would explain the necessity of specifically conserving these proteins throughout metazoan evolution.

Having answered the questions about the evolution of the SC in metazoans, the puzzle remains in regard to the general evolution of the SC in sexually reproducing multicellular organisms. Also yeast and plants assemble SCs during their first meiotic division. These SCs are (partially) characterized in *Saccharomyces cerevisiae* and *Arabidopsis thaliana* and again show the same tripartite structure as it is known from metazoans (Page and Hawley 2004; Mercier and Grelon 2008). But the respective protein components do not reveal any evolutionary relationship to SYCP1, SYCP2, SYCP3, SYCE1, SYCE2, SYCE3 or Tex12. Only the HIM-3 protein family of *C. elegans*, the *S. cerevisiae* LE protein Hop1p and the *Arabidopsis* LE associated Asy1 are related, all belonging to the HORMA domain protein family as do the murine HORMAD1 and HORMAD2 (Armstrong *et al.* 2002; Page and Hawley 2004; Wojtasz *et al.* 2009). Maybe one can imagine a similar dynamic model for the evolution of the SC in multicellular organisms in general from these rare homologies. An ancient inventory of proteins would have built a SC in the common ancestor of animals, plants and yeast definitely including HORMA-domain proteins as part of the chromosomal axes and large coiled coil proteins forming the TFs. However, during evolution of the different lineages, the set of proteins might have changed by strong diversification, addition and losses of individual components. This would have resulted in the variable SC protein components of the present-day multicellular organisms which only reveal relicts of their evolutionary history, e.g. the HORMA domain proteins and the archetypal secondary structure of the TF proteins.

## 10.2 The cnidarian SC: *Hydra* as model system for meiosis research?

According to the publication Fraune *et al.* 2014

As presented above, the analyses in chapter I, II and III revealed the existence of at least four cnidarian SC components being orthologous to the murine SYCP1, SYCP3, SYCE2 and Tex12. The presence of a SYCP2 orthologue is also possible but not yet definite because its characterization was not completed during the study of chapter III. And even more SC proteins could exist in *Hydra*. Their presence cannot be excluded and remains to be investigated. The following diagram (**Figure 10-2**) summarizes the lengths and the expansion of the respective coiled coil domains of HySYCP1, HySYCP3, HySYCE2 and HyTex12 in analogy to **Figure 5-2**. The detected HySYCP2 is not shown because the analyzed sequence is partial and most likely only reflects a small fragment of the full-length protein.

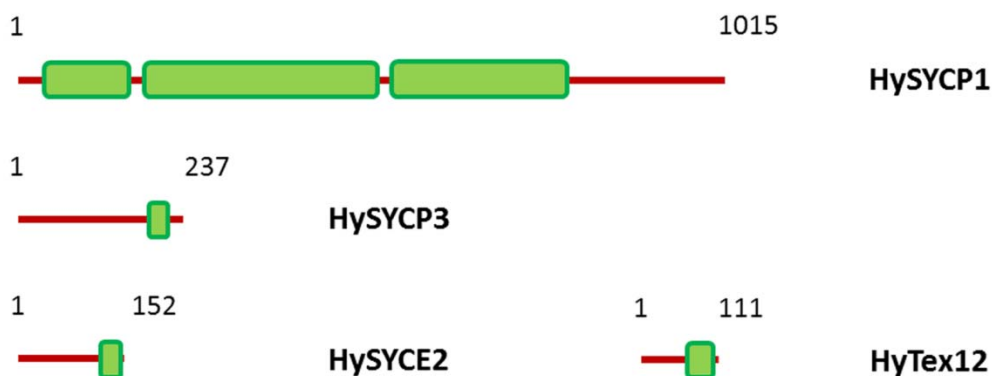


**Figure 10-2: The inventory of *Hydra* SC proteins.** The length of the proteins is indicated in numbers of amino acids. The extension and position of coiled coil domains, which were predicted by the Lupas algorithm, are represented by the green boxes. In HySYCP1 the coiled coil domains range from aa 36-157, from aa 180-515 and from aa 534-788. In HySYCP3, one coiled coil domain is predicted from aa 187-214, in HySYCE2 from aa 117-146 and in HyTex12 from aa 67-104. The figure is adopted from Fraune *et al.* 2014.

The localization of the proteins within the SC resembles very much the localization of the murine SC components according to the immunofluorescence analysis. Therefore, the following model of the cnidarian SC structure is proposed (**Figure 10-3**). In this model, HySYCP3 is a protein of the LEs while HySYCP1 is the component of the TFs. The TF protein's size and predicted secondary structure correlates with those of the TF proteins of *Drosophila*, *C. elegans* and mouse. This is why the model assumes HySYCP1 to dimerize as well and to span the distance from the LEs to the CE. HySYCE2 and HyTex12 most likely act together in the CE.

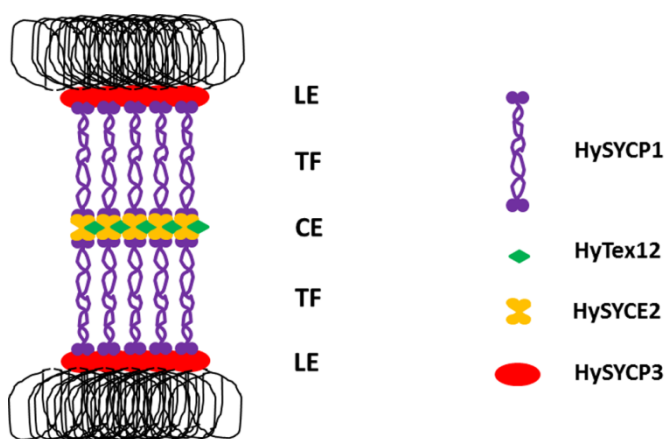


**Figure 10-3: Schematic diagram of the organization of the *Hydra* SC.** Two lateral elements, which are associated with the homologous chromosomes and consist of HySYCP3 (and maybe HySYCP2, not shown), are synapsed by the formation of the central region. The central region is probably formed by HySYCP1 dimers, which make the transverse filaments, and further proteins - HySYCE2 and HyTex12 - which are most likely specific for the central element. The figure is adopted from Fraune *et al.* 2014.

Now, the characterization of the SC proteins in the basal organism *Hydra* and their monophyletic origin in *Metazoa* further open the possibility to consider *Hydra* as a complementary but less complex model system for meiosis research. So what is known about the model organism *Hydra* and the cnidarian meiosis? In the following section, further available information about *Hydra* gametogenesis and meiosis will be recapitulated. Additionally it will be discussed which methods are practicable to study the SC and its function in this organism.

*Hydra* has been a model organism for biological research for more than 250 years (Galliot 2012). It belongs to the very old phylum of *Cnidaria* which is a sister group to the *Bilateria* (see also **Figure 6-1**). *Hydra* only has two epithelia, endoderm and ectoderm, which are separated by the mesogloea. The epithelia encase the gastric tube. A mouth opening is located at the top and is surrounded by a tentacle ring used for active capturing of prey. The foot is used for adhesion to the ground of fresh water (e.g. Steele 2012). Since the 18<sup>th</sup> century, *Hydra* has been used for classical topics in biology, e.g. regeneration, embryogenesis, patterning of body axes or cell signaling. Since the late 20<sup>th</sup> century, when new genetic approaches were developed and certainly since the genome of *Hydra magnipapillata* was sequenced and published for the first time (Chapman *et al.* 2010), *Hydra* became attractive for molecular biologists as well. Questions regarding innate immunity, tissue homeostasis, stem cells and metazoan evolution are now analyzed with the help of this simply built polyp. Although *Hydra* is known for its asexual reproduction and its immense regenerative capacity, it also reproduces sexually. Unknown extrinsic and/or intrinsic signals lead to the formation of the germ line and gonads along the body axes of the *Hydra* species (Littlefield *et al.* 1991). The gametes are derivatives of the interstitial cell stem cell lineage. Besides germ cells, these stem cells also give rise to specialized somatic cells, e.g. nematocytes, gland cells and nerve cells. The endodermal and ectodermal cells originate from the endodermal and ectodermal stem cell lineages (Bosch *et al.* 2010). Former analysis on *Hydra oligactis* and *Hydra magnipapillata* suggested that the interstitial stem cell population is heterogeneous harboring a self-renewing subpopulation which is committed to sperm differentiation (Littlefield 1985; Nishimiya-Fujisawa and Sugiyama 1993). Another subpopulation might be determined to the development of eggs and somatic cell types (Littlefield 1985). Indeed, the sex of the interstitial cells determines the sexual phenotype of the polyp. The genetic sex of the epithelial cells is irrelevant. In some species, also in *Hydra vulgaris* and *Hydra magnipapillata*, a reversal of the sex is possible (Bosch and David 1986). Molecular or cellular signals for the sex determination and reversal, however, are unknown. The karyotype of *Hydra magnipapillata* chromosomes did not reveal any heteromorphic chromosome pair which could be responsible for the determination of the sex as it is in higher metazoans (Anokhin *et al.* 2010).

The differentiation of gametes can be induced by starvation or low temperature in the lab depending on the *Hydra* species. Interstitial cells which are restricted to the female germ line proliferate and accumulate beneath the ectoderm during oogenesis. One of the centrally lying cells in the aggregate becomes the oocyte while the rest of the numerous cells turn into nutrient rich nurse cells. These will undergo apoptosis later and will be phagocytosed by the oocyte (Miller *et al.* 2000). Because there is only a small amount of oocytes per animal at a time, the female oogenesis is less convenient for meiosis research. Male animals in contrast produce a high amount of spermatocytes in their testes which makes them much more suitable for the analysis of the cnidarian SC and meiosis. When spermatogenesis is initiated, the interstitial cells, which are restricted to the production of sperms, accumulate between the mesogloea and the ectoderm. By lifting the epithelium, they form the conical swellings along the body

column which are characteristic for the *Hydra* testes. In the testis, the sperm precursors synchronously pass through the different developmental stages of gametogenesis in a spatial order, beginning with the spermatogonia at the testis base, followed by the meiotic stages of spermatocytes and the postmeiotic spermatids and finally the spermatozoa in the farthest tip of the testis. Ectodermal cells, which reach into the testis, separate it into distinct chambers (Figure 10-4) and it was speculated that the epithelial cells control the microenvironment of the adjacent developing germ cells similar to the mammalian Sertoli cells (Kuznetsov *et al.* 2001).

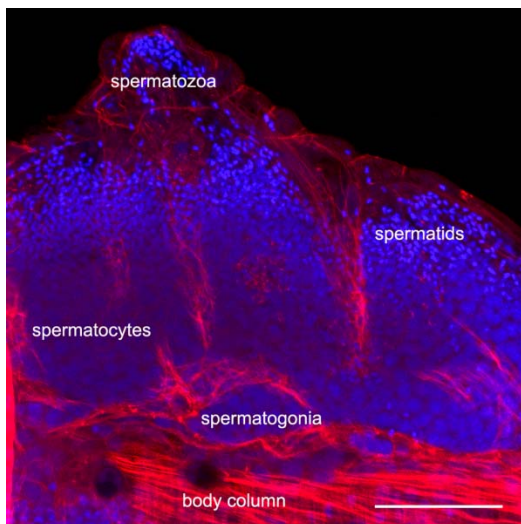


**Figure 10-4: A longitudinal section through the *Hydra* testis.** By the size of the cell nuclei, which are marked by the DNA staining (blue), the different developmental stages of the sperm precursor cells can be distinguished. Spermatogonia, spermatocytes, spermatids and spermatozoa occur in a spatial order from the testis base to the tip. Staining of the cellular actin skeleton with phalloidin-california red (red) illustrates the compartmentalization of the testes in distinct chambers. Scale bar, 50  $\mu$ m. The figure is adopted from Fraune *et al.* 2014.

In order that *Hydra* can advance to a complementary model system for meiosis research now, appropriate methods need to be available for comparative studies between the mammalian and the cnidarian system particularly in regard to the SC. These methods, which were tested and used for the expression analyses of the *Hydra* proteins in chapter I, II and III, were adapted from protocols for the characterization of murine SC proteins.

The spectrum of available methods includes the demonstration of gonad-specific expression of meiotic genes and proteins by RT-PCR or Western blot analysis on different tissues. Though *Hydra* has no differentiated organs, especially the testes can easily be separated from the body column which can be further split in head, mid-piece and foot. Additionally, whole mount *in situ* hybridization is a useful tool for gene expression analysis in *Hydra* and can be applied for the examination of cnidarian SC proteins as well.

Microscopic analysis is also practicable in *Hydra*. SCs can be detected in *Hydra* spermatocytes in the electron microscope and reveal the expected ultrastructural appearance (Figure 10-5).

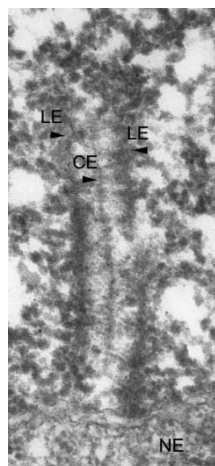


**Figure 10-5: Electron microscopical image of the *Hydra* SC.** Clearly, one can distinguish between the parallel running lateral elements (LE) and the central element (CE). The SC attaches to the nuclear envelope (NE) with its one end. The figure is photographed by Ricardo Benavente and adapted from Fraune *et al.* 2012b.

The preparation of the tissue can be performed following the standard fixation with glutaraldehyde and osmium tetroxide. Afterwards epon embedding is possible and suggested for the visualization of *Hydra* SCs (Fraune *et al.* 2012b). However, preembedding immunogold-labeling of specific SC proteins for electron microscopy was not yet successful. Especially the compact organization of the chromatin impaired the specific binding of the gold-labeled secondary antibody. But alternative microscopic methods for immunofluorescence analysis with a high resolution of the SC structure are also applicable in *Hydra*. Using confocal laser scanning microscopy, immuno-labeled SCs of chromosome spread preparations can be imaged to a resolution of 200-250 nm. Super-resolution immunofluorescence microscopy, such as the *d*STORM technology, with a resolution to down to 20 nm is currently tested on murine spermatocytes (Schücker *et al.* 2014). A preliminary experiment was also performed on *Hydra* chromosome spreads ( **Figure 10-6**).

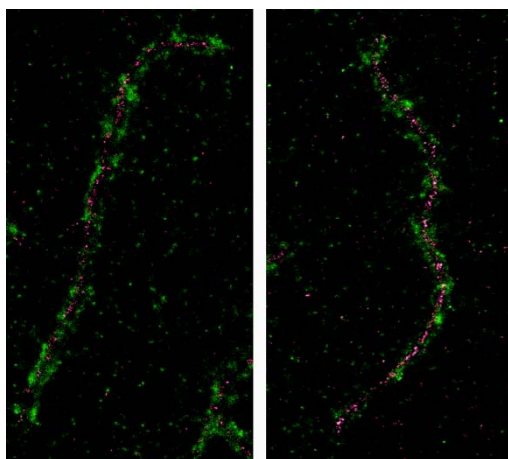


**Figure 10-6: *d*STORM microscopy on *Hydra* chromosome spreads.** The LEs can be observed as two distinct axes. They are stained with an  $\alpha$ -HySYCP3 antibody (rb  $\alpha$ -HySYCP3; 1:600) and labelled in green ( $\alpha$ -rb alexa 532, 1:200). HySYCP1 (gp  $\alpha$ -HySYCP1 N-terminal, 1:300;  $\alpha$ -gp alexa 647, 1:200), labelled in magenta, localizes as single line in the center of the SC. The image confirms the established model about the cnidarian SC organization. Furthermore, one can detect a left handed SC-twist which was also described in rat spermatocytes (Zickler and Kleckner 1999). The sample preparation and the imaging were performed under the instructions of Katharina Schücker and Thorge Holm (Schücker *et al.* 2014).

This super-resolution imaging could become an alternative to the immunogold-labeling technique for electron microscopy. With the high resolution capacity of the *d*STORM microscope it might be possible to illustrate the protein orientations and precise localizations within the SC. The required antibodies which were specifically generated for the examination of the cnidarian SC and meiosis I can be used for all the different immunofluorescence approaches and include not only antibodies against SC proteins but also antibodies which recognize components of the homologous recombination machinery (Wiesner 2013; Fraune *et al.* 2014; see also **Figure 10-7**).



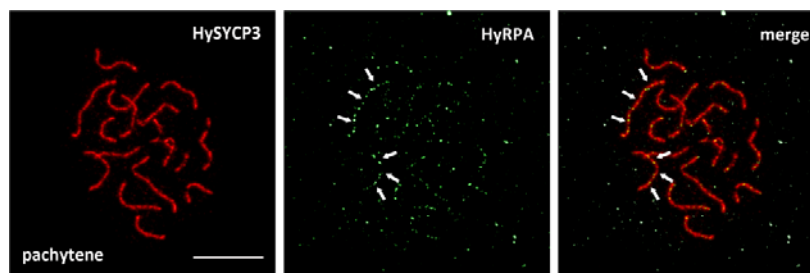


**Figure 10-7: HyRPA localizes in several foci along the *Hydra* SC in pachytene spermatocytes.** The localization pattern of HyRPA resembles the pattern of RPA along the mouse SC where it marks recombination nodules (TNs). The image was taken by Miriam Wiesner. It is adopted from Wiesner 2013 and Fraune *et al.* 2014.

Furthermore, polymerization properties of *Hydra* SC proteins were analyzed in analogy to the *ex vivo* polymerization studies with mammalian SC proteins. The ectopic expression of SC proteins in somatic cells has been developed to investigate binding and polymerization properties *in vitro* because culturing systems for meiotic cells are still not available. In transfected COS-7 cells, HySYCP1 and HySYCP3 do not form filamentous networks as do mammalian SYCP1 and SYCP3 (Yuan *et al.* 1998; Öllinger *et al.* 2005; Wiesner 2013). This could indeed be the result of different polymerization properties of the orthologues. But also improper culturing conditions could be the reason for the different features of the cnidarian proteins because COS-7 cells are cultured at 37°C while *Hydra* lives at 18°C. Though not yielding the same results for the *Hydra* proteins, the method could be successfully used to demonstrate that a) HySYCP3 is recruited into the filaments formed by mouse SYCP3 and thus can co-assemble with SYCP3 despite more than 500 million years of evolution (Wiesner 2013; see also see **Figure 7-9**) and b) HySYCE2 and HyTex12 can co-assemble into higher order structures indicating an ability of the proteins to interact as it is known from the mammalian orthologues (Hamer *et al.* 2006; Davies *et al.* 2012; see **Figure 8-5**).

With its considerable catalogue of orthologous SC protein components and many feasible methods which were adapted, *Hydra* seems to be an attractive invertebrate model system to complement the mammalian model for SC research. Only one methodical problem remains, which is related to the generation of genetically manipulated animals. In principle, transgenes can be successfully introduced into the genome of all three stem cell lineages of *Hydra* leading to either gene knock-down by siRNA or overexpression of exogenous genes (Wittlieb *et al.* 2006; Franzenburg *et al.* 2012).

In this study, *HySycp1* and *HySycp3* hairpin constructs fused to an *egfp* and under control of different promotor sequences were cloned for the injection into *Hydra* embryos to obtain knock-down lineages of the respective genes. These should be comparable to the existing *Sycp1*<sup>-/-</sup> and *Sycp3*<sup>-/-</sup> knock-out mice. However, a stable transmission into the germ line was not achieved although the *egfp* gene was obviously introduced into the I-cell lineage. An attempt failed to find the reason for this. By fluorescence *in situ* hybridization (FISH), it should be possible to distinguish between the possibilities of the hairpin construct not being inserted into the genome of the germ line cells and the possibility of the transgene not being expressed in the

germ line due to an inactive promotor sequence. But the FISH experiments which were performed did not yield convincing results. Yet it can be assumed that further techniques will be developed in the near future which will allow a reliable genetic manipulation of the germ line in *Hydra* as well. Then not only gene knock-down might be possible but also *in vivo* imaging of the dynamic of fluorescently tagged SC proteins in this transparent polyp.

Regardless of *Hydra's* suitability as complementary invertebrate model system for meiosis, comparative studies between distantly related metazoan species, as provided in this study, can be a useful tool to define evolutionary conserved properties of structural proteins. The comparison of orthologous SC proteins from various metazoan species revealed the existence of the conserved motifs CM1 and CM2 of SYCP1 and SYCP3 (Baier *et al.* 2007b; Winkel 2009). In the case of SYCP3, these domains were shown to be essential for the polymerization of the murine protein (Baier *et al.* 2007b). Additionally, the conserved distance of 146 aa between CM1 and CM2 might be the reason why HySYCP3 can co-assemble with the mammalian SYCP3 despite millions of years of evolution (Wiesner 2013). And also the observed conservation of the central domains of SYCE2 and Tex12 seems to be related to their polymerization properties (Davies *et al.* 2012). This finally means that the definition of highly conserved regions of SC proteins can provide a novel approach to investigate the protein interactions within the SC in more detail.

## 11 Perspectives

The presented analyses have demonstrated the monophyly of all mammalian SC proteins. Most of them were already part of an ancient SC as it can be observed in the present-day cnidarian species *Hydra*. According to the results, the mammalian-like SC emerged only once early in the evolution of *Metazoa*. Nevertheless, it evolved dynamically during the divergence of the animal lineages leading to a varying SC composition in different present-day organisms. But although all mammalian SC proteins and their evolution were examined in detail, several issues remain to be studied after this thesis.

In the near future, the expression analysis of HySYCP2 needs be completed to make assure statements about the identity of the ancestral protein as either SC protein component or component of the nucleolar cortical skeleton in oocytes. Furthermore, the functional relevance of the common conserved N-terminal domain of SYCP2 and NO145 should be determined. Maybe, an even closer inspection of potentially existing sequence domains and motifs might help to draw conclusions about the function of this protein region. This applies for the other SC proteins as well. As discussed above, the conservation of specific regions seems to be related to the polymerization and interaction properties of the proteins in most cases but specific sequence motif which would be conserved could not be identified yet.

The evolutionary study might also provide new approaches to further analyze the SC assembly process. Yet it is unknown how synapsis initiation takes place in *Hydra* in the absence of a mammalian-like initiation complex. Super-resolution imaging and biochemical binding assays could be applied to analyze if HySYCE2 can interact with HySYCP1 and if the dimensions of a HySYCE2/HyTex12 complex could substitute the lack of a SYCE1/SYCE3 complex in bridging the gaps between the TFs. This might provide new ideas for the model of the protein interactions in the SC assembly process also in the mouse model system.

Finally, *Hydra* can be further promoted as alternative model organism. The generation of a DNA expression construct which functions in the germline would open numerous possibilities to study a) the progression of the SC assembly *in vivo* by overexpression of fluorescently tagged proteins and b) the function of the cnidarian SC proteins by gene knock-down. Maybe, the key point is the selection of appropriate promotor and terminator sequences which would allow a reliable insertion and expression of the transgenes in the germ cells. Promotor and terminator sequences of *Sycp1* or *Sycp3* might be promising candidates for this and the 5' and 3' DNA regions of the respective genes need to be tested for functionality.

Generally, *Hydra* should be considered as alternative model organism also for other cell biological questions outside SC research. An ongoing study on the single *Hydra* lamin for example might result in new insights into the function of lamins and its relevance for tissue homeostasis.

## 12 Material

### 12.1 Biological material

#### 12.1.1 *Hydra* lineage: *Hydra vulgaris* AEP

*Hydra* medium

- Solution 1: 42 g/l  $\text{CaCl}_2 \cdot 2\text{H}_2\text{O}$   
in ddH<sub>2</sub>O, working concentration 1:1,000 in ddH<sub>2</sub>O
- Solution 2: 8.112 g/l  $\text{MgSO}_4 \cdot 7\text{H}_2\text{O}$   
4.238 g/l  $\text{NaHCO}_3$   
1.0958 g/l  $\text{K}_2\text{CO}_3$   
in ddH<sub>2</sub>O, working concentration 1:100 in ddH<sub>2</sub>O

*Hydra vulgaris* AEP was cultured in *Hydra* medium (HM) at 18°C. The animals were fed three times per week with *Artemia salina*, a brine shrimp (*Silver Star Artemia* dehydrated cysts, Inter Ryba GmbH). *Artemia* cysts were cultured in aerated saltwater with a concentration of 34 g NaCl/l to hatch for two days. Harvested *Artemia* were then rinsed and collected in ddH<sub>2</sub>O before feeding them to the *Hydra* cultures. The cultures had to be washed with new HM within 2-24 hours after feeding. For a detailed description of *Hydra* mass culturing, see also (Lenhoff and Brown 1970).

#### 12.1.2 Bacteria

##### **StrataClone SoloPack Competent Cells**

Competent bacterial cells from the *StrataClone* Blunt PCR Cloning Kit (Agilent, Böblingen) were used for transformation with the *Strata* pSC-B-amp/kan. Transformation was performed according to the manufacturer's instruction.

##### ***E. coli* XL1 blue**

Competent *E. coli* XL1 blue cells (Agilent, Böblingen) were transformed with a vector for clonal amplification of the plasmid after DNA cloning. The *E. coli* XL1 blue bacteria possess a tetracycline resistance. For efficient transformation, about 50-150 ng of the plasmid DNA were used.<sup>74</sup>

##### ***E. coli* Rosetta(DE3)<sup>TM</sup>**

Competent *E. coli* Rosetta<sup>TM</sup> cells were used for expression of eukaryotic proteins. The bacteria supply additional tRNAs for eukaryotic codons that are rarely used in bacteria on a chloramphenicol-resistant plasmid. The designation (DE3) indicates that the bacteria host contains an

---

<sup>74</sup> For the protocol of transformation of *E. coli* bacteria see on page 78.

IPTG inducible T7 RNA polymerase. Therefore this bacteria strain is suitable for protein expression from the pET vector or other T7-driven expression vectors. About 100-200 ng of plasmid DNA were used for transformation.<sup>75</sup>

### 12.1.3 Cell lines

#### COS-7 cells

The COS-7 cell line (ATTC CRL1651) originates from the kidney tissue of the African green monkey. Culturing of COS-7 cells occurred according to the description on page 94.

### 12.1.4 Antibodies

#### Primary antibodies

**Table 12-1:** Primary antibodies used in this study.

Antibody	Antigene	Host animal	Producer	Dilution and Incubation		Note
				IF	WB	
<b>Generated antibodies (polyclonal)</b>						
<b>α-HymSYCP1</b>	(C)ENRTDANVLKKNDSYK <i>Hydra magnipapillata</i>	Guinea-pig #31	SeqLab, Göttingen	1:50 2 h, RT		Final bleeding, purified
<b>α-HymSYCP3</b>	(C)SDEAPALLSKSSLKRRK <i>Hydra magnipapillata</i>	Guinea-pig #20, #21	SeqLab, Göttingen	1:150 2 h, RT	1:1,000 1 h, RT	Final bleeding, purified
<b>α-HySYCP1</b>	C-terminal peptide-6xHIS aa 789-1016 <i>Hydra AEP</i>	Rabbit #20	own synthesis (SeqLab, Göttingen)	1:900 1 h, RT	1:10,000 1 h, RT	Final bleeding, purified
<b>α-HySYCP1</b>	N-terminal peptide-6xHIS aa 1-137 <i>Hydra AEP</i>	Guinea-pig #44	own synthesis (SeqLab, Göttingen)	1:300 1 h, RT		Final bleeding, serum
<b>α-HySYCP3</b>	N-terminal peptide-6xHIS aa 1-84 <i>Hydra AEP</i>	Rabbit #58	own synthesis (SeqLab, Göttingen)	1:700 1 h, RT		Final bleeding, purified
<b>α-HySYCE2</b>	HySYCE2-6xHIS <i>Hydra AEP</i>	Rabbit #30, Guinea-pig #07	own synthesis (SeqLab, Göttingen)	1:200 1-2 d, 4°C	1:2,000 1 h, RT	Final bleeding, purified
<b>α-HyTex12</b>	HyTex12-6xHIS <i>Hydra AEP</i>	Guinea-pig #02,	own synthesis (SeqLab, Göttingen)	1:300 2 d, 4°C	no signal	2 <sup>nd</sup> bleeding, serum
		Rabbit #06		1:300 2 d, 4°C	no signal	Final bleeding, serum
<b>Purchased antibodies</b>						
<b>α-actin mono-</b>	Synthetic C-terminal peptide	Mouse	Sigma-Aldrich,		1:10,000 1 h, RT	

<sup>75</sup> For the protocol of transformation of *E. coli* bacteria see on page 78.

<b>clonal</b>			Steinheim (A4700)	
<b>α-myc</b>	Myc-Tag	Rabbit	Millipore, Darmstadt	1:200
<b>Dilution in ISH</b>				
<b>α-Dig-AP, fab frag- ments</b>	Digoxigenin	Sheep	Roche, Mannheim	1:2,000

## Secondary antibodies

**Table 12-2:** Secondary antibodies used in this study.

Antibody	Antigene	Host animal	Producer	Dilution	
				IF	WB
<b>α-Rb Texas Red</b>	IgG Rabbit	Goat	Dianova, Hamburg	1:50	
<b>α-Gp Texas Red</b>	IgG Guinea-pig	Goat	Dianova, Hamburg	1:50	
<b>α-Rb Cy2</b>	IgG Rabbit	Goat	Dianova, Hamburg	1:50	
<b>α-Gp Cy2</b>	IgG Guinea-pig	Goat	Dianova, Hamburg	1:50	
<b>α-Rb Alexa488</b>	IgG Rabbit	Goat	Dianova, Hamburg	1:600	
<b>α-Rb HRP</b>	IgG Rabbit	Goat	Dianova, Hamburg		1:10,000
<b>α-Gp HRP</b>	IgG Guinea-pig	Goat	Dianova, Hamburg		1:10,000
<b>α-mouse HRP</b>	IgG Mouse	Goat	Dianova, Hamburg		1:10,000

## 12.2 Molecular material

### 12.2.1 Plasmids

#### **Strata pSC-B-amp/kan**

The *Strata* pSC-B-amp/kan (Agilent, Böblingen) was used in combination with the *StrataClone* Blunt PCR Cloning Kit for efficient cloning of non-phosphorylated blunt-ended PCR products.<sup>76</sup> The plasmid encodes for a kanamycin- and an ampicillin-resistance and further allows blue/white screening. Standard primers (M13 forward, M13 revers, T7, T3) can be used for sequencing and colony PCR.<sup>77</sup>

#### **pET21a**

The pET21a plasmid (Novagen, Darmstadt) was used as expression vector system for proteins or peptides. It encodes for a 6xHIS tag that is fused to the target peptide C-terminally if it is cloned in the same reading frame. The expression is driven by a T7 promotor which is compatible for protein expression in competent *E. coli* Rosetta(DE3)<sup>TM</sup> cells.<sup>78</sup> The pET21a contains an ampicillin-resistance marker.

<sup>76</sup> For the protocol of DNA cloning with *Strata* see on page 83.

<sup>77</sup> For a description of DNA sequencing and a protocol of the colony PCR see on page 81. A list of the used primers is given in **Table 12-3**.

<sup>78</sup> For the description of the bacterial strain see on page 68 and for the protocol of protein expression see on page 88.

## pCMVmyc

pCMVmyc (Clontech, Heidelberg) is a plasmid encoding a c-myc upstream from the multiple cloning site. This results in a myc-tag that is fused to the N-terminus of a target peptide if this is cloned in frame. The expression is driven by a strong human cytomegalovirus (CMV) promoter. So the vector could be used for protein expression in eukaryotic cells, e.g. COS-7 cells.<sup>79</sup> For positive selection, the plasmid contains an ampicillin-resistance marker.

## pEGFP

pEGFP vectors (Clontech, Heidelberg) are eukaryotic expression systems including several different plasmids with the *EGFP* gene upstream (pEGFP C) or downstream (pEGFP N) of the multiple cloning site, each of them being available in all three possible reading frames (1, 2 or 3). By choosing the appropriate plasmid, it is possible to express every desired EGFP fusion protein. Alternatively, wild-type proteins can be expressed when cloned out of frame and with a stop codon in front of the tag of a pEGFP N vector. The expression is driven by the human cytomegalovirus (CMV) promoter that is active in eukaryotic cells. The plasmid encodes for a kanamycin-resistance to select for positive clones.

### 12.2.2 Oligonucleotides

**Table 12-3:** Oligonucleotides used in this study. Synthesis was performed by either Thermo Fisher Scientific (UlM) or Sigma-Aldrich (Steinheim).

Application	Oligo Name	Sequence (5' to 3')	Annealing Temperature
<b>HySycp1</b>			
<b>cDNA cloning/ sequencing</b>			
forward	HymSYCP1_5'ATG	ATGGAAAGTTTTCGAATGAATACTACTA-ACAAGCAA	65°C
revers	HymSYCP1_3'TGA_neu	GCAGACGTTCAACTATCA-AATCCAAAGACT	65°C
<b>Sequencing</b>			
revers	HymSYCP1_1012_3'	TTCAATTTTGGTTTGATTAAGAGTCA-AAGAAAGATT	62°C
revers	HymSYCP1_619_3'	CTACTTGATTTTCAAGATGATGAATAC-CTGACTCTAGACT	63°C
forward	HymSYCP1_1012_5'	CTTTCTTTGACTCTTAATCAAACCAAATT-GAA	60°C
forward	HymSYCP1_619_5'	AGTCTAGAGTCAGGTATTCATCATCTT-GAAAATCAAGTAG	63°
<b>RT/ ISH probe</b>			
forward	HymSYCP1_5'ATG	ATGGAAAGTTTTCGAATGAATACTACTA-ACAAGCAA	63°C/ 54°C
revers	HymSYCP1_1012_3'	TTCAATTTTGGTTTGATTAAGAGTCA-AAGAAAGATT	63°C
<b>Cloning of C-terminal antibody epitope</b>			
forward	Sycp1C-Term_NdeI_AS798_5'	CATATGAAGTTAAAGTCACAGACTGTTGAT-TCAC	62/68°C
revers	Sycp1C-	GTCGACACTATCAAATCCAAAGACTGT-	62/68°C

<sup>79</sup> For the protocol of transfection of DNA and protein expression in eukaryotic cells see on page 94.

	Term_ohneStop_Sall_3'	CAG	
<b>Cloning of N-terminal antibody epitope</b>			
forward	Sycp1N-Term_NdeI_5'	CATATGGAAAAGTTTTCGAATGAATACT	63°C
revers	Sycp1N-Term_AS137_Sall_3'	GTCGACACGTAGTATATTTGCCATT	63°C
<b>HySycp3</b>			
<b>cDNA cloning/ sequencing/ RT/ ISH probe</b>			
forward	Hym_SYCP3_5'	GTCCGCAATTAGTGAGCAATGAACGAT	64°C/ 54°C
revers	Hym_SYCP3_3'TAA	GACTTAAACACTGTGTAGCAAGCTTT-GAAGCGA	64°C
<b>Cloning of N-terminal antibody epitope</b>			
forward	Sycp3N-Term_NdeI_5'	CATATGAACGATAAAAAAAGAG-TAAGCAAAC	64°C/67°C
revers	Sycp3N-Term_Sall_3'	GTCGACTAGACTTTTACTAATGTCAGCAC-CAAAG	64°C/67°C
<b>HySyce2</b>			
<b>cDNA cloning/ sequencing/ RT/ ISH probe</b>			
forward	Hy_Syce2_ATG 5'	ATGACTAACAAACGCAAGTTTGTGAG	66°C/ 54°C
revers	Hy_Syce2_TGA 3'	CTACTGCAATGATGGATAGGTAGCTTG	66°C
<b>Cloning of antibody epitope (full-length protein)</b>			
forward	Syce2_NdeI_ATG_5'	CATATGACTAACAAACGCAAGTTTGTGAG	65°C
revers	Syce2_ohneStop_Sall_3'	GTCGACCTGCAATGATGGATAGGTAG	65°C
<b>HyTex12</b>			
<b>cDNA cloning/ sequencing/ RT/ ISH probe</b>			
revers	HyTex12 5'	CTGAACATGTGTA AAAATGTCTCAG	61°C
forward	HyTex12 3'	CAGTTTTAATATT-TAAGTGTAAAAGTGTTAATAG	61°C/ 60°C
<b>Cloning of antibody epitope (full-length protein)</b>			
forward	NdeI_HyTex12_ATG 5'	CATATGAATAACTGATAATAGTG-TATTTCTTACTC	62°C
revers	HyTex12_o.Stopp_Sall_3'	GTCGACAAGTTCGTTGTCG	62°C
<b>pCMVmyc vector cloning</b>			
forward	HyTex12_ATG_Sall 5'	GTCGACAATGAATAACTGATAATAGTG-TATTTTC	63°C
revers	HyTex12_Taa 3' II	TTAAAGTTCGTTGTCGCTTACAAG	63°C
<b>HySycp2, partial</b>			
<b>cDNA cloning/ sequencing/ ISH probe</b>			
forward	HySycp2_part_5'	ATGGTTTCAATTGATGACCG	60°C
revers	HySycp2_shortpart_3' neu	CATAGAATCATCTTGGACATAAGTTG	60°C
<b>Cloning of antibody epitope</b>			
forward	NdeI_HySycp2_ATG 5'	CATATGGTTTCAATTGATGACC	60°C
revers	HySycp2_Sall 3'	GTCGACCATAGAATCATCTTGG	60°C
<b>HyActin</b>			
<b>RT</b>			
forward	Hym_actin_5'	AAGCTCTTCCCTTGAGAAATC	60°C
revers	Hym_actin_3'	CCAAAATAGATCCTCCGATCC	60°C
<b>standard primer</b>			
<b>ISH probe</b>			
	T7	TAATACGACTCACTATAGGG	54°C/60°C
<b>Colony PCR/ sequencing in Strata pS-B-amp/kan</b>			
revers	M13 forward	TGTA AACGACGCGCCAGT	54°C
forward	M13 revers	CAGGAAACAGCTATGACC	54°C
forward	T3	ATTAACCTCACTAAAGGGA	54°C
revers	T7	TAATACGACTCACTATAGGG	54°C
<b>Colony PCR/ sequencing in pET21a</b>			
forward	pET 5'	CGATCCCGCAAATTAATACG	54°C



revers	pET 3'	GGCAGCAGCCAACTCAGCTTC	54°C
<b>Colony PCR/ sequencing in pCMV myc</b>			
forward	pCMV myc/HA 5'	AGCTGCGGAATTGTACCC	54°C
revers	pCMV myc/HA 3'	TGGTTTGTCCAAACTCATCAA	54°C
<b>Colony PCR/ sequencing in pEGFP N</b>			
forward	pEGFP N 5'	GCTGGTTTAGTGAACCGTCAGA	54°C
revers	pEGFP N 3'	CGTCGCCGTCCAGCTCGACCAG	54°C

### 12.2.3 Recombinant DNA constructs

The following recombinant DNA constructs were cloned for the expression in either bacteria or eukaryotic cells. For the respective protocols of DNA cloning, protein synthesis in bacteria or expression in somatic COS-7 cells, see on pages 83, 88 f. and 94. A list of the specific primers, which were used for cloning, is provided in **Table 12-3**.

#### ***HySycp1* N-terminus in pET21a**

##### **Protein product: HySYCP1 N-term-6xHIS**

The N-terminus of *HySycp1* encoding for aa 24-137 was amplified from the Strata\_*HySycp1* full length, K3 plasmid with the *Sycp1N-Term\_ NdeI\_5'/ Sycp1N-Term\_AS137\_Sall\_3'* primer pair and cloned into the pET21a via the NdeI and Sall restriction sites of the plasmid. The resultant plasmid was used for expression of the *HySycp1* N-terminus in *E. coli* Rosetta(DE3)<sup>™</sup> cells in the process of antibody synthesis.

#### ***HySycp1* C-terminus in pET21a**

##### **Protein product: HySYCP1 C-term-6xHIS**

The C-terminus of *HySycp1* encoding for aa 789-1016 was amplified from cDNA with the *Sycp1C-Term\_ NdeI\_AS798\_5'/Sycp1C-Term\_ohneStop\_Sall\_3'* primer pair and cloned into the pET21a via the NdeI and Sall restriction sites of the plasmid. The resultant plasmid was used for expression of the *HySycp1* C-terminus in *E. coli* Rosetta(DE3)<sup>™</sup> cells in the process of antibody synthesis.

#### ***HySycp3* N-terminus in pET21a**

##### **Protein product: HySYCP3 N-term-6xHIS**

The N-terminus of *HySycp3* encoding for aa 1-84 was amplified from the Strata\_*HySycp3* full length, K1 plasmid with the *Sycp3N-Term\_ NdeI\_5'/ Sycp3N-Term\_ Sall\_3'* primer pair and cloned into the pET21a via the NdeI and Sall restriction sites of the plasmid. The resultant plasmid was used for expression of the *HySycp3* N-terminus in *E. coli* Rosetta(DE3)<sup>™</sup> cells in the process of antibody synthesis.

### **HySyce2 in pET21a**

#### **Protein product: HySYCE2-6xHIS**

*HySyce2* was amplified from the Strata\_HySyce2 full length, K1 plasmid with the Syce2\_NdeI\_ATG\_5'/Syce2\_ohneStop\_Sall\_3' primer pair and cloned into the pET21a via the NdeI and Sall restriction sites of the plasmid. The resultant plasmid was used for expression of the *HySycp2* in *E. coli* Rosetta(DE3)<sup>™</sup> cells in the process of antibody synthesis.

### **HyTex12 in pET21a**

#### **Protein product: HyTex12-6xHIS**

*HyTex12* was amplified from the Strata\_HyTex12 full length, K4 plasmid with the NdeI\_HyTex12\_ATG 5'/HyTex12\_o.Stopp\_Sall\_3' primer pair and cloned into the pET21a via the NdeI and Sall restriction sites of the plasmid. The resultant plasmid was used for expression of the *HyTex12* in *E. coli* Rosetta(DE3)<sup>™</sup> cells in the process of antibody synthesis.

### **HySycp2 partial in pET21a**

#### **Protein product: HySYCP2 partial-6xHIS**

*HySycp2 partial* was amplified from the Strata\_HySycp2 shortpart, K15 plasmid with the NdeI\_HySycp2\_ATG 5'/HySycp2\_Sall\_3' primer pair and cloned into the pET21a via the NdeI and Sall restriction sites of the plasmid. The resultant plasmid was used for expression of the *HySycp2 fragment* in *E. coli* Rosetta(DE3)<sup>™</sup> cells in the process of antibody synthesis.

### **HySyce2 in pEGFP N3**

#### **Protein product: HySYCE2**

*HySyce2* was digested from the Strata\_HySyce2 full length, K8 with the restriction enzymes PstI and Sall and ligated into the corresponding restriction sites of the pEGFP N3 vector out of frame to the EGFP tag. The resultant plasmid was used for HySYCE2 expression in COS-7 cells.

### **HyTex12 in pCMV myc**

#### **Protein product: myc-HyTex12**

*HyTex12* was amplified from the Strata\_HyTex12 full length, K4 plasmid with the HyTex12\_ATG\_Sall 5'/HyTex12\_Taa 3' II primer pair and cloned into the pCMVmyc via the Sall and NotI restriction sites. The resultant plasmid was used for myc-HyTex12 expression in COS-7 cells.

## **12.3 Chemicals**

Chemicals used in this study were purchased from AppliChem (Darmstadt), Merck (Darmstadt), Roth (Karlsruhe), Serva (Heidelberg) and Sigma-Aldrich (Steinheim).

## 12.4 Computer software and Online Tools

**Table 12-4:** Computer software and Online tools used in this study.

Computer software	Application
Leica Confocal Software TCS SP2	Image acquisition
Adobe Photoshop	Image processing
Microsoft Office 2010	Scheme design
CLC DNA Workbench 6	DNA sequence analysis
Seaview 4.4.0	Protein alignment NJ tree and ML tree calculation
MAFFT	Protein alignment
BMGE	Adjustments of protein alignment
PhyML 3.0.1	ML tree calculation
MrBayes 3.2.1	BI tree calculation
CHROMA 1.0	Annotation of protein sequence alignment
Online Tools	
<b>BLAST at Compagen</b> <a href="http://www.compagen.org/">http://www.compagen.org/</a>	Transcriptome analysis of <i>Hydra vulgaris</i> AEP
<b>BLAST/PSI-BLAST at the NCBI</b> <a href="http://blast.ncbi.nlm.nih.gov">http://blast.ncbi.nlm.nih.gov</a>	Identification of homologues
<b>BLAST at Ensembl</b> <a href="http://www.ensembl.org/index.html">http://www.ensembl.org/index.html</a>	Identification of homologues
<b>BLAST at DFCI</b> <a href="http://compbio.dfci.harvard.edu">http://compbio.dfci.harvard.edu</a>	Identification of homologues
<b>BLAST at InParanoid 7</b> <a href="http://inparanoid.sbc.su.se/cgi-bin/index.cgi">http://inparanoid.sbc.su.se/cgi-bin/index.cgi</a>	Identification of homologues
<b>HMMer 3.0</b> <a href="http://hmmer.janelia.org">http://hmmer.janelia.org</a>	HMM profile Identification of homologues
<b>T-Coffee</b> <a href="http://www.t-coffee.org">www.t-coffee.org</a>	Protein alignment
<b>ClustalO</b> <a href="http://www.ebi.ac.uk/Tools/msa/clustalo/">http://www.ebi.ac.uk/Tools/msa/clustalo/</a>	Protein alignment
<b>SMART</b> <a href="http://smart.embl-heidelberg.de/">http://smart.embl-heidelberg.de/</a>	Identification of protein domains (coiled coils)
<b>PSORT II Prediction</b> <a href="http://psort.hgc.jp/form2.html">http://psort.hgc.jp/form2.html</a>	Identification of protein domains (coiled coils)
<b>IEDB Analysis Resource</b> <a href="http://tools.immuneepitope.org/tools/bcell/iedb_input">http://tools.immuneepitope.org/tools/bcell/iedb_input</a>	Antibody epitope prediction
<b>ExpASy Translate Tool</b> <a href="http://web.expasy.org/translate/">http://web.expasy.org/translate/</a>	Translation of a nucleotide sequence
<b>Bioinformatics Organization - Sequence manipulation Suite</b> <a href="http://www.bioinformatics.org/sms/">http://www.bioinformatics.org/sms/</a>	Format conversion: revers complement, prediction of protein molecular weight

## 12.5 Equipment

**Table 12-5:** Special equipment used in this study.

<b>Binocular SZ 61, equipped with Camera EC3</b>	Olympus, Hamburg Leica, Wetzlar
--	------------------------------------

---

<b>Centrifuge 6-16K</b>	Sigma, Osterode
<b>Centrifuge MIKRO 200/ 200R</b>	Hettich, Tuttlingen
<b>Confocal laser scanning microscope TCS-SP2 AOBS</b>	Leica, Wetzlar
<b>Electrophoresis Power Supply</b>	PeqLab, Erlangen
<b>Freezing microtom 2800 Frigocut E</b>	Reichert-Jung, Heidelberg
<b>Gradient Thermocycler T100</b>	BioRad, Munich
<b>Graphite blotting chamber</b>	LMS, Hartenstein Würzburg
<b>Hybridization oven MINI 10</b>	MWG Biotech, Ebersberg
<b>Infinite M200</b>	Tecan, Männerdorf
<b>Laboratory peristaltic pump Varioperpex® II</b>	LKB/Bromma, Schweden
<b>Protein gel electrophoresis chamber Mini V8</b>	Gibco BRL
<b>Thermocycler Primus 25 advanced</b>	PeqLab, Erlangen

---

## 13 Methods

### 13.1 Microbiological methods

#### 13.1.1 Culturing of bacteria

##### Liquid Culture

- LB medium (1L): 10 g bacto-trypton  
10 g NaCl  
5 g yeast-Extract  
pH 7.4, autoclavation
- Antibiotics: see **Table 13-1**:

**Table 13-1:** Antibiotic solutions used in this study.

	Stock solution	Working concentration
<b>Ampicillin</b>	50 mg/ml in ddH <sub>2</sub> O	100 µg/ml
<b>Kanamycin</b>	50 mg/ml in ddH <sub>2</sub> O	50 µg/ml
<b>Tetracyclin</b>	15 mg/ml in 70% ethanol	15 µg/ml
<b>Chloramphenicol</b>	34 mg/ml in ethanol	34 µg/ml

10 ml LB medium were filled in a 50 ml *Greiner* tube for a liquid overnight bacteria culture. The matching antibiotic was added to the appropriate working concentration in correspondence to the cultivated bacteria strain. Finally, the culture was inoculated with the respective bacteria from a glycerin stock or an agar plate and incubated at 37°C overnight while it was slightly shaken.

##### Glycerol stock

A glycerol stock from a certain bacteria strain, which allows long-term storage of the bacteria at -80°C, was made of 150 µl of a liquid culture and 850 µl glycerol. The liquids were mixed in a 1.5 ml *Eppendorf* tube very gently and frozen at -80°C.

##### Culturing on agar plates

- 1.5% agar in LB medium
- Antibiotics: see **Table 13-1**:

1.5% agar was suspended in LB medium and autoclaved. When the medium was cooled down to ca. 50°C, the desired antibiotic could be added in the appropriate working concentration. The agar LB medium was poured into steril plates and left at room temperature overnight to set it hard and dry. The plates were turned upside down and stored at 4°C. About 200 µl of a liquid bacteria culture could be streaked onto a plate after drying the plate again for at least 1 h at 37°C (lid open). This solid culture was incubated at 37°C overnight with the plate turned upside down again.

### 13.1.2 Production of competent bacteria

- TSS (Transformation and Storage Solution): 10% (w/v) PEG 3350 or 8000  
5% (v/v) DMSO  
50-70 mM Mg<sup>2+</sup> (MgCl<sub>2</sub>)  
pH 6.5, steril filtration, storage at -20°C
- LB medium<sup>80</sup>
- Antibiotics: see **Table 13-1**

To produce competent bacteria, which could efficiently take up foreign plasmid DNA, 200 ml LB medium mixed with the antibiotics that corresponded to the respective bacteria strain, were inoculated with 3 ml of a liquid overnight culture<sup>81</sup>. The bacteria were incubated on the shaker at 37°C until the culture reached the exponential growth phase (OD<sub>600</sub> 0.4-0.8). Then the culture was split to 50 ml *Greiner* tubes and centrifuged at 900g and 4°C for 10 min. The supernatants were removed and the pellets were resuspended quickly in X ml TSS, with X being 1/40 of the original culture volume thereby keeping the pellets cooled on ice. The bacteria were frozen in liquid N<sub>2</sub> in 100 µl aliquots (in 1.5 ml *Eppendorf* tubes) and stored at -80°C.

### 13.1.3 Transformation of *E. coli* bacteria with plasmid DNA

- LB medium<sup>82</sup>

Competent bacteria can be transformed with circular plasmid DNA that has an own replication origin and encodes a specific antibiotic resistance that allows selection of positive transformants.

An aliquot of competent bacteria<sup>83</sup> was thawed on ice for 15 min and mixed with ca. 5-150 ng of plasmid DNA or one ligation preparation. The bacteria were incubated on ice for 1 h. The following heat shock at 42°C for 60 sec improved the DNA take up of the bacteria. Finally, 900 µl LB medium were added and the bacteria were cultured at 37°C for 1 h by shaking them at roughly 200g. The bacteria established the new antibiotic resistance from the plasmid DNA during this time. Afterwards the bacterial solution was gently centrifuged at 700g for 3 min and the supernatant was removed leaving approximately 200 µl of LB medium in the tube. The bacterial pellet was resuspended in the remaining medium and streaked on an agar plate with the matching antibiotic resistance.<sup>84</sup>

The transformation of *StrataClone* SoloPack competent cells was performed according to the instructions of the manufacturer.

---

<sup>80</sup> For the recipe of LB medium see on page 77.

<sup>81</sup> For the protocol of a liquid overnight culture see on page 77.

<sup>82</sup> For the recipe of LB medium see on page 77.

<sup>83</sup> For the protocol of the production of competent bacteria see on the same page. A description of the bacterial strains is given on page 68.

<sup>84</sup> For the protocol of culturing bacteria on agar plates see on page 77.

## Testing transformation efficiency

After the production of competent bacteria, as described above, their transformation efficiency could be tested by transforming them with a serial DNA dilution of 100 µg, 10 µg and 1 µg of a standard pUC-vector. The transformation efficiency is defined as number of transformed bacterial colonies per 1 µg of used pUC-vector DNA and could be calculated from the number of bacterial colonies that resulted from the test transformation. The efficiency should be at approximately  $10^6$  transformants, at least.

## 13.2 Molecular methods

### 13.2.1 RNA extraction

- *peqGOLD Trifast<sup>TM</sup>* (PEQLAB, Erlangen)

Total mRNA was extracted from entire animals (5-10 animals/ preparation) or separated tissues (tissues of approximately 50 animals/ preparation) with the *peqGOLD Trifast<sup>TM</sup>* kit following the instruction of the manufacture. Accordingly, 250-300 µl *TriFast* were used for one preparation.

### 13.2.2 Purification of plasmid DNA

- *NucleoSpin<sup>®</sup> Plasmid* (Macherey-Nagel, Düren)

Plasmid DNA was purified from a 10 ml overnight culture<sup>85</sup> of the respective bacterial transformant with the *NucleoSpin<sup>®</sup> Plasmid* kit. The isolated DNA was eluted in 50 µl ddH<sub>2</sub>O. DNA concentration was measured at the *infiniteM200* of Tecan (Männedorf, Switzerland).

### 13.2.3 Polymerase chain reaction (PCR)

The polymerase chain reaction (PCR) is a method to easily amplify DNA fragments *in vitro*. The reaction is divided into three major steps:

1. **Denaturation** of the double stranded DNA template at 95-98°C.
2. **Annealing** of the short (approximately 18 bp) single stranded DNA oligonucleotides which define the respective DNA fragment (forward and reverse primer<sup>86</sup>) to the denatured template DNA. The primers are complementary to the 5' start and the 3' end of the DNA fragment and serve as starting point for DNA synthesis. The annealing temperature is specific for each primer depending on its sequence and should be between 50°C-70°C. The annealing temperatures for the two primers used in a PCR should nearly be equal.
3. **Elongation** of the new DNA strand that is catalyzed by a thermostable DNA polymerase at 72°C. The enzyme binds to the 3' end of the primers and synthesizes the new

---

<sup>85</sup> For the protocol of an overnight culture see on page 77.

<sup>86</sup> A list of the specific primers which were used in this study is provided in **Table 12-3**.

DNA strand complementary to the DNA template in 5' to 3' orientation. The elongation time is dependent on the enzyme and the length of the amplified DNA fragment.

### Reverse transcription (RT)-PCR

- *RiboLock<sup>TM</sup>* ribonuclease inhibitor (Fermentas, St. Leon Roth)
- *Reverse Transcriptase M-MLV* and *M-MLV RT 5x buffer* (Promega, Mannheim)
- dNTPs (Fermentas, St. Leon Roth)
- Oligo(dT)<sub>18</sub> primer (Fermentas, St. Leon Roth)

Extracted mRNA from entire animals or tissues<sup>87</sup> is converted (reversely transcribed) into complementary DNA (cDNA) by a RNA-dependent DNA polymerase in a first step. The resulting cDNA can be used as template for further cloning attempts of specific genes. In contrast to genomic DNA, cDNA has the advantage that it only contains the coding regions of the DNA. Introns as well as regulatory DNA sequences, e.g. promotor or terminator regions, are not present in the cDNA preparation.

Protocol for 20 µl preparation:

- 1 µg RNA
- 1 µl RNase inhibitor (40 U/µl)
- 4 µl 5x RT-buffer
- 1 µl dNTPs (10 mM/nucleotide)
- 1 µl oligo(dT) primer (500 µg/ml)
- 1 µl reverse transcriptase (200 U/µl)
- ddH<sub>2</sub>O to 20 µl

The mixture was incubated at 37°C for 1 h. Subsequently, the enzyme was heat inactivated at 95° for 5 min. Afterwards 1-2 µl of the cDNA could be used in a PCR reaction. The remaining cDNA preparation was stored at -20°C.

### *Phusion<sup>TM</sup>* PCR

- *Phusion<sup>TM</sup>* DNA polymerase and 5x *Phusion HF buffer* (Thermo Scientific, Schwerte)
- dNTPs (Fermentas, St. Leon Roth)
- specific primer pairs (Sigma-Aldrich, Steinheim)

The *Phusion<sup>TM</sup>* is a synthetic DNA polymerase with a proof-reading activity that was fused to a processivity-enhancing domain. This led to the improvement of fidelity and speed. The enzyme produces non-phosphorylated blunt ends. Because of its specific features, the *Phusion* was used for amplification of DNA that was further processed in a cloning approach.

Protocol for 50 µl preparation:

- 5-10 ng template DNA or 0.5-1 µl cDNA
- 1 µl 5' primer (10 pmol/µl)
- 1 µl 3' primer (10 pmol/µl)
- 1 µl dNTPs (10 mM/nucleotide)
- 1.5 µl DMSO
- 10 µl 5x HF reaction buffer
- 0.3 µl *Phusion<sup>TM</sup>* DNA polymerase (2 U/µl)
- ddH<sub>2</sub>O to 50 µl

cycling protocol:    initial denaturation            98°C    2 min

<sup>87</sup> For the protocol of mRNA extraction see on page 79.



denaturation	98°C	20 sec	} 35x
primer annealing	X°C <sup>88</sup>	30 sec	
elongation	72°C	1 kb/15 sec	
final elongation	72°C	10 min	
cooling down to	8°C		

### Colony PCR with Taq-polymerase

- Taq DNA polymerase and 10x Taq buffer (own synthesis)
- dNTPs (Fermentas, St. Leon Roth)
- specific primer pairs (Sigma-Aldrich, Steinheim)

The Taq polymerase is a DNA polymerase from the bacteria *Thermus aquaticus*. In contrast to the *Phusion<sup>TM</sup>*, it produces 5' adenine overhangs and does not possess a proof-reading activity. Therefore, it was used for colony PCR where mutations in the amplicates do not matter. Instead, colony PCR was used to check the success of a transformation of grown bacterial colonies with a certain cloned plasmid. A master-mix was prepared as X-fold enlargement of the following protocol.

Protocol for 25 µl preparation: 100 ng template DNA or one bacteria colony  
 0.25 µl 5' primer (10 pmol/µl)  
 0.25 µl 3' primer (10 pmol/µl)  
 0.5 µl dNTPs (10 mM/nucleotide)  
 1.5 µl MgCl<sub>2</sub> (25 mM)  
 2.5 µl 10x Taq buffer  
 0.5 µl Taq DNA polymerase (≈ 5 U/µl)  
 ddH<sub>2</sub>O to 25 µl

The master-mix was then split to X labeled PCR tubes (25 µl/ tube). Each tube was finally mixed with bacteria of one single colony from an agar plate by picking them with a pipette tip and resuspending them in the PCR preparation. Before, the picked bacterial colony was tipped to a new agar plate - the master plate - on which the tested colonies were cultured in a numbered order.

cycling protocol:	initial denaturation	95°C	2 min	} 25x
	denaturation	95°C	30 sec	
	primer annealing	X°C <sup>89</sup>	30 sec	
	elongation	72°C	1 kb/1 min	
	final elongation	72°C	7 min	
	cooling down to	8°C		

### 13.2.4 DNA sequencing

Sequencing of cloned DNA molecules was performed by GATC Biotech (Konstanz).

### 13.2.5 DNA gel electrophoresis

- 20x SB buffer: 200 mM NaOH

<sup>88</sup> X is the primer specific annealing temperature, usually between 60°C-70°C.

<sup>89</sup> X is the primer specific annealing temperature, usually between 50°C-60°C.

adjust to pH 8.0 with saturated boric acid

- 6x DNA loading buffer: 60% glycerol  
30% 0.2 M EDTA  
10% ddH<sub>2</sub>O  
+ 4% orange G  
+ 2% xylene cyanol  
1x working dilution
- $\lambda$  DNA EcoRI+HindIII DNA marker (Fermentas, St. Leon Roth)
- 0.8%-1.2% agarose (peqGOLD Universal Agarose from PeqLab, Erlangen) in 1x SB buffer
- ethidium bromide

DNA fragments of different electrophoretic mobility can be separated in a DNA agarose gel electrophoresis. The electrophoretic mobility is dependent on size, conformation and charge of the molecule.

A 0.8% agarose gel was used as standard to mainly separate linear fragments between 300-1,500 bp. Higher or lower agarose concentrations would be used to separate shorter or longer DNA molecules, respectively. The agarose was heated in 1x SB buffer until it was dissolved completely and mixed with 0.001% ethidium bromide to stain the DNA in the gel. The agarose solution was then poured into a cast which was prepared with a comb to leave wells for loading the samples and finally set completely dry before use. 50 ml agarose solution were used for a small cast. The set gel was placed in the electrophoresis chamber which was filled with 1x SB buffer. Then the DNA samples were mixed with 6x DNA loading buffer and loaded onto the gel. A voltage of 150-200 V was applied to the electrophoresis chamber. The negatively charged DNA molecules move through the agarose matrix to the positive electrical pole with different speed in the electric field depending on their size. A reference for the estimation of fragment's size, e.g. the  $\lambda$  DNA EcoRI+HindIII DNA marker, was always run in the first lane of the gel. The electrophoresis was run for 10 – 15 min. Finally, the DNA, which was stained with the intercalating ethidium bromide, could be visualized in the gel with UV light.

### 13.2.6 Preparative DNA gel electrophoresis and gel extraction

- *NucleoSpin® Gel and PCR Clean up* (Macherey-Nagel, Düren)

A certain DNA fragment with a specific size which is required for further usage can first be separated from other fragments in a DNA gel electrophoresis<sup>90</sup> and afterwards extracted from the gel.

A slice containing the respective DNA band was cut out from the gel under UV light and the DNA was finally purified from the remaining agarose matrix with the *NucleoSpin® Gel and PCR Clean up* kit. Additionally, the kit was used for the purification of PCR products.

---

<sup>90</sup> For the protocol of DNA gel electrophoresis see on page 81.

### 13.2.7 DNA cloning

#### **StrataClone**

- *StrataClone* Blunt PCR Cloning Kit (Agilent Technologies, Böblingen)

The *StrataClone* Blunt PCR Cloning Kit was used for fast and efficient cloning of non-phosphorylated blunt-ended PCR products from a *Phusion*<sup>TM</sup> PCR<sup>91</sup> into the standardized vector system of the *Strata* pSC-B-amp/kan<sup>92</sup>. The cloning procedure was performed according to the manufacturer's instructions, but with half of the recommended preparation per cloning attempt.

#### **Restriction digest**

- Restriction enzymes and corresponding 10x buffers (Fermentas, St. Leon Roth and New England Biolabs, Frankfurt am Main)

A DNA fragment can be inserted into a DNA plasmid via selected restriction sites that were cut by specific restriction endonucleases. Each restriction enzyme cuts a specific, palindromic recognition site in the DNA producing either 5'-phosphorylated blunt or sticky ends with a 5' or 3' overhang. Ends which are produced by the same enzyme can be efficiently joined by the DNA ligase.<sup>93</sup>

Protocol for 10 µl preparation: 1 µg DNA  
1 µl restriction enzyme 1 (10 U/µl)  
1 µl restriction enzyme 2 (10 U/µl), in a double digest  
1 µl 10x enzyme buffer (appropriate to enzyme 1 and 2)  
ddH<sub>2</sub>O to 10 µl

The preparation for the restriction digest was mixed and incubated at a temperature that was dependent on the applied enzymes, usually 37°C, for 1-2 h. Afterwards the enzymes were heat inactivated at 65°C-85°C for 20 min. Because of the required ratio of digested vector and insert during ligation, 3x vector and 5x-7x insert digests were usually prepared at the same time. After the reaction, the respective DNA fragments were extracted from a preparative agarose gel.<sup>94</sup>

#### **Ligation**

- *T4 DNA ligase* and *T4 10x ligation buffer* (Fermentas, St. Leon Roth)

DNA fragments, such as a vector and DNA insert, with complementary 5'- or 3'-overhangs which have been produced by the same restriction enzyme or blunt ends which were cut with a blunt end producing enzyme or by PCR, can be joined covalently during ligation. The enzyme, which is called ligase, catalyzes the formation of a phosphodiester bond between the 3' hydroxyl end of one DNA fragment and the 5' phosphate end of the other DNA molecule. There-

---

<sup>91</sup> For the protocol of the *Phusion*-PCR see on page 80.

<sup>92</sup> A description of the plasmid is given on page 70.

<sup>93</sup> For the protocol of DNA ligation see below.

<sup>94</sup> For the protocol of a preparative agarose gel and gel extraction see on page 82.

fore, at least one of the molecules needs to carry a phosphate at its 5' end of the respective ligation site. The insert molecules should be present in the preparation in a 5-fold excess over the vector molecules to achieve an efficient ligation reaction between a vector and an insert DNA.

Protocol for 20  $\mu$ l preparation:

- 150-300 ng vector DNA
- x  $\mu$ g insert DNA (molar ratio over vector 5:1)
- 2  $\mu$ l 10x ligation buffer
- 0.5  $\mu$ l ATP
- 1  $\mu$ l T4 ligase (5 U/ $\mu$ l)
- ddH<sub>2</sub>O to 20  $\mu$ l

The preparation was mixed according to the protocol and incubated overnight at 4°C. Afterwards the ligase was heat inactivated at 65°C for 15 min. Then the ligation preparation was ready to be used in a bacterial transformation of *E. coli* XL1 blue.<sup>95</sup>

## 13.3 Biochemical methods

### 13.3.1 Protein gel electrophoresis

Protein gel electrophoresis is a common method to separate proteins of different electrophoretic mobility in a gel matrix by application of an electric field. The molecular weight, the conformation and the charge of the molecule influence the protein mobility in the gel.

#### **Laemmli SDS-Page**

- Solution A: Acrylamide 4K, 30% (Applichem, Darmstadt)
- Solution B: 1 M Tris-HCl, pH 8.7
- Solution C: 1 M Tris-HCl, pH 6.8
- 20% (w/v) SDS in ddH<sub>2</sub>O
- Temed (Applichem, Darmstadt)
- 10% APS (w/v) in ddH<sub>2</sub>O
- 10x Running buffer: 250 mM Tris-HCl  
1.12 M glycine  
1% SDS  
pH 8.5  
1x working dilution
- 2x SDS sample buffer: 120 mM Tris-HCl  
10% (w/v) SDS  
20% (v/v) glycerol  
adjust to pH 6.8  
add 20% (v/v)  $\beta$ -mercaptoethanol  
bromophenol blue  
1x working dilution
- *PageRuler*<sup>™</sup> Prestained Protein ladder (Fermentas, St. Leon Roth)

---

<sup>95</sup> For the protocol of the bacterial transformation see on page 78 and for the description of the bacterial strain see on page 68.

**Table 13-2:** Pipetting schemes for separating gels of different polyacrylamid content and for the stacking gel. The mixtures last for at least two gels.

<b>Separating Gel</b>					
<b>Solutions</b>	<b>8%</b>	<b>9%</b>	<b>10%</b>	<b>12%</b>	<b>15%</b>
<b>Solution A</b>	4 ml	4.5 ml	5 ml	6 ml	7.5 ml
<b>Solution B</b>	5.6 ml	5.6 ml	5.6 ml	5.6 ml	5.6 ml
<b>20% SDS</b>	75 µl	75 µl	75 µl	75 µl	75 µl
<b>ddH<sub>2</sub>O</b>	5.215 ml	4.715 ml	4.215 ml	3.215 ml	1.715
<b>Temed</b>	20 µl	20 µl	20 µl	20 µl	20 µl
<b>10% APS</b>	100 µl	100 µl	100 µl	100 µl	100 µl

<b>Stacking Gel</b>	
<b>Solutions</b>	<b>5%</b>
<b>Solution A</b>	1.67 ml
<b>Solution C</b>	1.25 ml
<b>20% SDS</b>	50 µl
<b>ddH<sub>2</sub>O</b>	6.925 ml
<b>Temed</b>	20 µl
<b>10% APS</b>	150 µl

The SDS-Page uses a polyacrylamide gel matrix to separate proteins of different molecular weight. Different acrylamide concentrations in the separating gel can be used depending on the size range that needs to be resolved. High percentage gels are useful for the separation of small molecules while low percentage gels are useful for the separation of large molecules. Treatment of the samples with the detergent SDS (sodium dodecyl sulfate) results in the linearization/denaturation and negative charging of the proteins so that the influence of the individual conformation and charge on the mobility of the proteins in the gel can be neglected and a fractionation by size is achieved. In the electric field, the negatively charged proteins move through the matrix to the positive pole with different speed. The speed is depending on the molecular weight with small proteins moving faster than large proteins. The stacking gel, a gel with a large pore size, is needed to initially focus all proteins of a sample into a single sharp band before they enter the separating gel. A discontinuous buffer system, such as the *Laemmli* system, is necessary for this to work. It allows the formation of an ion gradient exclusively in the “stacking” region of the gel by choosing different pH values for the “stacking” and “resolving” region of the gel.

The samples were mixed with the 2x SDS sample buffer in 1.5 ml *Eppendorf* tubes and heated up to 95°C for at least 5 min or until the proteins or the tissue were solved. The samples were shortly centrifuged at high speed to collect the condensate.

To prepare the matrix, first, the ingredients for the separating gel were mixed<sup>96</sup> and polymerized between two glass plates. These glass plates had been separated by two laterally placed spacers and tightened with several fasteners before. The bottom side had been sealed with tape and a small layer of 0.5% agarose. The space between the glass plates was filled with the separating gel to a 2/3 height. A thin layer of ddH<sub>2</sub>O was pipetted onto the gel to obtain a

<sup>96</sup> For the pipetting scheme of the stacking and the separating gel see **Table 13-2**. Temed and APS were added last because they initiate the polymerization of the acrylamide.

smooth surface during the polymerization of the acrylamide. After the separating gel was set hard, the water was carefully removed and the remaining space between the glass plates was filled with the mixture of the stacking gel. A comb was inserted into the liquid stacking gel to create the wells for the samples. The gel was ready for use in the electrophoresis as soon as the stacking gel was polymerized.

The tape was removed from the bottom of the glass plates and the complete gel cassette was placed in the electrophoresis chamber. The anode and the cathode chamber were filled with 1x running buffer and the comb could be removed from the stacking gel. Now the samples were loaded. A protein ladder was run as reference for estimation of the protein size in the first lane. A voltage of 60 V was applied to the electrophoresis chamber until the samples were stacked in bands and reached the separating gel. Then the voltage was increased to 90 V and the electrophoresis was run for 1-2 h depending on the size range of the target proteins.

Afterwards the gel could be stained with coomassie to visualize the protein bands or could be used for Western blot analysis.<sup>97</sup>

### 13.3.2 Coomassie staining

- Coomassie staining solution: 0.05% (w/v) *Coomassie Brilliant blue R250* (Applichem)  
10% (v/v) isopropanol  
5% (v/v) acetic acid
- Coomassie destaining solution: 10% (v/v) isopropanol  
5% (v/v) acetic acid

Following a SDS-Page, a protein gel can be stained with coomassie, a dye which non-specifically binds to the proteins in a gel. Acetic acid is used to fix the proteins in the gel at the same time.

The protein gel was carefully taken from the glass plates. The stacking gel and the agarose that stuck to the top and the bottom side of the gel were removed. The remaining separating gel was stained in coomassie staining solution on a shaker for at least 2 h at room temperature. The excessive dye in the gel was removed by destaining in coomassie destaining solution until the protein bands could be seen. Usually, the incubation occurred on the shaker overnight.

### 13.3.3 Western Blot analysis

- CAPS buffer: 50 mM CAPS  
10% (v/v) methanol  
adjust to pH 10  
add 1 mM mercaptopropionic acid
- 1x TBST: 150 mM NaCl  
10 mM Tris-HCl  
0.1% (v/v) Tween  
pH 7.4
- 5-10% (w/v) milk in TBST, pH 7.4

---

<sup>97</sup> For the protocols of coomassie staining and Western blot analysis see sections below.

- Ponceau S: 0.2% Ponceau S in 3% TCA
- Western Lightning® *Plus*-ECL Enhanced Chemiluminescence Substrate (PerkinElmer, Waltham)

A Western blot analysis is used to detect a specific protein in a certain sample or tissue. Proteins that have been separated in a SDS-Page<sup>98</sup> can be transferred from the gel to a membrane during the blotting process. The membrane, which has a non-specific affinity for amino acids, can be incubated with specific antibodies to detect and visualize the band containing the protein of interest.

Subsequent to a SDS-Page, the separating gel was equilibrated in CAPS buffer for 10 min. A semidry blotting system was used as standard (Matsudaira 1987) which was set up in a graphite blotting chamber according to the following scheme:

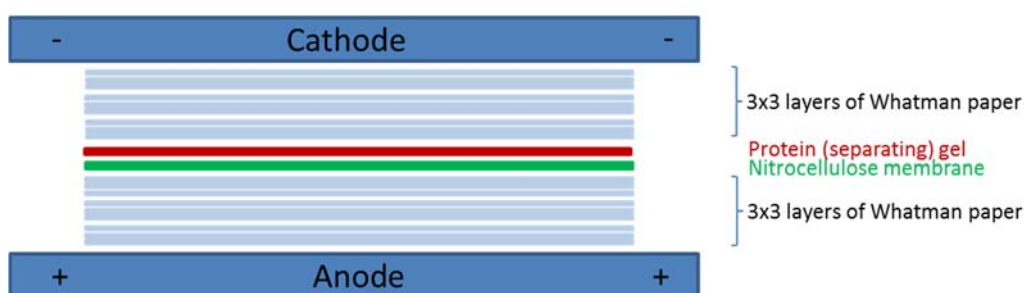


**Figure 13-1: Schematic illustration of the semidry Western blot set-up.**

The whatman papers as well as the nitrocellulose membrane (0.45  $\mu\text{m}$ , GE Healthcare, Munich) were cut in 9x5 cm pieces which was equal to the measurements of the protein gel. All layers were soaked in CAPS buffer before they were used in the set-up. To avoid air bubbles between the different layers of whatman paper, each layer was carefully pressed with a small *Greiner* tube. A blotting forceps was used during the whole experiment for handling of the nitrocellulose. A current of 1  $\text{mA}/\text{cm}^2$ , which was 45 mA for one blot by default, was applied to the blotting chamber for 45-60 min depending on the protein size. The negatively charged proteins move to the anode in the electric field, thereby leaving the gel and becoming immobilized onto the nitrocellulose membrane. When the blotting process was accomplished, the blot was deconstructed and the membrane had to remain moist for all following steps. The gel and the paper layers were disposed.

First, the membrane was stained in Ponceau S at room temperature for 3 min and washed in ddH<sub>2</sub>O to visualize the proteins in case of a successful transfer. The loaded lanes and the bands of the protein ladder were marked and traced with a graphite pencil.

Afterwards the membrane could be used for antibody detection. The nitrocellulose was washed in 1x TBST (3x 10 min) and blocked in milk at 4°C overnight to saturate its excessive binding capacities. The following day, the membrane was incubated in milk for 2 h at room temperature to restore a higher temperature before antibody incubation. The primary anti-

<sup>98</sup> For the protocol of protein gel electrophoresis see section above.

body was diluted in milk according to **Table 12-1** and added to the membrane at room temperature for at least 1 h. The membrane was washed again in 1x TBST (3x 10 min) and incubated with the secondary antibody which was diluted 1:10,000 in milk by default. The secondary antibody is coupled to a horseradish peroxidase (HRP) that catalyzes the chemical conversion of a supplied substrate. Light is emitted (chemiluminescence) during this process which is used to expose a radiographic film (AGFA Cronex 5, Hartenstein Laborversand, Würzburg). The membrane was incubated with the secondary antibody solution at room temperature for 45 min and could then be washed in 1x TBST for the last time. Eventually, the chemiluminescent ECL substrate was added to the membrane following manufacturer's instruction. The radiographic film was placed onto the membrane to become exposed by the emitted light in a dark-room. A dark band attested the existence of the target protein in a certain lane/sample after the development of the film.

### Stripping a nitrocellulose membrane

- Stripping buffer 1: 100 mM Glycin, pH 2
- Stripping buffer 2: 100 mM Tris-HCl  
2% SDS  
pH 6.7
- 1x TBST<sup>99</sup>

In case a second protein needs to be detected on the same nitrocellulose membrane, this membrane can be stripped to demolish the binding of the previous antibody and subsequently be incubated with another primary antibody. Therefore, the membrane was shortly washed in 1x TBST or alternatively stored in 1x TBST at 4°C overnight to remove all chemiluminescent substrate that remained from the first antibody detection. Then the membrane was successively incubated in stripping buffer 1 and 2 for 30 min each. After another short washing step with 1x TBST, the membrane was ready to be used in the next antibody incubation.

### 13.3.4 Expression and purification of HIS-tagged fusion proteins

An entire protein or protein fragments were expressed from the bacterial expression vector pET21a (Novagen, Darmstadt) in *E. coli* Rosetta™ bacteria.<sup>100</sup> After the expression, the protein can be purified from the bacteria through a nickel affinity chromatography matrix (nickel-nitrilotriacetic agarose) which is bound by the histidine residues of the 6xHis-tag with high specificity.

### Expression

- LB medium<sup>101</sup>

---

<sup>99</sup> For the recipe of 1xTBST see on page 86.

<sup>100</sup> For the description of the plasmid and the bacterial strain see on page 68 and 70. For the protocol of DNA cloning see on page 83. A list of recombinant DNA constructs which were used for this purpose is provided on page 73.

<sup>101</sup> For the recipe of the LB-medium see on page 77.



- IPTG (Isopropyl  $\beta$ -D-thiogalactopyranoside), stock solution 1M in ddH<sub>2</sub>O

To express enough protein, 2x-3x 200 ml LB medium with antibiotics were inoculated with 3 ml of a liquid overnight culture of the respective *E. coli* Rosetta™ strain. The cultures were incubated on a shaker at 37°C until they reached the exponential growth phase with an OD<sub>600</sub> between 0.4 and 0.9. The bacteria could be induced with 1 mM IPTG to efficiently stimulate the protein expression in this phase. The bacteria were further incubated at 37°C for 4 h. To check the efficiency of the induction, 1 ml of the bacterial cultures was taken just before the addition of IPTG and after the growth time of 4 h. The cultures could then be harvested by centrifugation at 3,000g for 10 min in 50 ml *Greiner* tubes. The supernatant was removed and the pellets were resuspended in X ml of buffer A with X being 1/20 of the original culture volume. The bacterial suspension was stored at 4°C overnight and could be processed further the next day. The two taken bacterial probes were likewise centrifuged and the pellets were resuspended in ca. 40  $\mu$ l 2x SDS sample buffer to test the protein content on a SDS-Page.<sup>102</sup>

### **Purification through a NTA (Nickel-nitrilotriacetic) agarose matrix**

- NTA (Nickel-nitrilotriacetic) agarose matrix suspension (Qiagen, Hilden)
- Buffer A: 8 M urea  
100 mM NaH<sub>2</sub>PO<sub>4</sub>  
10 mM Tris-HCl  
pH 8.0
- Buffer B: 8 M urea  
100 mM NaH<sub>2</sub>PO<sub>4</sub>  
10 mM Tris-HCl  
pH 6.3
- Buffer C: 8 M urea  
100 mM NaH<sub>2</sub>PO<sub>4</sub>  
10 mM Tris-HCl  
pH 5.9
- Buffer D: 8 M urea  
100 mM NaH<sub>2</sub>PO<sub>4</sub>  
10 mM Tris-HCl  
pH 4.5
- Neutralisation buffer: 1 M Tris-HCl, pH 9.5

The prepared suspension from the preceding day was sonicated 3x for 10 s. The application of ultrasound to the probe leads to disruption of cellular membranes and the release of the expressed protein into the lysate. After each sonication step, the sample was cooled on ice for 1 min to reestablish a low temperature. Then the suspension was incubated on a shaker for 1 h and subsequently could be centrifuged at 10,000g for 15 min. While insoluble bacterial substances, e.g. membranes, accumulate in the pellet, the soluble proteins remain in the supernatant. This clarified supernatant was loaded onto the NTA agarose matrix to efficiently purify the His-tagged target protein. To prepare the matrix, 2 ml of the NTA agarose matrix suspension was filled into a 5 ml polypropylene column (Qiagen, Hilden) which was equipped with a

---

<sup>102</sup> For the protocol of the SDS-Page see on page 84.

corresponding frit (Qiagen, Hilden). The frit in the column was profusely watered with ddH<sub>2</sub>O before use. The resulting matrix volume was 1 ml after the beads were sedimented because the matrix suspension is a 1:1 mix of beads and ethanol. The excessive ethanol was removed by gravity flow through the matrix which now, however, should never run dry. The matrix was then equilibrated with 20 ml of buffer A (flow by gravity) and could be loaded with the clarified lysate finally. During loading, the lysate was run along the column wall carefully to avoid swirling up the matrix. The lysate was filtered through the matrix by gravity flow. Afterwards the matrix with the bound protein was washed according to the following protocol (flow by gravity or assistance of a peristaltic pump):

- 20 ml buffer A (flow-through collected in a 50 ml *Greiner* tube)
- 15 ml buffer B (flow-through collected in a 50 ml *Greiner* tube)
- 10 ml buffer C (flow-through collected in 10x 1.5 ml *Eppendorf* tubes)
- 10 ml buffer D (flow-through collected in 10x 1.5 ml *Eppendorf* tubes)

The purification of the protein is achieved by a discontinuous pH gradient of the buffers. The elution of the protein from the matrix usually occurs during the pH shift from buffer B to C and buffer C to D. Therefore, the flow-through of buffer C and D was collected à 1 ml aliquots in 1.5 ml *Eppendorf* tubes. 50 µl of the neutralisation buffer were additionally added to each aliquot. To estimate the amount of the eluated protein, 7.5 µl of each protein fraction<sup>103</sup> were mixed with 7.5 µl 2x SDS sample buffer and loaded on a SDS-Page<sup>104</sup>. This finally could be stained with coomassie<sup>105</sup> and compared to a BSA standard<sup>106</sup>.

### 13.3.5 Concentration and purification of proteins from aqueous solutions

#### Protein precipitation

- Methanol, p.a. (Roth, Karlsruhe)
- Chloroform, p.a. (Applichem, Darmstadt)

The protein could be precipitated and subsequently solved in the appropriate volume of the desired solvent to increase the amount of protein in a solution or to purify the protein and change the solvent. Precipitation of proteins from solutions containing salt or detergents was achieved with methanol, chloroform and water. Organic solvents as methanol possess hydrophobic and hydrophilic features, similar to proteins themselves, and decrease the solvating power of an aqueous solution. Chloroform is used to efficiently remove lipids and detergents while the water is needed for separation of the aqueous phas, containing salt and nucleic acids and the chloroform phase containing detergents and lipids.

According to the method of Wessel and Flügge (Wessel and Flugge 1984) one part of a protein solution, usually 150 µl, was mixed with four parts cooled methanol and one part chloroform

---

<sup>103</sup> In the end, there are 24 probes: fraction A, fraction B, fraction C<sub>1</sub>-C<sub>10</sub>, fraction D<sub>1</sub>-D<sub>10</sub> and 2 bacterial probes.

<sup>104</sup> For the protocol of protein gel electrophoresis see on page 84.

<sup>105</sup> For the protocol of coomassie staining see on page 86.

<sup>106</sup> A BSA standard is a SDS-Page with 10 µg, 5 µg, 2 µg, 1 µg BSA stained with coomassie.

in a 1.5 ml *Eppendorf* tube by vortexing for 10 s. Phase separation was achieved by addition of three parts cooled water. The mixture was then incubated on ice for 10 min. Afterwards it was centrifuged at 13,000g for few minutes. The protein precipitates in the interphase between the upper aqueous phase and the lower chloroform phase. The upper phase was carefully removed. Four additional parts methanol were added to the remaining interphase/chloroform phase and centrifuged one more time to pellet the protein. The supernatant was removed and the pellet could air-dry. Finally, the protein was solved in accordance to its further use.

### Centrifugation

A protein solution can be filtrated through the semipermeable membrane of a centricon (*Amicon® Ultra*, Centrifugal Filter Units 3K-50K of Millipore, Tullagreen) to concentrate/dilute the protein or exchange the buffer. By centrifugation according to the manufacture's instructions, the primary solvent and its dissolved molecules and ions were removed through the filter to a minimal volume of 200 µl while the target protein should stay in the remaining solution<sup>107</sup>. The solution could be diluted with the new solvent afterwards and the procedure was repeated until the desired degree of dilution/concentration was achieved.

### Dialysis

- 2 mM EDTA, pH 8.0
- Dialysis buffer

Dialysis is another method to exchange a buffer of a protein solution and to remove excessive ions and molecules. However, it is not appropriate to increase the protein concentration. The principle of dialysis is based on the osmotic potential difference between the protein solution and a dialysis buffer. A semipermeable dialysis tube (Roth, Karlsruhe) allows the exchange of molecules to a certain molecular weight<sup>108</sup> between the protein solution in the tube and the surrounding dialysis buffer which is supplied in a large volume. This exchange occurs slowly overnight at 4°C until the equilibrium of the solved particle concentrations is reached. Before use, the dialysis tube was boiled in 2 mM EDTA for 30 min.

### 13.3.6 Synthesis of specific antibodies

If there is no specific antibody against a protein of interest available or purchasable, it can be synthesized in several steps. In a first step, a suitable antigen has to be selected and gained in a purified form. This antigen can be injected into a host animal which will produce polyclonal antibodies against the foreign peptide during a time of several weeks. Finally, the antibody can be purified from the blood serum of the host.

---

<sup>107</sup> Caution to the molecular weight cut off of the centricon.

<sup>108</sup> Caution to the molecular weight cut off of the tube.

## Selection of the antibody epitope

Several online services provide a prediction of suitable antibody epitopes in a protein sequence.<sup>109</sup> For an adequate antigenic polypeptide several features regarding sequence and structure need to be considered, e.g. hydrophilicity, accessibility and antigenic propensity.

## Immunization

The selected antigens were expressed as His-tagged fusion peptides from the pET21a vector and purified from the bacteria as described on p. 88. Immunization was carried out by SeqLab (Götting) in a 2-month protocol with three injections of the antigen at day 0, 21 and 49. For immunization of a rabbit or a guinea pig, at least 100 µg– 300 µg<sup>110</sup> of the protein in 500 – 1,000 µl PBS were needed per injection. If the protein was hard to dissolve, the solution could be heated up to 65°C and mixed with SDS to a maximum concentration of 4%. Blood serum, which contains the polyclonal antibodies, was taken at day 35 (1st bleeding), 53 (2nd bleeding) and 60 (final bleeding) and forwarded by SeqLab. The final bleedings could be affinity purified in the lab at the end. In the case of a rabbit, but not a guinea pig, the 1<sup>st</sup> and 2<sup>nd</sup> bleedings contained enough antisera for affinity purification as well.

## Purification

- Binding buffer: 200 mM NaCO<sub>3</sub>  
500 mM NaCl  
pH 8.3
- Washing buffer 1: 1 mM HCl, cooled to 4°C
- Buffer A: 500 mM ethanolamine  
500 mM NaCl  
pH 8.3
- Buffer B: 100 mM acetic acid  
500 mM NaCl  
pH 4.0
- Washing buffer 2: 3.5 M MgCl<sub>2</sub>
- PBS: 140 mM NaCl  
2.6 mM KCl  
6.4 mM Na<sub>2</sub>HPO<sub>4</sub>  
1.4 mM KH<sub>2</sub>PO<sub>4</sub>  
pH 7.4
- PBS + 350 mM NaCl, pH 7.4
- Elution buffer: 100 mM glycine, pH 2.5
- Neutralisation buffer: 1 M Tris-HCl, pH 9.5
- Storage buffer: 50 mM Na<sub>2</sub>HPO<sub>4</sub>  
0.1% (w/v) NaN<sub>3</sub> (toxic; addition to a maximum total volume of the storage buffer of 1 ml)  
pH 7.0

---

<sup>109</sup> See **Table 12-4** for the online services which were used in this study.

<sup>110</sup> 100 µg were used for the 2<sup>nd</sup> and the 3<sup>rd</sup> injection. 300 µg were needed for the 1<sup>st</sup> injection.

A HiTrap™ NHS-activated HP column 1ml (GE Healthcare, Munich) was used for affinity purification of the antibodies. It was operated with a syringe and a peristaltic pump. After washing out the isopropanol prior to the coupling reaction, it was important that the column never run dry. Furthermore, it should be avoided that air bubbles get into the column via the pump or the syringe.

### Antigenic ligand coupling

Ligands containing primary amino groups, just as the antigenic polypeptides, can be coupled to NHS-activated sepharose. Therefore, the isopropanol was washed out with 6 ml washing buffer 1 in a first step. 1-2 mg antigenic polypeptide were diluted in 1 ml binding buffer with up to 4% SDS, if necessary, to prepare the ligand solution. 1 ml of this ligand solution was injected onto the column with the aid of an appropriate syringe. The dilution was centrifuged with 3,000g at 4°C for 10 min before use. The column was sealed and incubated with the solution at room temperature for 1 h. Excessive active groups that were not coupled to the ligand were deactivated and non-specifically bound ligands were washed out by the following steps. Operation of the column occurred with the peristaltic pump at a maximum flow rate of 1 ml/min:

6 ml buffer A  
6 ml buffer B  
6 ml buffer A

The column was then incubated with buffer A at room temperature for 1 h for deactivation of the excessive active groups.

6 ml buffer B  
6 ml buffer A  
6 ml buffer B

Buffer B was finally substituted by PBS so that the column could be stored at 4°C for several days. If the column was not used during the next days, it was loaded with 1 ml storage buffer with the help of a syringe.

### Purification

3-5 ml serum of a guinea-pig or 7-10 ml serum of a rabbit were centrifuged at 4°C, 3,000g for 10 min to pellet insoluble particles. The supernatant was diluted in PBS to a 1:10 dilution. The column was equilibrated with 10 ml washing buffer 2 and washed with 30 ml PBS. Now the sample could be applied by pumping it onto the column with a maximum flow rate of 1 ml/min for three times. Afterwards the column was washed with 30 ml (guinea pig) or 50 ml (rabbit) PBS, 30 ml (guinea-pig) or 50 ml (rabbit) PBS + 350 mM NaCl and 10 ml (for both species) PBS. Elution of the antibody was achieved with 15 ml elution buffer that was pumped onto the column with a flow rate of 3 ml/min. The flow-through was collected in a 15 ml *Greiner* tube. 50 µl of the neutralization buffer were added to each ml of the eluate.

Finally, the column was washed with 20 ml PBS and loaded with 1 ml storage buffer for long term storage at 4°C.

## Dialysis and concentration of the antibody

### Dialysis<sup>111</sup>

- PBS<sup>112</sup>

A purified antibody was dialysed against 4 l cooled (4°C) PBS as dialysis buffer in a dialysis tubing with a molecular weight cut off of 14,000 (Roth, Karlsruhe).

### Concentration<sup>113</sup>

After dialysis the antibody solution was concentrated by centrifugation in a centricon with a molecular weight cut off of 50K. Centrifugation was carried out until the solution reached an OD<sub>280</sub> of at least 1.48 (photometric measurement in a cuvette, e.g. UVette, 220-1600 nm of Eppendorf, Hamburg). This OD<sub>280</sub> corresponds to an antibody concentration of 1mg/ml at which the antibody can be stored stably. Antibodies at lower concentrations needed to be stabilized with 1 mg/ml BSA. Finally, the antibody solution was stored in small aliquots at -80°C.

## 13.4 Cell culture

### 13.4.1 Culturing COS-7 cells

- Culturing medium: DMEM (1x) + GlutaMAX<sup>TM</sup>-I (Gibco by Life Technologies, Darmstadt)  
+10% FCS (PAA, Cölbe)  
+ 1% penicillin streptomycin
- Trypsin: 0.06% (w/v) trypsin  
0.02% (w/v) EDTA  
in PBS
- PBS<sup>114</sup>

COS-7 cells were cultured in Dulbeccos Modified Eagle Medium (DMEM) at 37°C with 5% CO<sub>2</sub>. 24 h prior to transfection, 1-4x10<sup>5</sup> cells were seeded in 30 mm dishes (Sarstedt, Nürnberg) which were equipped with 2-4 small and sterile 12 mm cover slips in a medium volume of 2.5 ml and incubated overnight by default. The dishes should have reached 40%-80% confluence on the day of transfection.

### 13.4.2 Transfection of COS-7 cells

- *Effectene*<sup>®</sup> transfection reagent (Qiagen, Hilden)

---

<sup>111</sup> For a detailed description of the dialysis protocol see on page 91.

<sup>112</sup> For the recipe of 1x PBS see on page 92.

<sup>113</sup> For a further description of the centrifugation protocol see on page 91.

<sup>114</sup> For the recipe of 1x PBS see on page 92.

Transfection describes the process of introducing foreign plasmid DNA in eukaryotic cells. The *Effectene* transfection reagent was used for transfection of COS-7 cells. The *Effectene* transfection is a two-step procedure in which first the DNA is condensed by the addition of the *Enhancer* and afterwards coated with cationic lipids by the *Effectene* reagent. This allows the passage of the *Effectene*-DNA complexes through the plasma membrane. The transfection was carried out under a sterile hood. For the transfection of cells in one 30 mm dish, 0.5 µg DNA were initially filled to 100 µl with the provided buffer, mixed with 4 µl *Enhancer*<sup>115</sup> in a 1.5 ml *Eppendorf* tube and incubated at room temperature for 5 min. Then 10 µl *Effectene* reagent were added. The mixture was vortexed briefly and incubated at room temperature for 10 min to allow the formation of the *Effectene*-DNA complexes. The prepared dish with the cells and the cover slips was taken from the incubator during this time. The medium was vacuumed and changed against 1.6 ml fresh and to 37°C pre-warmed DMEM. Then 600 µl DMEM were added to the DNA-*Enhancer-Effectene* mix and everything was carefully dropped onto the cells. The cells were finally placed back in the incubator for one night. After 24 h, the cells could be used for immunofluorescence analysis<sup>116</sup>.

## 13.5 Histochemistry

### 13.5.1 Hybridization histochemistry: Whole mount *in situ* hybridization

The whole mount *in situ* hybridization is a method to localize specific DNA or RNA sequences in an entire tissue or animal with the help of a labeled complementary DNA or RNA probe. The probe which is hybridized to the target sequence can be detected via its label and determines the position of the target DNA or RNA in the context of the surrounding tissue.

During this analysis, whole mount *in situ* hybridization was used to examine the expression of meiotic genes and therefore to localize specific mRNAs in an entire *Hydra* animal by the application of complementary RNA probes which were labeled with Digoxigenin. The probes could be detected with an  $\alpha$ -Dig antibody, finally.

#### RNA probe synthesis

- *RiboLock*<sup>TM</sup> ribonuclease inhibitor (Fermentas, St. Leon Roth)
- *T7 RNA polymerase* and *10x T7 buffer* (Roche, Mannheim)
- 10x NTP-Mix:       10 mM ATP, GTP, CTP  
                          5 mM UTP  
                          5 mM DIG-11-UTP  
                          (Fermentas, St. Leon Roth)
- Denaturation solution:   50% Formamide  
                                  25% 20x SSC<sup>117</sup>  
                                  25% ddH<sub>2</sub>O

---

<sup>115</sup> The DNA/Enhancer ratio should be 1:8.

<sup>116</sup> For the protocol of immunofluorescence analysis on cells see page on 102.

<sup>117</sup> For the recipe of 20x SSC see section below.

The RNA probe was synthesized by a T7 RNA polymerase from the *Strata* pSC-B-amp/kan vector that contained the entire or partial (700-1,000 bp probe length) cDNA sequence of the target mRNA. To finally obtain an antisense RNA probe, the cDNA needed to be in 5'-3' orientation, having the T7 promoter of the vector at its 3' end. To obtain a linear sense template for the *in vitro* transcription from this cDNA, a *Phusion* PCR was prepared with the 5' primer of the inserted cDNA and the T7 primer as reverse primer.<sup>118</sup> 5 µl of each PCR preparation were used to check the DNA amplification on an agarose gel.<sup>119</sup> The remaining 90 µl of the PCR product were purified with the *NucleoSpin® Gel and PCR Clean up* kit (Macherey-Nagel, Düren) and eluted in 30-40 µl ddH<sub>2</sub>O.<sup>120</sup> Subsequently, the preparation for the *in vitro* transcription was mixed according to the following protocol.

Protocol for 10 µl preparation: 6.5 µl PCR product (with T7 promoter),  
 0.5 µl RNase inhibitor (40 U/µl)  
 1 µl 10x T7-buffer  
 1 µl 10x NTP-Mix  
 1 µl T7 RNA polymerase (20 U/µl)

The mixture was incubated for 2 h at 37°C. Then 1 µl DNase I (10U/µl) was added and it was incubated at 37°C for further 15 min to digest the template DNA. At the end, the RNA probe was diluted 1:15 in denaturation solution and could be stored at -20°C.

### ***In situ* hybridization**

- Hydra medium (HM)<sup>121</sup>
- 2% (w/v) urethane in HM
- 4% (v/v) formaldehyde in HM, pH 7.4
- 4% (v/v) formaldehyde in PBT, pH 7.4
- PBT: PBS<sup>122</sup> + 0.1% (v/v) Tween
- Proteinase K: 10 µg/ml in PBT
- 20x SSC: 3 M NaCl  
 300 mM trisodium citrate  
 pH 7.8 (2x SSC, pH 7.4)
- 0.1% (w/v) CHAPS in 2x SSC
- MAB solution: 100 mM maleic acid  
 150 mM NaCl  
 pH 7.5
- MAB-B solution: MAB + 1% (w/v) BSA
- MAB-T solution: MAB + 0.1% (v/v) Tween
- NTM solution: 100 mM NaCl  
 100 mM Tris-HCl  
 adjust to pH 9.5  
 add 50 mM MgCl<sub>2</sub> (from 1 M stock solution)

<sup>118</sup> A description of the *Strata* plasmid is provided on page 70. For the protocol of the *Phusion*-PCR see on page 80. Two 50 µl preparations were used for each probe. A list of the specific primers which were used for this purpose is provided in **Table 12-3**.

<sup>119</sup> For the protocol of DNA gel electrophoresis see on page 81.

<sup>120</sup> For the description of the *NucleoSpin® Gel and PCR Clean up* kit see on page 82.

<sup>121</sup> For the recipe of HM see on page 68.

<sup>122</sup> For the recipe of 1x PBS see on page 92.



- NTMT solution: NTM + 0.1% (v/v) Tween
- Glycine solution: 4 mg/ml PBT
- Triethanolamine solution: 100 mM triethanolamine, pH 7.8
- 0.25% and 0.5% (v/v) acetic acid in 100 mM triethanolamine
- Hybridization solution: 50% (v/v) formamide  
25% (v/v) 20xSSC  
0.1% (v/v) Tween  
0.1% (w/v) CHAPS  
1x Denhardt's solution (from 50x stock solution)  
100 µg/ml heparin (from 10 mg/ml stock solution)
- tRNA stock solution: 10 mg/ml tRNA from baker's yeast (Roche, Mannheim)
- Blocking solution: 80% (v/v) MAB-B  
20% (v/v) FCS or sheep serum (heat inactivated)
- NBT/BCIP tablets (Roche, Mannheim): 1 tablet/10 ml ddH<sub>2</sub>O
- Methanol, p.a.
- Ethanol, p.a.

The protocol of the *in situ* hybridization takes four days consisting of several different steps:

1. Fixation of the animals.
2. Permeabilization of the tissue and hybridization of the probe.
3. Probe detection.
4. Visualization.

About 10 animals were starved for two days prior to the experiment. On day 1 of the protocol, these animals were initially relaxed in 2% urethane for 2 min and then fixed in 4% formaldehyde (in HM) at 4°C overnight. The following day (day 2), the animals were prepared for the hybridization reaction. All steps were carried out at room temperature placing the animals in a 12-well plate and shaking them gently. The fixative was replaced by 100% methanol. After 10 min, the methanol was discarded and replaced by 100% ethanol wherein the animals were incubated for additional 10 min. Then the samples were rehydrated in a declining alcohol series, staying in 75% ethanol/25% ddH<sub>2</sub>O, 50% ethanol/50% PBT and 25% ethanol/75% PBT for 5 min each. The animals were washed in PBT for 10 min to completely remove the ethanol. Afterwards the tissue was permeabilized for the RNA probe by digesting the proteins with a proteinase K treatment for 20 min. The samples were rinsed twice in glycine solution for 5-10 min and washed with PBT for 2x 15 min. The samples were treated with triethanolamine solution for 10 min and 0.25% and 0.5% acetic anhydride for 5 min each to further increase the accessibility of the mRNA and the specificity of the signal. Afterwards the animals were washed again in PBT (3x 5 min) and refixed in 4% formaldehyde (in PBT) for 1 h. The fixative was washed out with PBT (20 min). Then the samples were incubated in 2x SSC at room temperature for 10 min and at 70°C for 20 min to destroy secondary RNA structures and inhibit endogenous alkaline phosphatases. The solution was subsequently replaced by first 50% 2x SSC/50% hybridization solution (incubation for 10 min) and then 100% hybridization solution (incubation for 10 min) to equilibrate the tissue to the following hybridization reaction. This reaction was carried out in 2 ml *Eppendorf* tubes in a rotating hybridization oven at 57°C with solutions that were likewise pre-warmed to 57°C. First the prehybridization was performed in 2 ml hybridization solution containing 2% (v/v) tRNA from the stock solution for 1 h (57°C). During the last 10 min, 4

$\mu$ l of the 1:15 probe dilution were denatured in 100  $\mu$ l denaturation solution at 70°C. Finally, this denatured probe was added to the 2 ml pre-warmed hybridization solution containing 2% (v/v) tRNA wherein the samples were incubated for 16-24 h.<sup>123</sup> On day 3, the probe detection was performed. Therefore, the samples were subsequently washed in pre-warmed (57°C) 100% hybridization solution, 75% hybridization solution/25% 2x SSC, 50% hybridization solution/50% 2x SSC and 25% hybridization solution/75% 2x SSC at 57°C for 10 min each and then incubated in 2x SSC containing 0.1% CHAPS for 2x 30 min. Afterwards the samples were prepared for the antibody reaction. They were washed with MAB-T at room temperature for 10 min. The samples were then incubated in blocking solution at 4°C for 2 h to saturate unspecific binding sites followed by the staining reaction with the  $\alpha$ -Dig antibody which is fused to an alkaline phosphatase (fab fragment, Roche, Mannheim) and diluted 1:2,000 in blocking solution. The incubation with the antibody was performed at 4°C overnight. Eventually, on day 4, the antibody localization was visualized by the enzymatic reaction of the alkaline phosphatase. For this reaction, the samples were washed in MAB-T for 4x 30 min and in NTMT for 10 min. Then a NBT/BCIP tablet was dissolved in ddH<sub>2</sub>O and the solution was applied to the samples. The alkaline phosphatase converts the substrate NBT/BCIP to a black-purple precipitate and therewith stains the region of the target gene expression. The reaction was checked every 5 min until a specific staining was observed (ca. 20 min) and stopped in ddH<sub>2</sub>O (washing 5x 1 min). For storage, the animals were dehydrated in an increasing alcohol series of 25%, 50% and 75% ethanol and kept in 75% ethanol. Furthermore, a strong background signal could be reduced by destaining the animals in 100% methanol at 4°C overnight.

### 13.5.2 Immunohistochemistry

#### Whole mount immunofluorescence for confocal laser scanning microscopy

- 2% (w/v) urethane in HM
- 4% (v/v) formaldehyde in HM
- PBS<sup>124</sup>
- PBS + 0.1% (v/v) Tween
- PBS + 0.5% (v/v) Triton
- PBS + 1% (w/v) BSA + 0.1% (v/v) Tween
- PBS + 1% (w/v) BSA + 0.5% (v/v) Tween
- PBS + 1% (w/v) BSA + 0.5% (v/v) Tween + 0.5% (v/v) Triton
- Phalloidin-California red
- Hoechst 33258: working concentration 1:333 in PBS (Roche, Mannheim)
- Mounting medium: 50% (v/v) glycerol  
50% (v/v) PBS

Whole mount immunofluorescence analysis is useful to illustrate the localization of a protein in the context of the whole animal.

---

<sup>123</sup> The final probe dilution will be 1:7500 which corresponds to approximately 5-10 ng/ml.

<sup>124</sup> For the recipe of 1x PBS see on page 92.

First, several sexual animals were selected, relaxed in 2% urethane for 2 min and fixed in 4% formaldehyde for at least 1 h. The samples were then permeabilized and blocked by several incubation steps: 4x 15 min in PBS + 0.1% Tween, 30 min in PBS + 0.5% Triton and 1 h in PBS + 1% BSA + 0.1% Tween. The primary antibodies were diluted in in PBS + 1% BSA + 0.1% Tween.<sup>125</sup> The incubation with this antibody dilution was performed at 4°C overnight. The following day, the animals were washed 4x 15 min with PBS + 1% BSA + 0.1% Tween and then were incubated with the secondary antibodies at room temperature for 2 h which were likewise diluted in PBS + 1% BSA + 0.1% Tween.<sup>126</sup> After the second incubation period, the samples were washed again 4x 15 min in PBS + 1% BSA + 0.5% Tween. A treatment with phalloidin-california red (1:1,000 in PBS + 1% BSA + 0.5% Tween + 0.5% Triton, 1 h at room temperature) could be performed to stain the actin skeleton. A last washing step was done in PBS + 1% BSA + 0.5% Tween (4x 15 min). A few drops of Hoechst were added during the last 10 min to stain the DNA. Finally, the animals were mounted onto a *SuperFrost Plus* glass slide (Thermo Scientific, Menzel Gläser, Braunschweig) with glycerol/PBS and analyzed with the CLSM.

### Immunofluorescence on cryosections for confocal laser scanning microscopy

- 2% (w/v) urethane in HM<sup>127</sup>
- Tissue freezing medium (Jung Leica Microsystems, Nussloch)
- 2-methylbutane
- PBS<sup>128</sup>
- 1% (v/v) formaldehyde in PBS
- 0.05% (v/v) Triton in PBS
- PBT: 0.15% (w/v) BSA  
0.1% Tween  
in PBS, pH 7.4
- Hoechst 33258: working concentration 1:333 in PBS (Roche, Mannheim)
- Mounting medium: 50% (v/v) glycerol  
50% (v/v) PBS

For the immunofluorescence analysis on cryosections, the tissue has to be frozen quickly to avoid formation of water crystals in the tissue. The frozen tissue can be cut in thin sections of 5-10 µm and transferred to a *SuperFrost Plus* glass slide (Thermo Scientific, Menzel Gläser, Braunschweig) or a cover slip of 12 mm where the immunofluorescence can finally be performed to localize proteins in the context of the surrounding tissue. In this thesis, cryosections were made from frozen *Hydra* testis tissue to analyze the localization of meiotic proteins in the gonads.

<sup>125</sup> For the dilution of the primary antibodies in immunofluorescence analysis see **Table 12-1**.

<sup>126</sup> For the dilution of the secondary antibodies in immunofluorescence analysis see **Table 12-2**.

<sup>127</sup> For the recipe of HM see on page 68.

<sup>128</sup> For the recipe of 1x PBS see on page 92.

### Tissue embedding

*Hydra* animals with testes were selected and relaxed in 2% urethane in HM. The heads were removed with a scalpel. A small droplet of tissue freezing medium was dripped on a small piece of aluminum foil and 1-2 animals were placed in the medium. A pointed forceps was used to position the animal in the droplet. The piece of aluminum foil was then carefully placed in a beaker with 2-methylbutane that was cooled to  $-70^{\circ}\text{C}$  in the freezer. To keep it cool, the beaker itself was placed in styrofoam box with liquid  $\text{N}_2$ . After 2-3 min the aluminum foil with the frozen medium droplet was taken from the 2-methylbutan using a forceps. The droplet was peeled of the foil and quickly placed in a pre-cooled 1.5 ml *Eppendorf* tube with  $-70^{\circ}\text{C}$  cold 2-methylbutan and transferred into the  $-70^{\circ}\text{C}$  freezer where it could be stored for long term.

### Preparation of cryosections

The embedded tissue was transported to the freezing microtom 2800 FRIGOCUT E (Reichert-Jung, Heidelberg; cooled to  $-20^{\circ}\text{C}$ ) in a cooling block, taken from the tube and fastened on an object plate with tissue freezing medium. Usually,  $6\ \mu\text{m}$  thin sections were cut with the microtom and were transferred to a 12 mm cover slip. The sections were dried at room temperature for about 30 min.

### Immunofluorescence analysis

After drying, the sections were fixed and permeabilized with formaldehyde and Triton. Therefore, the samples were incubated in 1% formaldehyde for 3 min and in 0.05% Triton for 10 min. Afterwards the sections were washed in PBS (3x 5 min). The tissue was incubated in PBT in a moist chamber for 1 h to saturate unspecific binding sites. Now the primary antibodies were given to the samples (50  $\mu\text{l}$ / sample). They were diluted in PBS as indicated in **Table 12-1**. The incubation was performed in the moist chamber for at least 1 h. The samples were washed in PBS (3x 5 min) and then incubated with the secondary antibodies, which were diluted according to the information of **Table 12-2**, in the moist chamber for 30 min. During the last 10 min of incubation, few droplets of Hoechst were added. The sections were washed in PBS for the last time (3x 5 min). The bottom side of the cover slips was then carefully dried with a tissue to avoid salt crystals before the upper side with the samples was mounted onto a *Super-Frost Plus* glass slide (Thermo Scientific, Menzel Gläser, Braunschweig) with glycerol/PBS.

### **13.5.3 Immunocytochemistry**

#### **Immunofluorescence on chromosome spread preparations for confocal laser scanning microscopy**

- Hypotonic buffer: 30 mM Tris-HCl  
17 mM trisodium citrate  
5 mM EDTA  
50mM sucrose

adjust to pH 8.2  
add 5 mM DTT (from 1 M stock solution)

- 1% (w/v) paraformaldehyde (soluble at 60°C with few drops of 1 M NaOH) + 0.15% (v/v) Triton, pH 9.2, steril filtrated
- 100 mM sucrose, steril filtrated
- PBS<sup>129</sup>
- Blocking solution: 5% (w/v) milk  
5% (v/v) FCS  
in PBS, pH 7.4  
stored at -20°C  
centrifuge at 16,000g for 30 min before use; use only supernatant
- Mounting medium: 50% (v/v) glycerol  
50% (v/v) PBS

Immunofluorescence analysis on chromosome spreads bear the advantage that the cells are flattened and chromosome structures such as the SC are stretched out. This allows a very accurate and specific binding of an antibody to target proteins of the chromosome axis and reduces background signals. Chromosome spreads were used in this study to analyze the localization pattern of different SC proteins along the chromosome axes of *Hydra* spermatocytes.

### Chromosome spread preparation

The chromosome spreads were prepared according to the dry-down procedure of de Boer (De Boer *et al.* 2009) with some adjustments to the *Hydra* tissue. Mid-pieces of male *Hydra* animals - head and foot were removed - were incubated in hypotonic buffer for 20 min.<sup>130</sup> In this buffer, the cells were macerated and the tissue could easily be suspended in sucrose. Therefore, 20 µl sucrose were placed on a slide, two swollen mid-pieces were transferred into the sucrose droplet and with the help of 1-10 µl pipette the cells were suspended completely. Then a new *SuperFrost Plus* slide (Thermo Scientific, Menzel Gläser, Braunschweig) was dipped into the paraformaldehyde solution. Excess of solution was drained carefully by dripping it onto a tissue paper. The “last” droplet was finally kept in one corner of the slide and the cell suspension was placed into this droplet. The suspension was dispersed over the entire slide by gently swerving the slide. It was then placed in a moist chamber where it was incubated successively with the lid closed for 30 min, with the lid ajar for 1 h and with the lid completely removed until it was dry. At the end, the slide was wrapped in aluminum foil and could be stored at -70°C for a long time period. Usually, about 10 slides (20 animals) were prepared at once.

### Immunofluorescence analysis

The needed number of slides was taken from the freezer. After ca. 15 min the slides reached room temperature. Then they were unwrapped and washed in PBS (3x 7m min). Immediately

---

<sup>129</sup> For the recipe of 1x PBS see on page 92.

<sup>130</sup> Longer incubation times can lead to a complete disruption of the spermatocytes and the synaptonemal complexes!

after this step, the slides could already be blocked with ca. 300  $\mu$ l blocking solution per slide in a moist chamber for at least 30 min. The primary antibodies were prepared during this time. They were diluted in blocking solution as indicated in **Table 12-1** and centrifuged at 16,000g and 4°C for 30 min to pelletize antibody fragments. At least 150  $\mu$ l of the supernatant from the antibody dilution was then pipetted onto the cells of each slide from which the blocking solution has been removed by tilting the slide and a cover slip was placed on top to assure an equal dispersion of the antibody across the entire slide. The chromosome spreads were incubated with the primary antibodies in a closed moist chamber at room temperature for at least 1 h and up to 2 nights at 4°C depending on the antibody.<sup>131</sup> Then the cover slips were slid down and the samples were washed in PBS (3x 5 min). Prior to the incubation with the secondary antibodies, the slides were again incubated in blocking solution in the moist chamber for 30 min. The secondary antibodies were diluted in blocking solution<sup>132</sup> and centrifuged at 16,000g and 4°C for 30 min just as the primary antibodies. After pipetting the secondary antibody dilution onto the slides, cover slips were again put on top. The slides were incubated in the moist chamber for 30 min. Then the cover slips were removed<sup>133</sup> and few drops of Hoechst were added. After 10 min incubation, the slides were washed again in PBS (3x 5 min) and mounted with glycerol/PBS.

### Immunofluorescence on cells for confocal laser scanning microscopy

- PBS<sup>134</sup>
- 1% (v/v) formaldehyde in PBS
- 0.1% (v/v) Triton in PBS
- PBT<sup>135</sup>
- Mounting medium:     50% (v/v) glycerol  
                              50% (v/v) PBS

Immunofluorescence analysis can also be performed on cells from a cell culture. As there is no meiotic cell culture system available, this method was used to examine endogenous binding and polymerization properties of meiotic proteins in the heterologous system of transfected somatic cells.

24 h after transfection of COS-7 cells<sup>136</sup> with the eukaryotic expression vector which encodes the proteins of interest the overgrown cover slips were taken from the dishes and washed in PBS for 3x 5min. The cells that adhered to the cover slips were then fixed in 1% formaldehyde for 3 min and treated with 0.1% Triton for 10 min. Afterwards PBT was used as blocking solution to saturate unspecific binding sites. The cells were blocked with 50-100  $\mu$ l PBT per cover

---

<sup>131</sup> For the dilution and incubation time of the primary antibodies in immunofluorescence analysis see **Table 12-1**.

<sup>132</sup> For dilution of the secondary antibodies in immunofluorescence analysis see **Table 12-2**.

<sup>133</sup> Caution that not too much dilution is lost to avoid drying-out of the samples.

<sup>134</sup> For the recipe of 1x PBS see on page 92.

<sup>135</sup> For the recipe of 1x PBT see in the previous section on page 99.

<sup>136</sup> For the protocol of the transfection of eukaryotic cells see on page 94.

slip in a moist chamber for 30 min and could subsequently be incubated with the primary antibodies which were diluted in PBT as indicated in **Table 12-1**. The incubation occurred in the moist chamber for 30 min. The cover slips were washed again in PBS (3x 5 min) and the cells were then incubated with the secondary antibodies, which were again diluted in PBT as indicated in **Table 12-2**, in the moist chamber. Few droplets of Hoechst were added after 20 min and the cells were incubated for 10 more min. Finally, the cover slips were washed in PBS for the last time (3x 5 min) and mounted onto a glass slide with glycerol/PBS.

## 13.6 Phylogenetic analysis

For the phylogenetic analysis of a protein complex, it is the first step to identify homologues for each protein component using the BLAST - Basic Local Alignment Search Tool - which is based on finding core similarities of preset length - the word size - with a certain minimum score<sup>137</sup> between a query and the database sequences of various gene and protein databases. These can be used to reconstruct the phylogeny of each protein in a phylogenetic tree. A comparison of the resultant trees with a reference tree, e.g. the tree of metazoan species, finally allows conclusions about the origin and the evolution of the protein complex. In this study, the evolutionary history of the SC ought to be analyzed.

### 13.6.1 Dataset assembly

Depending on the question which had to be answered<sup>138</sup>, annotated and characterized protein sequences were used as initial seeds to query public sequence databases. Homologous sequences available in the *non-redundant* (*nr*) database at the NCBI were identified using the BLASTp program which is a program to search the protein database using a protein query (Altschul *et al.* 1997). Algorithm parameters were chosen in respect to the search request. Usually, a maximum number of 500 aligned sequences - the *maximum target sequences* - were selected. The e-value threshold<sup>139</sup>, the *word size*<sup>140</sup> and the *gap costs*<sup>141</sup> were chosen by default. The substitution matrix BLOSUM45<sup>142</sup> was selected to search for divergent protein se-

---

<sup>137</sup> The score is the likelihood that a query sequence is a true homologue of a database sequence compared to the likelihood that the sequence was aligned randomly just by chance.

<sup>138</sup> For example, there is a methodical difference when asking "How did the mouse synaptonemal complex evolve?" versus "How did the synaptonemal complex evolve in *Metazoa*?". In the first case, the SC is analyzed only from the mouse perspective, using only the mouse SC components as starting point for the search of homologues. In the second case, the SC has to be analyzed from all different perspectives regarding metazoans. So not only the mouse SC proteins but also the other characterized SC proteins from *D. melanogaster* and *C. elegans* need to be used as starting point for the phylogenetic analysis.

<sup>139</sup> The *expected threshold* is 10 by default. The e-value is basically the number of alignments that would match with a score greater or equal to X by chance alone searching the complete database.

<sup>140</sup> The *word size* is 3 by default. It is defined as the length of a seed that can initiate an alignment.

<sup>141</sup> The gap costs are a penalty of introducing or extending gaps into an alignment that reduces the score.

<sup>142</sup> BLOSUM is a scoring matrix to find conserved regions of proteins.

quences. The PSI-BLAST program was used with BLOSUM45 and default values for all other parameters to ensure that all homologues were sampled (Altschul *et al.* 1997). It is an iterative BLAST search that constructs an own position-specific scoring matrix from the best multiple alignment of the previous BLAST search and uses this new matrix to query the database in a new search attempt. More homologues could be retrieved from the *nr/nt*, *est*, *wgs* databases<sup>143</sup> and ongoing genome project data available at the NCBI, Ensembl database, release 71, the DFCI and the InParanoid project using BLASTp and tBLASTn to search a translated nucleotide database using a protein query. All BLASTp and tBLASTn searches were repeated several times by using each newly detected homologue as seed for a new search. The absence of any homologous sequence in a given species/lineage, for which the complete genome is available, was checked by screening the corresponding genome with the tBLASTn program. The sequences retrieved were used for reciprocal BLAST analyses. If this analysis resulted in hits that were already identified as homologues, it was justified to assume that they really represented putative homologues of the analyzed protein and not false positives.

The retrieved sequences were aligned using ClustalO (Sievers *et al.* 2011) implemented in the *Seaview* program, version 4.4.0 (Gouy *et al.* 2010) for each protein. The alignment was edited with the G-Blocks option to only keep the best local alignments for tree calculations. A preliminary neighbor-joining (NJ) tree was inferred with the same program. Parameters were chosen by default. The NJ is a distance method that calculates a matrix containing the evolutionary distances<sup>144</sup> between multiple aligned sequences and step-by-step builds a tree which represents these distances best by adjusting tree topology and branch lengths. The method is fast, but lacks accuracy and was only used for preliminary analysis. Based on this tree, the closest homologues of the sequences that were experimentally demonstrated as part of the protein complex - this is the mouse SC - were selected, realigned and used to build a specific Hidden Markov Model (HMM; statistical model) profile, which is a specific sequence profile of a homologous protein family with position-specific scores and gap penalties, using the HMMer 3.0 webserver. The resulting profile could be used to query the *nr* database with the *hmmsearch* option as well as to individually verify all the other sequences present in the initial alignment by starting from the closest and progressing to the more distantly related sequences according to the NJ tree. New and verified sequences were added to the new alignment step-by-step and used to update the HMM profile. This procedure was repeated iteratively until no further homologues could be identified.

### 13.6.2 Multiple sequence alignment

Multiple alignments for phylogenetic tree construction need to be very accurate and only include the best local alignments of the sequences. In order to reduce potential tree reconstruc-

---

<sup>143</sup> *nr/nt*: non redundant nucleotide sequences; *est*: *expressed sequence tags* containing mRNA sequences; *wgs*: *whole genome shotgun sequences* containing genomic sequences.

<sup>144</sup> The conversion of the substitution matrix into a distance matrix occurs via the evolutionary models, e.g. LG or WAG.



tion artifacts linked to the overrepresentation of a few lineages, a taxonomically balanced subset of homologues was selected as a first step for final phylogenetic analyses. Several bioinformatic programs and services can then be used to align these sequences. Besides the ClustalO option in the *Seaview* program, the T-Coffee webserver and MAFFT , version 7 (Kato *et al.* 2002) were used to receive the optimal alignments. These were inspected using *Seaview* and ambiguously aligned regions were removed with the BMGE (Crisuolo and Gribaldo 2010) Annotation of sequence alignments were designed using CHROMA Version 1.0 (Goodstadt and Ponting 2001). The identity threshold for grouping of the residues was set to 60%-80%. Seven groups were created, depending on different features of the amino acids: Identical, charged, Ser/Thr, aliphatic, aromatic, polar and hydrophobic. Sparse regions longer than four residues were removed by the program if at least 80% of the sequences were blank gaps at these positions. The number of removed residues is indicated by numbers in brackets in the corresponding sequences at those positions.

### 13.6.3 Phylogenetic tree construction

Maximum Likelihood (ML) and Bayesian Inference (BI) were used to accurately construct the final phylogenetic trees.<sup>145</sup>

In contrast to the NJ method, the ML does not consider evolutionary distances between sequences but estimates the probability of observing the present data, which is the sequence alignment, given certain parameters, such as tree topology, branch length and evolutionary model. Optimizing these parameters by testing all possible trees will lead to the maximum probability or maximum likelihood for the alignment data. Each site of the alignment is considered as independent event and assumed to evolve uniformly during this procedure. ML trees were inferred with the ML option implemented in the *Seaview* program or with PhyML version 3.0.1 (Guindon *et al.* 2009) with the LG model , option NNI+SPR and a gamma distribution to take into account heterogeneous evolutionary rates of different sites with four categories of sites and an estimated alpha parameter. The robustness of the resulting ML tree was assessed with the bootstrap procedure. A bootstrap value corresponds to a branch and indicates the number of trees - usually out of 100 replicates - that have rebuilt this certain branch.

The most important contrast between ML and BI is that BI considers the data to be given and the parameters to be random. It estimates the probability of a certain parameter given the observed data, the posterior probability, by applying the Bayesian theorem. Therefore, it assumes an *a-priori* set probability distribution of the parameter taking into account some uncertainty about it. Accordingly, the branch robustness was estimated by calculation of the posterior probabilities of the branches. The BI trees were constructed using MrBayes 3.2.1. (Ronquist *et al.* 2012) with a mixed amino acid substitution model and gamma distribution

---

<sup>145</sup> MAFFT and BMGE were applied by Céline Armenant-Brochier, University of Lyon, France who calculated the final phylogenetic trees of SYCE1, SYCE2, SYCE3 and Tex12 with PhyML 3.0.1 and MrBayes 3.2.1.

---

with four categories of sites and an estimated alpha parameter. The search was run with four independent chains for 1 million generations. Trees were sampled every 100 generations. The first 2,000 trees were discarded as 'burnin'.

## 14 References

- Agarwal, S., and G. S. Roeder, 2000 Zip3 provides a link between recombination enzymes and synaptonemal complex proteins. *Cell* 102: 245-255.
- Aguinaldo, A. M., J. M. Turbeville, L. S. Linford, M. C. Rivera, J. R. Garey *et al.*, 1997 Evidence for a clade of nematodes, arthropods and other moulting animals. *Nature* 387: 489-493.
- Alsheimer, M., A. Baier, S. Schramm, W. Schutz and R. Benavente, 2010 Synaptonemal complex protein SYCP3 exists in two isoforms showing different conservation in mammalian evolution. *Cytogenet Genome Res* 128: 162-168.
- Altschul, S. F., T. L. Madden, A. A. Schaffer, J. Zhang, Z. Zhang *et al.*, 1997 Gapped BLAST and PSI-BLAST: a new generation of protein database search programs. *Nucleic Acids Res* 25: 3389-3402.
- Anderson, L. K., S. M. Royer, S. L. Page, K. S. McKim, A. Lai *et al.*, 2005 Juxtaposition of C(2)M and the transverse filament protein C(3)G within the central region of *Drosophila* synaptonemal complex. *Proc Natl Acad Sci U S A* 102: 4482-4487.
- Anokhin, B., G. Hemmrich-Stanisak and T. C. G. Bosch, 2010 Karyotyping and single-gene detection using fluorescence in situ hybridization on chromosomes of *Hydra magnipapillata* (Cnidaria:Hydrozoa). *Comp Cytogenet* 4: 97-110.
- Armstrong, S. J., A. P. Caryl, G. H. Jones and F. C. Franklin, 2002 Asy1, a protein required for meiotic chromosome synapsis, localizes to axis-associated chromatin in *Arabidopsis* and *Brassica*. *J Cell Sci* 115: 3645-3655.
- Baier, A., M. Alsheimer and R. Benavente, 2007a Synaptonemal complex protein SYCP3: Conserved polymerization properties among vertebrates. *Biochim Biophys Acta* 1774: 595-602.
- Baier, A., M. Alsheimer, J. N. Volff and R. Benavente, 2007b Synaptonemal complex protein SYCP3 of the rat: evolutionarily conserved domains and the assembly of higher order structures. *Sex Dev* 1: 161-168.
- Baker, S. M., A. W. Plug, T. A. Prolla, C. E. Bronner, A. C. Harris *et al.*, 1996 Involvement of mouse Mlh1 in DNA mismatch repair and meiotic crossing over. *Nat Genet* 13: 336-342.
- Bannister, L. A., L. G. Reinholdt, R. J. Munroe and J. C. Schimenti, 2004 Positional cloning and characterization of mouse mei8, a disrupted allele of the meiotic cohesin Rec8. *Genesis* 40: 184-194.
- Baudat, F., K. Manova, J. P. Yuen, M. Jasin and S. Keeney, 2000 Chromosome synapsis defects and sexually dimorphic meiotic progression in mice lacking Spo11. *Mol Cell* 6: 989-998.
- Bickel, S. E., D. W. Wyman, W. Y. Miyazaki, D. P. Moore and T. L. Orr-Weaver, 1996 Identification of ORD, a *Drosophila* protein essential for sister chromatid cohesion. *EMBO J* 15: 1451-1459.
- Bogdanov, Y. F., T. M. Grishaeva and S. Y. Dadashev, 2007 Similarity of the domain structure of proteins as a basis for the conservation of meiosis. *Int Rev Cytol* 257: 83-142.

- Bolcun-Filas, E., Y. Costa, R. Speed, M. Taggart, R. Benavente *et al.*, 2007 SYCE2 is required for synaptonemal complex assembly, double strand break repair, and homologous recombination. *J Cell Biol* 176: 741-747.
- Bolcun-Filas, E., E. Hall, R. Speed, M. Taggart, C. Grey *et al.*, 2009 Mutation of the mouse *Syce1* gene disrupts synapsis and suggests a link between synaptonemal complex structural components and DNA repair. *PLoS Genet* 5: e1000393.
- Bolcun-Filas, E., and J. C. Schimenti, 2012 Genetics of meiosis and recombination in mice. *Int Rev Cell Mol Biol* 298: 179-227.
- Borner, G. V., N. Kleckner and N. Hunter, 2004 Crossover/noncrossover differentiation, synaptonemal complex formation, and regulatory surveillance at the leptotene/zygotene transition of meiosis. *Cell* 117: 29-45.
- Bosch, T. C., F. Anton-Erxleben, G. Hemmrich and K. Khalturin, 2010 The *Hydra* polyp: nothing but an active stem cell community. *Dev Growth Differ* 52: 15-25.
- Bosch, T. C., and C. N. David, 1986 Male and female stem cells and sex reversal in *Hydra* polyps. *Proc Natl Acad Sci U S A* 83: 9478-9482.
- Botelho, R. J., L. DiNicolo, N. Tsao, A. Karauskakis, M. Tarsounas *et al.*, 2001 The genomic structure of *SYCP3*, a meiosis-specific gene encoding a protein of the chromosome core. *Biochim Biophys Acta* 1518: 294-299.
- Carpenter, A. T., 1975 Electron microscopy of meiosis in *Drosophila melanogaster* females: II. The recombination nodule—a recombination-associated structure at pachytene? *Proc Natl Acad Sci U S A* 72: 3186-3189.
- Chapman, J. A., E. F. Kirkness, O. Simakov, S. E. Hampson, T. Mitros *et al.*, 2010 The dynamic genome of *Hydra*. *Nature* 464: 592-596.
- Colaiacono, M. P., A. J. MacQueen, E. Martinez-Perez, K. McDonald, A. Adamo *et al.*, 2003 Synaptonemal complex assembly in *C. elegans* is dispensable for loading strand-exchange proteins but critical for proper completion of recombination. *Dev Cell* 5: 463-474.
- Cole, F., S. Keeney and M. Jasin, 2010 Evolutionary conservation of meiotic DSB proteins: more than just Spo11. *Genes Dev* 24: 1201-1207.
- Costa, Y., R. Speed, R. Ollinger, M. Alsheimer, C. A. Semple *et al.*, 2005 Two novel proteins recruited by synaptonemal complex protein 1 (SYCP1) are at the centre of meiosis. *J Cell Sci* 118: 2755-2762.
- Couteau, F., and M. Zetka, 2005 HTP-1 coordinates synaptonemal complex assembly with homolog alignment during meiosis in *C. elegans*. *Genes Dev* 19: 2744-2756.
- Crisuolo, A., and S. Gribaldo, 2010 BMGE (Block Mapping and Gathering with Entropy): a new software for selection of phylogenetic informative regions from multiple sequence alignments. *BMC Evol Biol* 10: 210.
- Daniel, K., J. Lange, K. Hached, J. Fu, K. Anastassiadis *et al.*, 2011 Meiotic homologue alignment and its quality surveillance are controlled by mouse HORMAD1. *Nat Cell Biol* 13: 599-610.
- Davies, O. R., J. D. Maman and L. Pellegrini, 2012 Structural analysis of the human SYCE2-TEX12 complex provides molecular insights into synaptonemal complex assembly. *Open Biol* 2: 120099.
- de Boer, E., F. G. Lhuissier and C. Heyting, 2009 Cytological analysis of interference in mouse meiosis. *Methods Mol Biol* 558: 355-382.

- de Massy, B., 2003 Distribution of meiotic recombination sites. *Trends Genet* 19: 514-522.
- de Vries, F. A., E. de Boer, M. van den Bosch, W. M. Baarends, M. Ooms *et al.*, 2005 Mouse *Sycp1* functions in synaptonemal complex assembly, meiotic recombination, and XY body formation. *Genes Dev* 19: 1376-1389.
- Dehal, P., and J. L. Boore, 2005 Two rounds of whole genome duplication in the ancestral vertebrate. *PLoS Biol* 3: e314.
- Dobson, M. J., R. E. Pearlman, A. Karaiskakis, B. Spyropoulos and P. B. Moens, 1994 Synaptonemal complex proteins: occurrence, epitope mapping and chromosome disjunction. *J Cell Sci* 107 ( Pt 10): 2749-2760.
- Fawcett, D. W., 1956 The fine structure of chromosomes in the meiotic prophase of vertebrate spermatocytes. *J Biophys Biochem Cytol* 2: 403-406.
- Franzenburg, S., S. Fraune, S. Kunzel, J. F. Baines, T. Domazet-Lošo *et al.*, 2012 MyD88-deficient *Hydra* reveal an ancient function of TLR signaling in sensing bacterial colonizers. *Proc Natl Acad Sci U S A* 109: 19374-19379.
- Fraune, J., S. Schramm, M. Alsheimer and R. Benavente, 2012a The mammalian synaptonemal complex: protein components, assembly and role in meiotic recombination. *Exp Cell Res* 318: 1340-1346.
- Fraune, J., M. Alsheimer, J. N. Volff, K. Busch, S. Fraune *et al.*, 2012b *Hydra* meiosis reveals unexpected conservation of structural synaptonemal complex proteins across metazoans. *Proc Natl Acad Sci U S A* 109: 16588-16593.
- Fraune, J., C. Brochier-Armanet, M. Alsheimer and R. Benavente, 2013 Phylogenies of central element proteins reveal the dynamic evolutionary history of the Mammalian synaptonemal complex: ancient and recent components. *Genetics* 195: 781-793.
- Fraune, J., M. Wiesner and R. Benavente, 2014 The synaptonemal complex of the basal metazoan *Hydra*: more similarities to vertebrate than invertebrate meiosis model organism. *J Genet Genomics, in revision*.
- Galliot, B., 2012 *Hydra*, a fruitful model system for 270 years. *Int J Dev Biol* 56: 411-423.
- Gause, M., Z. Misulovin, A. Bilyeu and D. Dorsett, 2010 Dosage-sensitive regulation of cohesin chromosome binding and dynamics by Nipped-B, Pds5, and Wapl. *Mol Cell Biol* 30: 4940-4951.
- Gillies, C. B., 1975 Synaptonemal complex and chromosome structure. *Annu Rev Genet* 9: 91-109.
- Goodstadt, L., and C. P. Ponting, 2001 CHROMA: consensus-based colouring of multiple alignments for publication. *Bioinformatics* 17: 845-846.
- Goodyer, W., S. Kaitna, F. Couteau, J. D. Ward, S. J. Boulton *et al.*, 2008 HTP-3 links DSB formation with homolog pairing and crossing over during *C. elegans* meiosis. *Dev Cell* 14: 263-274.
- Gouy, M., S. Guindon and O. Gascuel, 2010 SeaView Version 4: A multiplatform graphical user interface for sequence alignment and phylogenetic tree building. *Mol Biol Evol* 27: 221-224.
- Guindon, S., F. Delsuc, J.-F. Dufayard and O. Gascuel, 2009 Estimating maximum likelihood phylogenies with PhyML, pp. 113-137 in *Bioinformatics for DNA Sequence Analysis*, edited by D. Posada. Humana Press.

- Hamer, G., K. Gell, A. Kouznetsova, I. Novak, R. Benavente *et al.*, 2006 Characterization of a novel meiosis-specific protein within the central element of the synaptonemal complex. *J Cell Sci* 119: 4025-4032.
- Hamer, G., H. Wang, E. Bolcun-Filas, H. J. Cooke, R. Benavente *et al.*, 2008 Progression of meiotic recombination requires structural maturation of the central element of the synaptonemal complex. *J Cell Sci* 121: 2445-2451.
- Hawley, R. S., 2011 Solving a meiotic LEGO puzzle: transverse filaments and the assembly of the synaptonemal complex in *Caenorhabditis elegans*. *Genetics* 189: 405-409.
- Hemmrich, G., B. Anokhin, H. Zacharias and T. C. Bosch, 2007 Molecular phylogenetics in *Hydra*, a classical model in evolutionary developmental biology. *Mol Phylogenet Evol* 44: 281-290.
- Hemmrich, G., K. Khalturin, A. M. Boehm, M. Puchert, F. Anton-Erxleben *et al.*, 2012 Molecular signatures of the three stem cell lineages in *Hydra* and the emergence of stem cell function at the base of multicellularity. *Mol Biol Evol*.
- Iwai, T., A. Yoshii, T. Yokota, C. Sakai, H. Hori *et al.*, 2006 Structural components of the synaptonemal complex, SYCP1 and SYCP3, in the medaka fish *Oryzias latipes*. *Exp Cell Res* 312: 2528-2537.
- Jeffress, J. K., S. L. Page, S. K. Royer, E. D. Belden, J. P. Blumenstiel *et al.*, 2007 The formation of the central element of the synaptonemal complex may occur by multiple mechanisms: the roles of the N- and C-terminal domains of the *Drosophila* C(3)G protein in mediating synapsis and recombination. *Genetics* 177: 2445-2456.
- Katoh, K., K. Misawa, K. Kuma and T. Miyata, 2002 MAFFT: a novel method for rapid multiple sequence alignment based on fast Fourier transform. *Nucleic Acids Res* 30: 3059-3066.
- Kneissel, S., W. W. Franke, J. G. Gall, H. Heid, S. Reidenbach *et al.*, 2001 A novel karyoskeletal protein: characterization of protein NO145, the major component of nucleolar cortical skeleton in *Xenopus* oocytes. *Mol Biol Cell* 12: 3904-3918.
- Kolas, N. K., and P. E. Cohen, 2004 Novel and diverse functions of the DNA mismatch repair family in mammalian meiosis and recombination. *Cytogenet Genome Res* 107: 216-231.
- Kouznetsova, A., R. Benavente, A. Pastink and C. Hoog, 2011 Meiosis in mice without a synaptonemal complex. *PLoS ONE* 6: e28255.
- Kuznetsov, S., M. Lyanguzowa and T. C. Bosch, 2001 Role of epithelial cells and programmed cell death in *Hydra* spermatogenesis. *Zoology* 104: 25-31.
- Lake, C. M., and R. S. Hawley, 2012 The molecular control of meiotic chromosomal behavior: events in early meiotic prophase in *Drosophila* oocytes. *Annu Rev Physiol* 74: 425-451.
- Lammers, J. H., H. H. Offenbergh, M. van Aalderen, A. C. Vink, A. J. Dietrich *et al.*, 1994 The gene encoding a major component of the lateral elements of synaptonemal complexes of the rat is related to X-linked lymphocyte-regulated genes. *Mol Cell Biol* 14: 1137-1146.
- Lenhoff, H. M., and R. D. Brown, 1970 Mass culture of *Hydra*: an improved method and its application to other aquatic invertebrates. *Lab Anim* 4: 139-154.
- Li, X. C., E. Bolcun-Filas and J. C. Schimenti, 2011 Genetic evidence that synaptonemal complex axial elements govern recombination pathway choice in mice. *Genetics* 189: 71-82.
- Liebe, B., M. Alsheimer, C. Hoog, R. Benavente and H. Scherthan, 2004 Telomere attachment, meiotic chromosome condensation, pairing, and bouquet stage duration are modified in spermatocytes lacking axial elements. *Mol Biol Cell* 15: 827-837.

- Littlefield, C. L., 1985 Germ cells in *Hydra oligactis* males. I. Isolation of a subpopulation of interstitial cells that is developmentally restricted to sperm production. *Dev Biol* 112: 185-193.
- Littlefield, C. L., C. Finkemeier and H. R. Bode, 1991 Spermatogenesis in *Hydra oligactis*. II. How temperature controls the reciprocity of sexual and asexual reproduction. *Dev Biol* 146: 292-300.
- Liu, J. G., L. Yuan, E. Brundell, B. Bjorkroth, B. Daneholt *et al.*, 1996 Localization of the N-terminus of SCP1 to the central element of the synaptonemal complex and evidence for direct interactions between the N-termini of SCP1 molecules organized head-to-head. *Exp Cell Res* 226: 11-19.
- Llano, E., Y. Herran, I. Garcia-Tunon, C. Gutierrez-Caballero, E. de Alava *et al.*, 2012 Meiotic cohesin complexes are essential for the formation of the axial element in mice. *J Cell Biol* 197: 877-885.
- MacQueen, A. J., M. P. Colaiacovo, K. McDonald and A. M. Villeneuve, 2002 Synapsis-dependent and -independent mechanisms stabilize homolog pairing during meiotic prophase in *C. elegans*. *Genes Dev* 16: 2428-2442.
- Manheim, E. A., and K. S. McKim, 2003 The synaptonemal complex component C(2)M regulates meiotic crossing over in *Drosophila*. *Curr Biol* 13: 276-285.
- Martin, V. J., C. L. Littlefield, W. E. Archer and H. R. Bode, 1997 Embryogenesis in *Hydra*. *Biol Bull* 192: 345-363.
- Matsudaira, P., 1987 Sequence from picomole quantities of proteins electroblotted onto polyvinylidene difluoride membranes. *J Biol Chem* 262: 10035-10038.
- Mercier, R., and M. Grelon, 2008 Meiosis in plants: ten years of gene discovery. *Cytogenet Genome Res* 120: 281-290.
- Meuwissen, R. L., H. H. Offenberg, A. J. Dietrich, A. Riesewijk, M. van Iersel *et al.*, 1992 A coiled-coil related protein specific for synapsed regions of meiotic prophase chromosomes. *EMBO J* 11: 5091-5100.
- Miller, M. A., U. Technau, K. M. Smith and R. E. Steele, 2000 Oocyte development in *Hydra* involves selection from competent precursor cells. *Dev Biol* 224: 326-338.
- Moens, P. B., N. K. Kolas, M. Tarsounas, E. Marcon, P. E. Cohen *et al.*, 2002 The time course and chromosomal localization of recombination-related proteins at meiosis in the mouse are compatible with models that can resolve the early DNA-DNA interactions without reciprocal recombination. *J Cell Sci* 115: 1611-1622.
- Moens, P. B., E. Marcon, J. S. Shore, N. Kochakpour and B. Spyropoulos, 2007 Initiation and resolution of interhomolog connections: crossover and non-crossover sites along mouse synaptonemal complexes. *J Cell Sci* 120: 1017-1027.
- Moses, M. J., 1956 Chromosomal structures in crayfish spermatocytes. *J Biophys Biochem Cytol* 2: 215-218.
- Nishimiya-Fujisawa, C., and T. Sugiyama, 1993 Genetic analysis of developmental mechanisms in hydra. XX. Cloning of interstitial stem cells restricted to the sperm differentiation pathway in *Hydra magnipapillata*. *Dev Biol* 157: 1-9.
- Offenberg, H. H., J. A. Schalk, R. L. Meuwissen, M. van Aalderen, H. A. Kester *et al.*, 1998 SCP2: a major protein component of the axial elements of synaptonemal complexes of the rat. *Nucleic Acids Res* 26: 2572-2579.

- Öllinger, R., M. Alsheimer and R. Benavente, 2005 Mammalian protein SCP1 forms synaptonemal complex-like structures in the absence of meiotic chromosomes. *Mol Biol Cell* 16: 212-217.
- Page, S. L., and R. S. Hawley, 2001 c(3)G encodes a *Drosophila* synaptonemal complex protein. *Genes Dev* 15: 3130-3143.
- Page, S. L., and R. S. Hawley, 2003 Chromosome choreography: the meiotic ballet. *Science* 301: 785-789.
- Page, S. L., and R. S. Hawley, 2004 The genetics and molecular biology of the synaptonemal complex. *Annu Rev Cell Dev Biol* 20: 525-558.
- Page, S. L., R. S. Khetani, C. M. Lake, R. J. Nielsen, J. K. Jeffress *et al.*, 2008 Corona is required for higher-order assembly of transverse filaments into full-length synaptonemal complex in *Drosophila* oocytes. *PLoS Genet* 4: e1000194.
- Pelttari, J., M. R. Hoja, L. Yuan, J. G. Liu, E. Brundell *et al.*, 2001 A meiotic chromosomal core consisting of cohesin complex proteins recruits DNA recombination proteins and promotes synapsis in the absence of an axial element in mammalian meiotic cells. *Mol Cell Biol* 21: 5667-5677.
- Peter, A., and R. Stick, 2012 Evolution of the lamin protein family: What introns can tell. *Nucleus* 3: 44-59.
- Petronczki, M., M. F. Siomos and K. Nasmyth, 2003 Un menage a quatre: the molecular biology of chromosome segregation in meiosis. *Cell* 112: 423-440.
- Philippe, H., R. Derelle, P. Lopez, K. Pick, C. Borchiellini *et al.*, 2009 Phylogenomics revives traditional views on deep animal relationships. *Curr Biol* 19: 706-712.
- Revenkova, E., M. Eijpe, C. Heyting, C. A. Hodges, P. A. Hunt *et al.*, 2004 Cohesin SMC1 beta is required for meiotic chromosome dynamics, sister chromatid cohesion and DNA recombination. *Nat Cell Biol* 6: 555-562.
- Revenkova, E., and R. Jessberger, 2005 Keeping sister chromatids together: cohesins in meiosis. *Reproduction* 130: 783-790.
- Romanienko, P. J., and R. D. Camerini-Otero, 2000 The mouse *Spo11* gene is required for meiotic chromosome synapsis. *Mol Cell* 6: 975-987.
- Ronquist, F., M. Teslenko, P. van der Mark, D. L. Ayres, A. Darling *et al.*, 2012 MrBayes 3.2: efficient Bayesian phylogenetic inference and model choice across a large model space. *Syst Biol* 61: 539-542.
- Schalk, J. A., A. J. Dietrich, A. C. Vink, H. H. Offenberger, M. van Aalderen *et al.*, 1998 Localization of SCP2 and SCP3 protein molecules within synaptonemal complexes of the rat. *Chromosoma* 107: 540-548.
- Scherthan, H., S. Weich, H. Schwegler, C. Heyting, M. Harle *et al.*, 1996 Centromere and telomere movements during early meiotic prophase of mouse and man are associated with the onset of chromosome pairing. *J Cell Biol* 134: 1109-1125.
- Schild-Prüfert, K., T. T. Saito, S. Smolikov, Y. Gu, M. Hincapie *et al.*, 2011 Organization of the synaptonemal complex during meiosis in *Caenorhabditis elegans*. *Genetics* 189: 411-421.
- Schmekel, K., and B. Daneholt, 1995 The central region of the synaptonemal complex revealed in three dimensions. *Trends Cell Biol* 5: 239-242.



- Schmekel, K., and B. Daneholt, 1998 Evidence for close contact between recombination nodules and the central element of the synaptonemal complex. *Chromosome Res* 6: 155-159.
- Schmekel, K., R. L. Meuwissen, A. J. Dietrich, A. C. Vink, J. van Marle *et al.*, 1996 Organization of SCP1 protein molecules within synaptonemal complexes of the rat. *Exp Cell Res* 226: 20-30.
- Schramm, S., 2011 SYCE3, ein neues Synaptonemalkomplexprotein: Expression, funktionelle Analyse und Bindungspartner. Dissertation thesis, University of Würzburg.
- Schramm, S., J. Fraune, R. Naumann, A. Hernandez-Hernandez, C. Hoog *et al.*, 2011 A novel mouse synaptonemal complex protein is essential for loading of central element proteins, recombination, and fertility. *PLoS Genet* 7: e1002088.
- Schücker, K., T. Holm, M. Sauer, R. Benavente, 2014 Elucidation of synaptonemal complex organization by super-resolution imaging. *In preparation*.
- Severson, A. F., L. Ling, V. van Zuylen and B. J. Meyer, 2009 The axial element protein HTP-3 promotes cohesin loading and meiotic axis assembly in *C. elegans* to implement the meiotic program of chromosome segregation. *Genes Dev* 23: 1763-1778.
- Sievers, F., A. Wilm, D. Dineen, T. J. Gibson, K. Karplus *et al.*, 2011 Fast, scalable generation of high-quality protein multiple sequence alignments using Clustal Omega. *Mol Syst Biol* 7: 539.
- Smolikov, S., A. Eizinger, K. Schild-Prufert, A. Hurlburt, K. McDonald *et al.*, 2007 SYP-3 restricts synaptonemal complex assembly to bridge paired chromosome axes during meiosis in *Caenorhabditis elegans*. *Genetics* 176: 2015-2025.
- Smolikov, S., K. Schild-Prufert and M. P. Colaiacovo, 2009 A yeast two-hybrid screen for SYP-3 interactors identifies SYP-4, a component required for synaptonemal complex assembly and chiasma formation in *Caenorhabditis elegans* meiosis. *PLoS Genet* 5: e1000669.
- Steele, R. E., 2012 The *Hydra* genome: insights, puzzles and opportunities for developmental biologists. *Int J Dev Biol* 56: 535-542.
- Storlazzi, A., L. Xu, A. Schwacha and N. Kleckner, 1996 Synaptonemal complex (SC) component Zip1 plays a role in meiotic recombination independent of SC polymerization along the chromosomes. *Proc Natl Acad Sci U S A* 93: 9043-9048.
- Tarsounas, M., T. Morita, R. E. Pearlman and P. B. Moens, 1999 RAD51 and DMC1 form mixed complexes associated with mouse meiotic chromosome cores and synaptonemal complexes. *J Cell Biol* 147: 207-220.
- Turner, J. M., S. K. Mahadevaiah, O. Fernandez-Capetillo, A. Nussenzweig, X. Xu *et al.*, 2005 Silencing of unsynapsed meiotic chromosomes in the mouse. *Nat Genet* 37: 41-47.
- von Wettstein, D., S. W. Rasmussen and P. B. Holm, 1984 The synaptonemal complex in genetic segregation. *Annu Rev Genet* 18: 331-411.
- Webber, H. A., L. Howard and S. E. Bickel, 2004 The cohesion protein ORD is required for homologue bias during meiotic recombination. *J Cell Biol* 164: 819-829.
- Wessel, D., and U. I. Flugge, 1984 A method for the quantitative recovery of protein in dilute solution in the presence of detergents and lipids. *Anal Biochem* 138: 141-143.
- Wiesner, M., 2013 Assembly des Synaptonemalkomplexes und homologe Rekombination in der Meiose des Modellorganismus *Hydra vulgaris*. Master thesis, University Würzburg.
- Wilkins, A. S., and R. Holliday, 2009 The evolution of meiosis from mitosis. *Genetics* 181: 3-12.

- Winkel, K., 2009 Synaptonemalkomplexprotein SYCP1: Bindungspartner, Polymerisationseigenschaften und evolutionäre Aspekte. Dissertation thesis, University of Würzburg.
- Winkel, K., M. Alsheimer, R. Ollinger and R. Benavente, 2009 Protein SYCP2 provides a link between transverse filaments and lateral elements of mammalian synaptonemal complexes. *Chromosoma* 118: 259-267.
- Wittlieb, J., K. Khalturin, J. U. Lohmann, F. Anton-Erxleben and T. C. Bosch, 2006 Transgenic *Hydra* allow in vivo tracking of individual stem cells during morphogenesis. *Proc Natl Acad Sci U S A* 103: 6208-6211.
- Wojtasz, L., K. Daniel, I. Roig, E. Bolcun-Filas, H. Xu *et al.*, 2009 Mouse HORMAD1 and HORMAD2, two conserved meiotic chromosomal proteins, are depleted from synapsed chromosome axes with the help of TRIP13 AAA-ATPase. *PLoS Genet* 5: e1000702.
- Yang, F., R. De La Fuente, N. A. Leu, C. Baumann, K. J. McLaughlin *et al.*, 2006 Mouse SYCP2 is required for synaptonemal complex assembly and chromosomal synapsis during male meiosis. *J Cell Biol* 173: 497-507.
- Yuan, L., J. G. Liu, J. Zhao, E. Brundell, B. Daneholt *et al.*, 2000 The murine SCP3 gene is required for synaptonemal complex assembly, chromosome synapsis, and male fertility. *Mol Cell* 5: 73-83.
- Yuan, L., J. Pelttari, E. Brundell, B. Bjorkroth, J. Zhao *et al.*, 1998 The synaptonemal complex protein SCP3 can form multistranded, cross-striated fibers in vivo. *J Cell Biol* 142: 331-339.
- Zacharias, H., B. Anokhin, K. Khalturin and T. C. Bosch, 2004 Genome sizes and chromosomes in the basal metazoan *Hydra*. *Zoology* 107: 219-227.
- Zetka, M. C., I. Kawasaki, S. Strome and F. Muller, 1999 Synapsis and chiasma formation in *Caenorhabditis elegans* require HIM-3, a meiotic chromosome core component that functions in chromosome segregation. *Genes Dev* 13: 2258-2270.
- Zheng, Y. H., D. Rengaraj, J. W. Choi, K. J. Park, S. I. Lee *et al.*, 2009 Expression pattern of meiosis associated SYCP family members during germline development in chickens. *Reproduction* 138: 483-492.
- Zickler, D., and N. Kleckner, 1998 The leptotene-zygotene transition of meiosis. *Annu Rev Genet* 32: 619-697.
- Zickler, D., and N. Kleckner, 1999 Meiotic chromosomes: integrating structure and function. *Annu Rev Genet* 33: 603-754.

# 15 Supplements

## 15.1 Supplementary Figures

```

>Mus_musculus      MERH-----GVAAPPVELKDQE-----PPAI---VESGKH-RQSENHEETPGSVA---PSASC---QL-----PGPFSSLD--S
>Homo_sapiens      MERQ-----GVDVPHVKCKDQE-----PQPL---GESKEHPRWEENCEEEAGGGP---ASASC---QLTVLE---GKSGLYFSSLD--S
>Canis_lupus       MERQ-----GVDMPHVECKDQE-----PQLL---GESKEQPQGEESREEEAGRGP---ASANR---QLMMLE---GKSGSCFSSLD--S
>Monodelphis_domestica (192) AKKPLGTMSEQDLKNKEQDQNDQAGPSIF---SELERSSSPNDVQGRHRFSSPSSLVSNADS---HTETLD---GKTS SFFVALD--A
>Sarcophilus_harrisii -----MSEQDLKNKEQDQCQDQAGPSIF---CDLEKSSTPCEVQGRHRFSSPSSLVSNADS---HTETLD---GKTS SFFAALD--A
>Macropus_eugenii -----D---GKTS SFFAALD--A
>Ornithorhynchus_anatinus -----KERESVSWAP---ISASERENPERVEPAENPFSESHELQGDRS---RVENPN---YTS SLPFPVPD--K
>Gallus_gallus     -----MTSHHPNVSTALQDNEAALQEPEETQNDTAC---CPGPGREKAHEESSRVEARGAAVLDR-----QASSRYFAALD--S
>Taeniopygia_guttata -----MSSNQEFLFEEAEQNKSNSPF---FSNVQRSTLSDDLRLKE SPNLRLLSSPLTS-----GGSD---SRST SFFMALN--S
>Anolis_carolinensis -----RKE SPSTSLLCPTADV---PVAALD---GKS ANYFTALD--S
>Pelodiscus_sinensis -----MSNQECE---SPEPEEEQAKPDS-----P
>Chelonia_mydas   -----GV---QRNTTHAHLFQFKCRKE SPSTSLLCPTADG---PVAALD---GKS NYFAALD--S
>Chrysemys_picta  -----RKN SPKTPL--PNANI---SGGRPD---SKAS NYFIALD--A
>Python_molurus   -----RKE PPPXSPTYPGADT---AMAALD---GKS NYLAALD--A
>Alligator_mississippiensis -----
>Xenopus_tropicalis -----
>Latimeria_chalumnae -----
>Danio_rerio      (23) HTSAKVPDDGLNSTGGTLSFVTLDDSSDLQND---DSGIGVSKTSSRSSPANNT-----AEDVAILPPNN--S
>Oryzias_latipes  -----MDFYFDDL PSTSQSTP---KKA-----QDDTQMVPEQS SSSL
>Oreochromis_niloticus (7) FTTIMFNSDLALQSQTQMDGFEDIPSNFYQYTP---KKGCEVSRMTEEDTDCDS SRGESS-----SVSVTEIQEH HSSS
>Tetraodon_nigroviridis -----MDFYLD DTPSSSQST (17) EKGGLVRRADSEEE TTSYGGPAC-----PVTVAIVDS--S
>Branchiostoma_floridae (6) SAKAGTVPASQQESRDATKDDKMFKHPGEPAAAT---RET---AVQEAPTS ETD SVSYSEPAIPAFT---SETLTE---NPMAS TIESGM--P
>Strongylocentrotus_purpuratus -----MS---NVGPVR---SDDKVTRQRPL--L
>Capitella_teleta (70) ADGNI FVRNSHGRVQMVNRNLSQLDSV NQQLAA---AASASEERDEVDANSTHDDTHSRQTRSAQT (71) ETGYLS (11) KPSTNVRDDQA--K
>Alvinella_pompejana -----SVYKLF DLETVMADTSTGMNYTESGNTSRCQ---ESDPDITRNPEDTAPGSDLDSNLNLH-----NNSHIV (11) TGE SSGVQAKL--S
>Lottia_gigantea  -----MTKRNWE SMQDMFNSSSSSNQLSIPHTD-----PFPEKVVISSE--I
>Crassostrea_gigas -----MTEPAINEETEFFANEIESEKALT---AEGDFSEKPLEDAKE ICNYQSGEFSS-----EHVFKIPENKG--L
>Daphnia_pulex    (72) LENFKVSSSGSVAGGQSPYFNVTNTPTKKSAI---QDTQVVKPLNAESP EADATPSNAV TQKEQM (14) ENNVEE---NKPRKLRPIGE--Y
>Nematostella_vectensis -----MEGESEENGLQNK EIDSASEST---NLNSEVT SENNDTKKEENVSLADTI TPCEP---E EKARE (11) PHLSDVSKTKL--L
>Hydra_magnipapillata -----MTNK---RK F---VREKVEADSDKIGNVEDEVKQL---EE--TD---HNLSTDLDKPLSSL
Consensus          :      :      :      :      :      :      :      :      :      :
    
```

```

>Mus_musculus      SIETLKKK-AQELIENINERQKDHALMTNFRDSLKMKVS-DLTEKLEERMYQV SHHSKIIQERLQEFQKMAKINHLEME
>Homo_sapiens      SIDILQKR-AQELIENINKSRQKDHALMTNFRNSLTKVS-DLTEKLEERIQI NDHNKIIQEKLEFTQKMAKISHLETE
>Canis_lupus       SIDILKKR-AQELIENINERQKDHALMTNFRDSLKIKVS-DLTEKLEERMYQI NHHNKIIQDKLEFTQKMAKISHLETE
>Monodelphis_domestica SIETLQKR-AQQLIDSINERQKDHLMNSNFRDSLKMKVS-DLVEKLEERMYQI DHHNKLIQEKLEFSEKMEKINNLETE
>Sarcophilus_harrisii SIETLQKR-AQQLIDSINERQKDHLMNSNFRDSLKMKVS-DLVEKLEERMYQI DHHNKLIQDKLEFSEKIEKINNLETE
>Macropus_eugenii  SIETLQKR-AQQLIDSINERQKDHLMNSNFRDSLKMKVS-DLVEKLEERMYQI DHHNKLIQEKLEFSEKIEKINNLETE
>Ornithorhynchus_anatinus NVGHMQKR-SEILLKHINDSRKKDYKIMQNKRTVYMKKAVAMNKIEGKFCQF NHQTNYIQEKLEFKRSLASASNLEND
>Gallus_gallus     SVGDLRQR-AQGLIDRLNDSRKEDHTVMSGFRDSLQLEVS-NLAEQLEERLQFL SLHNELIQERLQELAEVMERVRQAEDA
>Taeniopygia_guttata -----XXXQVS-ELTEQLEERLFHG GFHNGLIQERLQALSEVLERVEGVQAE
>Anolis_carolinensis TIENMEQR-TQQLIDKINGNRKNDHEFMNTFRENLLMKVS-SLAEKLEERVYFV DHNSKLIQDKLVFSEIMERIRQIETE
>Pelodiscus_sinensis NIENLQKR-TQQLIEKINENRKKDHT-XXXXXXXXXXLQVS-SLAEKLEEMMFLI DRHNKMQDKLQELSEIMERISQIQAE
>Chelonia_mydas    FFEDIERRELHSEILSRSDSKGKDKGFTFSIE-----QVS-SLAEKLEEMMFLI DRHNKMQDKLQELSEIMERISQIQTE
>Chrysemys_picta   NIENLQRR-TQQLIEKINENRKKDHTVMSNFRSLLMKVS-SLAEKLEEMMFLI DRHNKMQDKLQELSEIMERISQIQTE
>Python_molurus    TIENLQER-TQHLIDKINENRKKDHTVMSNFRSLLMKVS-SLAEKLEESVFPV DHNNKLIQDKLQELSEIMERIRQIETE
>Alligator_mississippiensis NIENLQKR-TQQLIDKINENRKKDHTVMSNFRSLLMKVS-TLAEKLEEMMFLI DLHNKLMQDKLQELSDAMGRISQIGAE
>Xenopus_tropicalis -----MKNFNESLAKKVA-ELSKILEARMYCM DEHNKLLQERLQELPEIMDRIGELQSE
>Latimeria_chalumnae -----VS-ELIQKLEEGIYEI DHHNKMMQDKLQELTEIMGRIGQLEIE
>Danio_rerio       PIDEIGKK-AHDLIERINERRALDQHVMTSFEEQLIKKT-EMCQQVKDQMFKY EEHSQGIESSITELSEVLERSSQLSME
>Oryzias_latipes   GIEDISRR-AQETVEDINHSRTNDQKVMDDFQEKLAEKKT-ETCRQMKEHMYTV EENSDEMQLQELSKVLESCSKLNRE
>Areochromis_niloticus RTDDISRK-AQESVQKINQSRISNQMIDSFQEKLEVEKKT-DLCMQMKEHMYKV EENSQKMQVNLQELQEVLESCTKFSHE
>Tetraodon_nigroviridis VIDEISSK-VQDLVEKINNSRASDQRMDSFQEEELMTKKT-EVCQEMKESMYTV EDNSNEMHVKLKELSRVLESCTRLHQE
>Branchiostoma_floridae TREMLNQS-AQKLVDDINSKRKRDAALLSDFKKALEIQG-NSCSLLESSEMYQT ETTGGRMQEKLELFAVLDRVSKLEAE
>Strongylocentrotus_purpuratus SREALNDQ-AQQLIEKINEKRRKRDNTVLDLDFRKKVLQDKVA-LTCGALERMYRV ETSQKMQPKLEFFATLDRVAIERE
>Capitella_teleta  DRESISND-LQVLVGEINSRRESDMKLLSDFKSEIMMQAH-KACSVLEQKIFDM NYQSGQVPMMEALVATLERVKGHEAE
>Alvinella_pompejana TKEVIEK-VQQLVQGLNDRKQDTPVMDHFKKNLQMHFE-KASKAMEENLFQI QRQSERIQVVLNLFLLNRIAAIENE
>Lottia_gigantea   NRDSLSTA-AQQIIDLNAKRRKQDTQLLIDLKKALEKQTE-KVYKATEQHLFAV DKQGGKIVQDKIQQLFSDIENISKLETE
>Crassostrea_gigas TRLEIQDA-ANNIEATNKKRKRDSMDLRDFKKTAEYQLS-ATLLEMQHIIHKV ERQGGKLMEDKQELMARLEKIGKLEQE
>Daphnia_pulex     TVSSLDKE-FQDIMHLKQERERDKQLFLQCSKALREKTE-SIIEENLENIKGR QSLDENLHLSVIEFVKEWESGRKLEEE
>Nematostella_vectensis SSEELQRG-VQELIDSVNTRSRDNTNLTDFKKALEMQLS-KSCTALEEALVQS EQNNQTIQSKLEFFAVIERIGQLETE
>Hydra_magnipapillata TSESIINH-VQSIIDMEVKKRDETLIVEFRKSMEIQTE-IWCDLLEKTLAKV MKNNNTCQEKFQQLHTILGRISQLEQE
Consensus          ::::: :*:*:*:*:*:*:*:*:*:*:*:*:*:*:*:*:*:*:*:*:*:*:*:*:*:*:*:*:*:*:*:*:*:*:*:*:*:*:*:*:*:*:*:*:*:*:*:*:*:*:*:*:*:*:*:*:*:*:*:*:*

```

```

>Mus_musculus      LKQVCQTVETVYKDLCVQS-----E-(13)C
>Homo_sapiens      LKQVCHSVETVYKDLCLQP-----EQ(51)C
>Canis_lupus       LKQVCHTVETVYKDLCIQP-----E-----V
>Monodelphis_domestica LKQVCHTVETVYKDLCVQP-----E-----I
>Sarcophilus_harrisii LKQVCHTVETVYKDLCVQP-----E-----I
>Macropus_eugenii  LKQVCHTVETVYKDLCVQP-----E-----I
>Ornithorhynchus_anatinus IQDICQAMEETLTECIVNM---ADHSCL--E
>Gallus_gallus     LQQVCHTVEAATRDLCLOP-----E-----T

```

```

>Taeniopygia_guttata      LRRICCTVEAVYQDLCLQP-----E-----D
>Anolis_carolinensis     LRQVCNTVEILTKDLCGQA-----E-----L
>Pelodiscus_sinensis     LRQVCHTVEAAVKDLCMQP-----E-----
>Chelonia_mydas         LRQVCHTVEAAVKDLCVQP-----E-----V
>Chrysemys_picta        LRQVCHTVEAAVKDLCVQP-----E-----V
>Python_molurus         LRQVCHTVEEMTKDLCGQS-----E-----L
>Alligator_mississippiensis LRQVCHAVEAAVKDLCIQP-----E-----M
>Xenopus_tropicalis     LKQVCQTVVTVYQDLCVHP-----D-----V
>Latimeria_chalumnae    LKQVCRTVVTVYKDLCVQP-----EL(50)V
>Danio_rerio            LQGASQTLAIINKGLQHGT-----E-----Q
>Oryzias_latipes       LLEAAQALAFLEGLAMSQ-----RSE---S
>Oreochromis_niloticus  LLEANRALACLREGDM-----P
>Tetraodon_nigroviridis LMEATQALTGLRVSIGVKK-----QD---C
>Branchiostoma_floridae LKQFRQALGMLYTDVQAPQ-----T-----Q
>Strongylocentrotus_purpuratus LAHFKEALGVLYIDIQTK-----R
>Capitella_teleta      LSDFRQTMHMIYQDM-----A
>Alvinella_pompejana    LSQFKQVMGNLYEQLNCS-----D
>Lottia_gigantea       LKEFKQALQILYQDMK-----D
>Crassostrea_gigas     LGEFRKALQLLYHDMNKSE(992)KS(51)V
>Daphnia_pulex         FNVLRNHMSSIMNNILQDPCL-----E
>Nematostella_vectensis LAEFKATLGPPKNEEHKKH-----FN(20)S
>Hydra_magnipapillata  MSSFKQSLNSLYAEVQATY----- (3)-Q
Consensus              *:.....*:...:

```

**Supplementary Figure 1: Multiple alignment of SYCE2 homologues.** The alignments were created by MAFFT and annotated with CHROMA. Identical residues are marked with a star in the consensus line while colons indicate residues with similar features. The threshold for grouping of the residues was set to 60%. Positions kept for phylogenetic inferences are indicated in red.











```

>Xenopus_tropicalis      IYTRLCQEWEAARK-----NMSEDSVDQMACGVGAEGAQKEQAGALQEEQP-----
>Latimeria_chalumnae    KCN-----
>Danio_rerio            -----
>Oryzias_latipes        -----
>Oreochromis_niloticus  -----
>Ictalurus_punctatus    -----
>Branchiostoma_floridae -----
>Asterina_pectinifera   -----
>Capitella_teleta       -----
>Crassostrea_gigas      KLTTLKA-----
>Lottia_gigantea        KLKESLE-----
>Mytilus_californianus  LIEAI-----
Consensus                :: ::::

```

**Supplementary Figure 3: Multiple alignment of SYCE1 homologues.** The alignments were created by MAFFT and annotated with CHROMA. Identical residues are marked with a star in the consensus line while colons indicate residues with similar features. The threshold for grouping of the residues was set to 60%. Positions kept for phylogenetic inferences are indicated in red.

```

>Mus_musculus      ---MADSDPGERSYDNMLKMLSDLNKDLEKLLLEEMEKIS--VQATMAYDMVMRTNPFLAESMRRLDAFLNCKEEMKKN--QELLTETKRKQ----
>Homo_sapiens      ---MDADAPEERNYDNMLKMLSDLNKDLEKLLLEEMEKIS--VQATMAYDMVMRTNPFLAESMRRLDAFVNCKEEMKKN--QELLHETKQRL----
>Canis_lupus       ---MADSEPGERNYDNMLKMLSDLNKDLEKLLLEEMEKIS--VQATMAYDMVMRTNPFLAESMRRLDAFLNCKEEMKKN--QELLNETKHKQ----
>Monodelphis_domestica -----XXXXXXXXX--LQATMAYDMVMRTNPALADSMRRLDAFLNCKEEMKKN--QELLNETKPKQ----
>Sarcophilus_harrisii -----XXXXXXXXX--VQATMAYDMVMRTNPALADSMRRLDAFLNCKEEMKKN--QELLNETKPKQ----
>Macropus_eugenii  ---QGDAKSGD-NYDNILKMLSN-----LKD LKME--NQATMAYDMVMRTNPALADSMRRLDAFLNCKEEMKKN--QELLNETKPKP----
>Ornithorhynchus_anatinus ---MAETDPGERSYD-MPKSLSDLNRDLENLLEEMEKIS--VQATMAYDMVMRTNPFLADTLRRLRLEGSFLDCKEEMKKN--QALLQETQSAPSR--
>Gallus_gallus     ---MARQEPQERNYDNMLKMVEDLNRDLEKLLLEIEKLT--VQATMAYDMVMRTNPDLTNSMRRLDAFLNCKEEMKKN--QEVLRSEKGEQKK--
>Taeniopygia_guttata ---MDESESQKENYNEGKMVENFNMDMEELDEMEKLT--VRAAMAYDYVAIQTNPGPYNAMQHLEDAFLMCKEQMEKK--QEVLLFRGEGQKK--
>Meleagris_gallopavo ---MARQEPQERNYDNMLKMIEDLNRDLEKLLLEEMEKLT--VQATMAYDMVMRTNPDLTNSMRRLDAFLNCKEEMKKN--QEVLRSEKGEQKK--
>Anolis_carolinensis ---MAKCEPTYERNYDNIVKQLEDLNRDLEKLLLEEMEKLSIPVQATMAYDMVMRTNPDLANSRRLDAFLNCKEEMERN--QEMLKETKGAEQRP--
>Pelodiscus_sinensis ---MAKSEPQERNYDNMVKMLEDLNRDLEKLLLEEMEKLSVAVQATMAYDMVMRTNPDLANSRRLDAFLNCKEEMKKN--KEMLKETKGNEQKQ--
>Chelonia_mydas    ---MAKSEPRERNYDNMVKMLEDLNRDLEKLLLEEMEKLSVAVQATMAYDMVMRTNPDLANSRRLDAFLNCKEEMKKN--QEMLKETKGTEQKQ--
>Chrysemys_picta   ---MAKSEPQERNYDNMVKMLEDLNRDLEKLLLEEMEKLSVAVQATMAYDMVMRTNPDLANSRRLDAFLNCKEEMKKN--QEMLKETKGTEQKQ--
>Python_molurus    -----VS-----VQATMAYDMVMRTNPDLANSRRLDAFLNCKEEMKKN--QEMLKETKGAEQPK--
>Alligator_mississippiensis ---MAKSEPQERNCDNMVKMLEDLNRDLEKLLLEEMEKLSVAVQATMAYDMVMRTNPDLANSRRLDAFLNCKEEMKKN--QEMLKETKDGGEKK--
>Xenopus_tropicalis ---MAEPEQTSVQSSQEDVSRMLRDLDNDDLENMLEKMETLS--VRTTEMAYDMVALRTPALAQSMKRLDAFFKCKREEIEKN--QEMLEETKQTKPEP--
>Latimeria_chalumnae ---MAESELCEKKHNDNILKMLCDLNRDLEKMLEDIEKISGRVQATMAYDMVMRTNPALTDMSMKLEDAFLNCKEEVERN--QEMLSETKGNQ----
>Danio_rerio       ---MSGGLSDVQLCEDFSSSELQLNQHLEKMTQMEDVVS--VKLSCMTYDMVLRTPDLAESFKSLENEFQKCKAVLCGL--TDGQEVKCHPADEEQV--
>Oryzias_latipes   (4)MSDSSASALPG--SNDDVLELNKNLERMVEDTENMS--AQLTMAAYDMVALRTPALAEFGASMRQLEAYQRCCRAAVFGDSAPPEPEGETDSASAKP--
>Oreochromis_niloticus ---MADSARSALPRISDDDKLEMNKELERMIEDVESMS--AHLTMAAYDMVALRTPALAEFGASMRQLEAYQRCCRAAVCGD--PDQESQIDKYAETAVT--
>Tetraodon_nigroviridis ---MS-----ELTEDLERMTEHTEKMS--LQLTMAHDLVLRASELSSMRKLEAYRGCRAAVCGD--PEPDKSPAAPGAQP--
>Ictalurus_punctatus ---MVDNASAGEQYEDFGRETLECSKDLEERMTEQMEKIS--VNVVMTYDMVLRTPDLAKSLKRLKNEFVQCKAVICGS--GDNLVQDRIVANQKT--
Consensus          *::: :::: :::: :::: :::: :::: :::: :::: :::: :::: :::: :::: :::: :::: :::: :::: :::: :::: :::: :::: :::: ::::

```

```

>Mus_musculus      -----
>Homo_sapiens      -----
>Canis_lupus       -----
>Monodelphis_domestica -----
>Sarcophilus_harrisii -----
>Macropus_eugenii  -----
>Ornithorhynchus_anatinus -----
>Gallus_gallus     -----E
>Taeniopygia_guttata -----E
>Meleagris_gallopavo -----E
>Anolis_carolinensis -----E
>Pelodiscus_sinensis -----E
>Chelonia_mydas    -----E
>Chrysemys_picta   -----E
>Python_molurus    -----
>Alligator_mississippiensis -----E

```

---

```
>Xenopus_tropicalis      EANTD
>Latimeria_chalumnae   -----
>Danio rerio            SPKTN
>Oryzias_latipes       --TEM
>Oreochromis_niloticus TLSQM
>Tetraodon_nigroviridis ----D
>Ictalurus_punctatus   --TQE
Consensus
```

**Supplementary Figure 4: Multiple alignment of SYCE3 homologues.** The alignments were created by MAFFT and annotated with CHROMA. Identical residues are marked with a star in the consensus line while colons indicate residues with similar features. The threshold for grouping of the residues was set to 60%. Positions kept for phylogenetic inferences are indicated in red.











## 15.2 Supplementary Tables

Supplementary Table 1

Origin of SYCP1 homologues		
Species name	Taxonomic rank	Accession number or source
<i>A. carolinensis</i>	Tetrapoda	XP_003220552
<i>G. gallus</i>	Tetrapoda	NW_001471609.1
<i>C. lupus</i>	Tetrapoda	XP_857086
<i>E. caballus</i>	Tetrapoda	XP_001496166
<i>M. musculus</i>	Tetrapoda	BAA13639
<i>M. mulatta</i>	Tetrapoda	XP_001111808
<i>H. sapiens</i>	Tetrapoda	EAW56624
<i>T. guttata</i>	Tetrapoda	NW_002205215.1
<i>X. tropicalis</i>	Tetrapoda	EL822968
<i>D. rerio</i>	Actinopterygii	AAH54660
<i>O. latipes</i>	Actinopterygii	JQ906936
<i>B. floridae</i>	Cephalochordata	ABEP02021905
<i>C. savignyi</i>	Tunicata	AACT01000684
<i>C. intestinalis</i>	Tunicata	XP_002126213
<i>S. purpuratus</i>	Echinodermata	AAGJ04087648
<i>C. teleta</i>	Annelida	<a href="http://genome.jgi.doe.gov/">http://genome.jgi.doe.gov/</a>
<i>A. pompejana</i>	Annelida	GO222799
<i>L. gigantea</i>	Mollusca	FC693207
<i>C. gigas</i>	Mollusca	AM861984
<i>A. californica</i>	Mollusca	<a href="http://genome.ucsc.edu/">http://genome.ucsc.edu/</a>
<i>P. cinctipes</i>	Crustacea	FE795932, FE750881
<i>H. vulgaris</i>	Cnidaria	JQ906934
<i>N. vectensis</i>	Cnidaria	FC319267
<i>P. pileus</i>	Ctenophora	FP999277
<i>A. queenslandica</i>	Porifera	ACUQ01003074
Origin of CCDC39 homologues		
<i>H. sapiens</i>	Tetrapoda	NP_852091

<i>S. purpuratus</i>	Echinodermata	XP_781717
<i>D. melanogaster</i>	Hexapoda	ACD81657

Supplementary Table 2

Origin of SYCP3 homologues		
Species name	Taxonomic rank	Accession number or source
<i>M. musculus</i>	Tetrapoda	P70281
<i>R. norvegicus</i>	Tetrapoda	NP_037173
<i>C. griseus</i>	Tetrapoda	XP_003499744
<i>M. mulatta</i>	Tetrapoda	XP_001092064
<i>H. sapiens</i>	Tetrapoda	NP_710161
<i>B. Taurus</i>	Tetrapoda	EV636425
<i>S. scrofa</i>	Tetrapoda	XP_003126725
<i>G. gallus</i>	Tetrapoda	XP_416330
<i>X. laevis</i>	Tetrapoda	NP_001108302
<i>D. rerio</i>	Actinopterygii	NP_001035440
<i>T. nigroviridis</i>	Actinopterygii	CAF89756
<i>O. latipes</i>	Actinopterygii	NP_001098182
<i>B. floridae</i>	Cephalochordata	XP_002590403
<i>C. savignyi</i>	Tunicata	AACT01005945.1
<i>C. intestinalis</i>	Tunicata	XP_002125203
<i>M. tectiformis</i>	Tunicata	CJ405176
<i>P. lividus</i>	Echinodermata	AM591176
<i>S. purpuratus</i>	Echinodermata	<a href="http://www.spbase.org/">http://www.spbase.org/</a>
<i>A. pompejana</i>	Annelida	GO140558, GO140559
<i>E. clavigera</i>	Annelida	FR757763
<i>L. gigantea</i>	Mollusca	<a href="http://genome.jgi-psf.org/">http://genome.jgi-psf.org/</a>
<i>A. purpuratus</i>	Mollusca	ES469350
<i>H. vulgaris</i>	Cnidaria	JQ906932
<i>C. hemisphaerica</i>	Cnidaria	CU427518
<i>N. vectensis</i>	Cnidaria	XM_001635156
<i>M. leidy</i>	Ctenophora	FC471529
<i>A. queenslandica</i>	Porifera	ACUQ01004382
<i>T. adhaerens</i>	Placozoa	XM_002115536
Origin of SYCP2 homologues		
<i>H. sapiens</i>	Tetrapoda	CAM28337

---

<i>M. musculus</i>	Tetrapoda	BAC26589
<i>G. gallus</i>	Tetrapoda	BU226441
<i>X. tropicalis</i>	Tetrapoda	CX939648
<i>D. rerio</i>	Actinopterygii	XP_685048

Supplementary Table 3

Origin of the SYCE2 homologues						
Species name	Taxonomic rank	Accession number	sequence	Method/database	seed	E-value
<i>M. musculus</i>	Tetrapoda	NP_082230	complete	BLASTp/ NCBI nr		0
<i>P. paniscus</i>	Tetrapoda	XP_003814885	complete	BLASTp /NCBI nr	<i>M. musculus</i>	1e-70
<i>R. norvegicus</i>	Tetrapoda	EDL92193	complete	BLASTp /NCBI nr	<i>M. musculus</i>	5e-123
<i>H. sapiens</i>	Tetrapoda	NP_001099048	complete	BLASTp /NCBI nr	<i>M. musculus</i>	1e-70
<i>P. troglodytes</i>	Tetrapoda	XP_001155819	complete	BLASTp /NCBI nr	<i>M. musculus</i>	1e-70
<i>P. abelii</i>	Tetrapoda	XP_002828793	complete	BLASTp /NCBI nr	<i>M. musculus</i>	4e-71
<i>P. anubis</i>	Tetrapoda	XP_003915053	complete	BLASTp /NCBI nr	<i>M. musculus</i>	5e-70
<i>N. leucogenys</i>	Tetrapoda	XP_003256956	complete	BLASTp /NCBI nr	<i>M. musculus</i>	2e-70
<i>L. africana</i>	Tetrapoda	XP_003413389	complete	BLASTp /NCBI nr	<i>M. musculus</i>	8e-75
<i>S. boliviensis</i>	Tetrapoda	XP_003941778	complete	BLASTp /NCBI nr	<i>M. musculus</i>	2e-69
<i>C. jacchus</i>	Tetrapoda	XP_002761833	complete	BLASTp /NCBI nr	<i>M. musculus</i>	1e-66
<i>C. lupus</i>	Tetrapoda	XP_542039	complete	BLASTp /NCBI nr	<i>M. musculus</i>	2e-73
<i>B. taurus</i>	Tetrapoda	DAA28039	complete	BLASTp /NCBI nr	<i>M. musculus</i>	4e-74
<i>M. mulatta</i>	Tetrapoda	XP_002801138	complete	BLASTp /NCBI nr	<i>M. musculus</i>	1e-54
<i>C. porcellus</i>	Tetrapoda	XP_003468209	complete	BLASTp /NCBI nr	<i>M. musculus</i>	7e-58
<i>O. cuniculus</i>	Tetrapoda	XP_002724280	complete	BLASTp /NCBI nr	<i>M. usculus</i>	1e-64
<i>S. scrofa</i>	Tetrapoda	XP_003480827	complete	BLASTp /NCBI nr	<i>M. musculus</i>	4e-63
<i>C. griseus</i>	Tetrapoda	EGW00612	partial	BLASTp /NCBI nr	<i>M. musculus</i>	2e-45
<i>A. melanoleuca</i>	Tetrapoda	EFB28619	Complete	BLASTp /NCBI nr	<i>M. musculus</i>	4e-65
<i>M. putorius</i>	Tetrapoda	AES07688	Complete	BLASTp /NCBI nr	<i>M. musculus</i>	2e-64
<i>O. garnettii</i>	Tetrapoda	XP_003798068	partial	BLASTp /NCBI nr	<i>M. musculus</i>	1e-39
<i>M. domestica</i>	Tetrapoda	XP_001377747	complete	BLASTp /NCBI nr	<i>M. musculus</i>	6e-57
<i>S. harrisi</i>	Tetrapoda	XP_003760717	complete	BLASTp /NCBI nr	<i>M. musculus</i>	4e-56
<i>M. eugenii</i>	Tetrapoda	ABQO021047289	partial	tBLASTn/NCBI wgs	<i>S. harrisi</i>	3e-41
<i>O. anatinus</i>	Tetrapoda	ENSOANP00000014450	partial	BLASTp/UniProtKB	<i>M. musculus</i>	2x10-5
<i>G. gallus</i>	Tetrapoda	XP_003643433	complete	BLASTp /NCBI nr	<i>M. musculus</i>	1e-37
<i>T. guttata</i>	Tetrapoda	XP_002194928	partial	BLASTp /NCBI nr	<i>M. musculus</i>	4e-15
<i>A. carolinensis</i>	Tetrapoda	XP_003216437	complete	BLASTp /NCBI nr	<i>M. musculus</i>	6e-36
<i>P. sinensis</i>	Tetrapoda	ENSPSIP00000014147	partial	BLASTp/ UniProtKB	<i>A. carolinensis</i>	9x10-31
<i>P. molurus</i>	Tetrapoda	AEQU010394814	partial	tBLASTn/NCBI wgs	<i>A. carolinensis</i>	3e-30

<i>A. mississippiensis</i>	Tetrapoda	AKHW01024067	partial	tBLASTn/NCBI wgs	<i>A. carolinensis</i>	2e-18
<i>C. mydas</i>	Tetrapoda	EMP37242	complete	BLASTp /NCBI nr	<i>A. carolinensis</i>	3e-23
<i>C. picta</i>	Tetrapoda	AHGY01185898	partial	tBLASTn/NCBI wgs	<i>A. carolinensis</i>	1e-21
<i>X. tropicalis</i>	Tetrapoda	XP_002939167	partial	BLASTp /NCBI nr	<i>M. musculus</i>	1e-19
<i>L. chalumnae</i>	Coelacanth	AFYH01158832	partial	tBLASTn/NCBI wgs	<i>A. carolinensis</i>	8e-17
<i>D. rerio</i>	Actinopterygii	NP_001018339	complete	BLASTp /NCBI nr	<i>M. musculus</i>	2e-11
<i>O. mykiss</i>	Actinopterygii	BX_298349	complete	tBLASTn/Gene Indices	<i>D. rerio</i>	1,6e-44
<i>O. latipes</i>	Actinopterygii	FS528043	complete	tBLASTn/Gene Indices	<i>D. rerio</i>	1,1e-22
<i>O. niloticus</i>	Actinopterygii	XP_003453800	complete	BLASTp /NCBI nr	<i>M. musculus</i>	2e-06
<i>T. nigroviridis</i>	Actinopterygii	CAG03308	complete	BLASTp /NCBI nr	<i>M. musculus</i>	6e-10
<i>B. floridae</i>	Cephalochordata	XP_002591412	complete	BLASTp /NCBI nr	<i>M. musculus</i>	8e-15
<i>C. savignyi</i>	Tunicata	BW516106	complete	tBLASTn/NCBI est	<i>H. diversicolor</i>	2e-09
<i>C. intestinalis</i>	Tunicata	XP_002130896	complete	BLASTp /NCBI nr	<i>M. musculus</i>	0,008
<i>P. misakiensis</i>	Tunicata	AU036426	complete	tBLASTn/NCBI est	<i>H. diversicolor</i>	2e-06
<i>S. purpuratus</i>	Echinodermata	XP_003726746	complete	BLASTp /NCBI nr	<i>M. musculus</i>	1e-13
<i>A. pompejana</i>	Annelida	GO169636	complete	tBLASTn/NCBI est	<i>L. gigantea</i>	2e-14
<i>C. teleta</i>	Annelida	Jgi 210482 AMQN01004103	complete	Blastp/InParanoid tBLASTn/NCBI wgs	<i>M. musculus</i> <i>C. teleta</i>	4,9e-06
<i>S. nudus</i>	Annelida	FR768618	complete	tBLASTn/NCBI est	<i>L. gigantea</i>	2e-23
<i>L. stagnalis</i>	Mollusca	ES573602	complete	tBLASTn/NCBI est	<i>L. gigantea</i>	1e-09
<i>L. gigantea</i>	Mollusca	jgi 158004 AMQO01001743	complete	Blastp/InParanoid tBLASTn/NCBI wgs	<i>M. musculus</i> <i>L. gigantea</i>	1,8e-08
<i>C. gigas</i>	Mollusca	EKC37702	complete	BLASTp /NCBI nr	<i>M. musculus</i>	1e-04
<i>H. diversicolor</i>	Mollusca	GT866818	complete	tBLASTn/NCBI est	<i>L. gigantea</i>	2e-32
<i>D. pulex</i>	Crustacea	EFX69051	complete	Hmmsearch/NCBI est	<i>hmmprofil</i>	0,023
<i>H. magnipapillata</i>	Cnidaria	XP_002165182	complete	BLASTp /NCBI nr	<i>M. musculus</i>	5e-06
<i>N. vectensis</i>	Cnidaria	XP_001625149	complete	BLASTp /NCBI nr	<i>M. musculus</i>	2e-11

Supplementary Table 4

Origin of the Tex12 homologues						
Species name	Taxonomic rank	Accession number	sequence	Method/database	seed	E-value
<i>M. musculus</i>	Tetrapoda	NP_079963	complete	BLASTp /NCBI nr		0
<i>S. boliviensis</i>	Tetrapoda	XP_003923759	complete	BLASTp /NCBI nr	<i>M. musculus</i>	2e-60
<i>C. griseus</i>	Tetrapoda	XP_003498567	complete	BLASTp /NCBI nr	<i>M. musculus</i>	2e-68
<i>L. africana</i>	Tetrapoda	XP_003415682	complete	BLASTp /NCBI nr	<i>M. musculus</i>	3e-63
<i>B. taurus</i>	Tetrapoda	NP_001029435	complete	BLASTp /NCBI nr	<i>M. musculus</i>	2e-63
<i>M. mulatta</i>	Tetrapoda	NP_001181321	complete	BLASTp /NCBI nr	<i>M. musculus</i>	1e-61
<i>O. garnettii</i>	Tetrapoda	XP_003794793	complete	BLASTp /NCBI nr	<i>M. musculus</i>	1e-59
<i>O. cuniculus</i>	Tetrapoda	XP_002708480	complete	BLASTp /NCBI nr	<i>M. musculus</i>	7e-64
<i>E. caballus</i>	Tetrapoda	XP_001501942	complete	BLASTp /NCBI nr	<i>M. musculus</i>	1e-63
<i>P. abelii</i>	Tetrapoda	XP_002822521	complete	BLASTp/NCBI nr	<i>M. musculus</i>	6e-62
<i>H. sapiens</i>	Tetrapoda	NP_112565	complete	BLASTp /NCBI nr	<i>M. musculus</i>	9e-62
<i>A. melanoleuca</i>	Tetrapoda	XP_002921152	complete	BLASTp /NCBI nr	<i>M. musculus</i>	5e-61
<i>S. scrofa</i>	Tetrapoda	XP_003357347	complete	BLASTp /NCBI nr	<i>M. musculus</i>	7e-63
<i>C. porcellus</i>	Tetrapoda	XP_003472874	complete	BLASTp /NCBI nr	<i>M. musculus</i>	2e-57
<i>R. norvegicus</i>	Tetrapoda	NP_001178035	complete	BLASTp /NCBI nr	<i>M. musculus</i>	1e-72
<i>C. lupus</i>	Tetrapoda	XP_854089	complete	BLASTp/NCBI nr	<i>M. musculus</i>	2e-64
<i>H. glaber</i>	Tetrapoda	EHB18703	complete	BLASTp /NCBI nr	<i>M. musculus</i>	7e-18
<i>C. jacchus</i>	Tetrapoda	XP_003734157	complete	BLASTp /NCBI nr	<i>M. musculus</i>	3e-37
<i>S. harrisii</i>	Tetrapoda	XP_003764283	complete	BLASTp /NCBI nr	<i>M. musculus</i>	1e-36
<i>M. domestica</i>	Tetrapoda	AAFR03009835	complete	tBLASTn/NCBI wsg	<i>S. harrisii</i>	2e-23
<i>M. eugenii</i>	Tetrapoda	ENSMEUP00000005950	partial	tBLASTn/Ensembl genomic sequence	<i>S. harrisii</i>	5.4e-59
<i>M. gallopavo</i>	Tetrapoda	XP_003212810	complete	BLASTp /NCBI nr	<i>M. musculus</i>	3e-29
<i>G. gallus</i>	Tetrapoda	XP_001233099	complete	BLASTp /NCBI nr	<i>M. musculus</i>	3e-27
<i>T. guttata</i>	Tetrapoda	ABQF01045735	partial	tBLASTn/NCBI wsg	<i>G. gallus</i>	7e-16
<i>A. carolinensis</i>	Tetrapoda	FG795025	complete	tBLASTn/NCBI est	<i>O. niloticus</i>	1e-06
<i>P. sinensis</i>	Tetrapoda	AGCU01007591	partial	tBLASTn/NCBI wsg	<i>A. carolinensis</i>	9e-12
<i>P. molurus</i>	Tetrapoda	AEQU010325864	partial	tBLASTn/NCBI wsg	<i>A. carolinensis</i>	2e-16
<i>C. mydas</i>	Tetrapoda	AJIM01191925	partial	tBLASTn/NCBI wsg	<i>A. carolinensis</i>	1e-12
<i>C. picta</i>	Tetrapoda	AHGY01090089	partial	tBLASTn/NCBI wsg	<i>A. carolinensis</i>	3e-12

<i>A. mississippiensis</i>	Tetrapoda	AKHW01088812	partial	tBLASTn/NCBI wsg	<i>A. carolinensis</i>	1e-10
<i>X. tropicalis</i>	Tetrapoda	XP_002942798	complete	BLASTp /NCBI nr	<i>M. musculus</i>	5e-15
<i>L. chalumnae</i>	Coelacanth	BAH001008061	partial	tBLASTn/NCBI wsg	<i>A. carolinensis</i>	8e-09
<i>D. rerio</i>	Actinopterygii	XP_003200088	complete	BLASTp /NCBI nr	<i>M. musculus</i>	2e-10
<i>A. fimbria</i>	Actinopterygii	ACQ58790	complete	BLASTp /NCBI nr	<i>M. musculus</i>	2e-08
<i>O. niloticus</i>	Actinopterygii	XP_003453604	complete	BLASTp /NCBI nr	<i>M. musculus</i>	0,21
<i>O. latipes</i>	Actinopterygii	FS551872	complete	tBLASTn/NCBI est	<i>O. niloticus</i>	4e-39
<i>T. nigroviridis</i>	Actinopterygii	CR716219	Complete	tBLASTn/NCBI nr	<i>O. niloticus</i>	5e-22
<i>R. rutilus</i>	Actinopterygii	EG548787	complete	tBLASTn/NCBI est	<i>O. niloticus</i>	1e-21
<i>P. promelas</i>	Actinopterygii	DT342891	complete	tBLASTn/NCBI est	<i>O. niloticus</i>	5e-21
<i>D. labrax</i>	Actinopterygii	FM002700	complete	tBLASTn/NCBI est	<i>O. niloticus</i>	1e-41
<i>O. mykiss</i>	Actinopterygii	CR370999	complete	tBLASTn/NCBI est	<i>O. niloticus</i>	1e-26
<i>I. furcatus</i>	Actinopterygii	FD158102	complete	tBLASTn/NCBI est	<i>O. niloticus</i>	6e-11
<i>G. morhua</i>	Actinopterygii	EY966699	complete	tBLASTn/NCBI est	<i>O. niloticus</i>	3e-20
<i>P. olivaceus</i>	Actinopterygii	CX286679	complete	tBLASTn/NCBI est	<i>O. niloticus</i>	3e-18
<i>S. salar</i>	Actinopterygii	CB508238	partial	tBLASTn/NCBI est	<i>O. niloticus</i>	2e-24
<i>B. floridae</i>	Cephalochordata	XP_002590156	complete	BLASTp /NCBI nr	<i>M. musculus</i>	0,15
<i>S. purpuratus</i>	Echinodermata	AAGJ04009105	partial	tBLASTn/NCBI wsg	<i>A. pompejana</i>	0,35
<i>C. teleta</i>	Annelida	AMQN01002974	partial	tBLASTn/NCBI wsg	<i>L. gigantea</i>	8e-05
<i>A. pompejana</i>	Annelida	GO142621	complete	tBLASTn/NCBI est	<i>G. gallus</i>	0,009
<i>L. gigantea</i>	Mollusca	AMQO01006439	complete	tBLASTn/NCBI wsg	<i>B. floridae</i>	2e-09
<i>H. vulgaris</i>	Cnidaria	CN567182	complete	tBLASTn/NCBI est	<i>B. floridae</i>	3e-09



Supplementary Table 5

Origin of the SYCE1 homologues						
Species name	Taxonomic rank	Accession number	sequence	Method/database	seed	E-value
<i>M. musculus</i>	Tetrapoda	NP_001137237	complete	BLASTp/NCBI nr		0
<i>R. norvegicus</i>	Tetrapoda	NP_001020229	complete	BLASTp/NCBI nr	<i>M. musculus</i>	0
<i>H. sapiens</i>	Tetrapoda	NP_001137236	complete	BLASTp/NCBI nr	<i>M. musculus</i>	7e-119
<i>P. troglodytes</i>	Tetrapoda	XP_001146521	complete	BLASTp/NCBI nr	<i>M. musculus</i>	1e-117
<i>P. abelii</i>	Tetrapoda	XP_002821352	complete	BLASTp/NCBI nr	<i>M. musculus</i>	1e-120
<i>C. porcellus</i>	Tetrapoda	XP_003479623	complete	BLASTp/NCBI nr	<i>M. musculus</i>	2e-144
<i>N. leucogenys</i>	Tetrapoda	XP_003275547	complete	BLASTp/NCBI nr	<i>M. musculus</i>	6e-117
<i>P. paniscus</i>	Tetrapoda	XP_003805584	complete	BLASTp/NCBI nr	<i>M. musculus</i>	2e-115
<i>A. melanoleuca</i>	Tetrapoda	XP_002928741	complete	BLASTp/NCBI nr	<i>M. musculus</i>	1e-138
<i>C. griseus</i>	Tetrapoda	XP_003514379	complete	BLASTp/NCBI nr	<i>M. musculus</i>	4e-169
<i>L. africana</i>	Tetrapoda	XP_003423552	complete	BLASTp/NCBI nr	<i>M. musculus</i>	3e-122
<i>M. mulatta</i>	Tetrapoda	XP_002805923	complete	BLASTp/NCBI nr	<i>M. musculus</i>	4e-116
<i>E. caballus</i>	Tetrapoda	XP_001497316	complete	BLASTp/NCBI nr	<i>M. musculus</i>	1e-126
<i>P. anubis</i>	Tetrapoda	XP_003904501	complete	BLASTp/NCBI nr	<i>M. musculus</i>	2e-120
<i>O. cuniculus</i>	Tetrapoda	XP_002718820	complete	BLASTp/NCBI nr	<i>M. musculus</i>	2e-123
<i>B. taurus</i>	Tetrapoda	NP_001033238	complete	BLASTp/NCBI nr	<i>M. musculus</i>	5e-128
<i>C. lupus</i>	Tetrapoda	XP_537943	complete	BLASTp/NCBI nr	<i>M. musculus</i>	4e-144
<i>O. garnettii</i>	Tetrapoda	XP_003803715	complete	BLASTp/NCBI nr	<i>M. musculus</i>	7e-140
<i>M. fascicularis</i>	Tetrapoda	Q4R7J8	complete	BLASTp/NCBI nr	<i>M. musculus</i>	3e-101
<i>H. glaber</i>	Tetrapoda	EHB13133	complete	BLASTp/NCBI nr	<i>M. musculus</i>	1e-94
<i>M. domestica</i>	Tetrapoda	ADB77889	complete	BLASTp/NCBI nr	<i>M. musculus</i>	4e-55
<i>S. harrisii</i>	Tetrapoda	ENSSHAP00000009845	partial	BLASTp/UniProtKB	<i>M. domestica</i>	1x10-52
<i>M. eugenii</i>	Tetrapoda	FY576800	complete	tBLASTn/NCBI est	<i>M. domestica</i>	7e-109
<i>S. boliviensis</i>	Tetrapoda	XP_003938136	complete	BLASTp/NCBI nr	<i>M. musculus</i>	3e-38
<i>C. jacchus</i>	Tetrapoda	XP_003735392	complete	BLASTp/NCBI nr	<i>M. musculus</i>	2e-39
<i>O. anatinus</i>	Tetrapoda	ESOANP00000022990	complete	BLASTp/UniProtKB	<i>M. domestica</i>	4x10-76
<i>A. carolinensis</i>	Tetrapoda	XP_003216702	complete	BLASTp/NCBI nr	<i>M. musculus</i>	5e-44
<i>C. mydas</i>	Tetrapoda	EMP26554	partial	BLASTp/NCBI nr	<i>A. carolinensis</i>	6e-33

<i>P. sinensis</i>	Tetrapoda	ENSPSIP00000010027	partial	BLASTp/UniProtKB	<i>A. carolinensis</i>	2x10 <sup>-38</sup>
<i>X. tropicalis</i>	Tetrapoda	XP_002943661	complete	BLASTp /NCBI nr	<i>M. musculus</i>	3e-20
<i>L. chalumnea</i>	Coelacanth	H3ALY1	complete	Hmmsearch/UniProt	<i>hmmprofil</i>	8,7e-77
<i>P. reticulata</i>	Actinopterygii	ES386322	complete	tBLASTn/NCBI est	<i>O. latipes</i>	2e-49
<i>R. rutilus</i>	Actinopterygii	EG545611	complete	tBLASTn/NCBI est	<i>O. latipes</i>	3e-36
<i>P. promelas</i>	Actinopterygii	DT113652	partial	tBLASTn/NCBI est	<i>O. latipes</i>	2e-23
<i>S. maximus</i>	Actinopterygii	HQ603845	partial	tBLASTn/NCBI est	<i>O. latipes</i>	3e-23
<i>P. maniculatus</i>	Actinopterygii	GH530402	complete	tBLASTn/NCBI est	<i>O. latipes</i>	3e-09
<i>O. niloticus</i>	Actinopterygii	XP_003444205	complete	BLASTp /NCBI nr	<i>M. musculus</i>	1e-17
<i>D. rerio</i>	Actinopterygii	XP_694355	complete	tBLASTn/NCBI est	<i>M. musculus</i>	5e-14
<i>O. latipes</i>	Actinopterygii	XP_004074263	complete	BLASTp/NCBI nr	<i>D. rerio</i>	1e-32
<i>B. floridae</i>	Cephalochordata	XP_002592847	complete	tBLASTn/NCBI nr	<i>O. latipes</i>	0,16
<i>A. pectinifera</i>	Echinodermata	DB424359	complete	tBLASTn/NCBI est	<i>L. gigantea</i>	1e-12
<i>C. teleta</i>	Annelida	AMQN01011277	complete	tBLASTn/NCBI wsg	<i>L. gigantea</i>	2e-12
<i>M. californianus</i>	Mollusca	ES407417	partial	tBLASTn/NCBI est	<i>B. floridae</i>	1e-10
<i>L. gigantea</i>	Mollusca	jgi 156257 AMQO01001205	complete	Blastp/InParanoid tBLASTn/NCBI wsg	<i>M. musculus</i> <i>L. gigantea</i>	<0,01
<i>C. gigas</i>	Mollusca	AM858590	complete	tBLASTn/NCBI est	<i>L. gigantea</i>	3e-48

Supplementary Table 6

Origin of the SYCE3 homologues						
Species name	Taxonomic rank	Accession number	sequence	Method/database	seed	E-value
<i>M. musculus</i>	Tetrapoda	NP_001156352	complete	BLASTp /NCBI nr		0
<i>A. melanoleuca</i>	Tetrapoda	XP_002917318	complete	BLASTp /NCBI nr	<i>M. musculus</i>	6e-57
<i>C. porcellus</i>	Tetrapoda	XP_003461608	complete	BLASTp /NCBI nr	<i>M. musculus</i>	1e-54
<i>C. griseus</i>	Tetrapoda	XP_003515506	complete	BLASTp /NCBI nr	<i>M. musculus</i>	5e-59
<i>B. taurus</i>	Tetrapoda	XP_001193262	complete	BLASTp /NCBI nr	<i>M. musculus</i>	2e-54
<i>R. norvegicus</i>	Tetrapoda	NP_001128725	complete	BLASTp /NCBI nr	<i>M. musculus</i>	3e-59
<i>E. caballus</i>	Tetrapoda	XP_003364377	complete	BLASTp /NCBI nr	<i>M. musculus</i>	8e-58
<i>L. africana</i>	Tetrapoda	XP_003423236	complete	BLASTp/NCBI nr	<i>M. musculus</i>	3e-46
<i>S. scrofa</i>	Tetrapoda	NP_001193291	complete	BLASTp /NCBI nr	<i>M. musculus</i>	9e-56
<i>O. cuniculus</i>	Tetrapoda	XP_002723272	complete	BLASTp /NCBI nr	<i>M. musculus</i>	4e-56
<i>C. lupus</i>	Tetrapoda	XP_003431525	complete	BLASTp /NCBI nr	<i>M. musculus</i>	7e-57
<i>S. boliviensis</i>	Tetrapoda	XP_003932838	complete	BLASTp /NCBI nr	<i>M. musculus</i>	7e-53
<i>M. mulatta</i>	Tetrapoda	NP_001180282	complete	BLASTp /NCBI nr	<i>M. musculus</i>	1e-53
<i>O. garnettii</i>	Tetrapoda	XP_003783125	complete	BLASTp /NCBI nr	<i>M. musculus</i>	3e-56
<i>P. troglodytes</i>	Tetrapoda	XP_001156556	complete	BLASTp /NCBI nr	<i>M. musculus</i>	2e-52
<i>H. sapiens</i>	Tetrapoda	NP_001116697	complete	BLASTp /NCBI nr	<i>M. musculus</i>	2e-52
<i>O. anatinus</i>	Tetrapoda	XP_003430278	complete	BLASTp /NCBI nr	<i>M. musculus</i>	2e-43
<i>H. glaber</i>	Tetrapoda	EHB03472	complete	BLASTp /NCBI nr	<i>M. musculus</i>	9e-50
<i>N. leucogenys</i>	Tetrapoda	XP_003281537	partial	BLASTp /NCBI nr	<i>M. musculus</i>	2e-28
<i>M. domestica</i>	Tetrapoda	XP_003341970	partial	BLASTp /NCBI nr	<i>M. musculus</i>	2e-28
<i>S. harrisii</i>	Tetrapoda	XP_003770860	partial	BLASTp /NCBI nr	<i>M. musculus</i>	2e-28
<i>M. eugenii</i>	Tetrapoda	ENSMEUP00000004105	partial	tBLASTn/Ensembl genomic	<i>S. harrisii</i>	1.2e-38
<i>O. anatinus</i>	Tetrapoda	XP_003430278	complete	BLASTp /NCBI nr	<i>G. gallus</i>	9e-35
<i>G. gallus</i>	Tetrapoda	XP_001231764	complete	BLASTp /NCBI nr	<i>M. musculus</i>	5e-44
<i>T. guttata</i>	Tetrapoda	XP_002188999	complete	BLASTp /NCBI nr	<i>M. musculus</i>	1e-24
<i>M. gallopavo</i>	Tetrapoda	XP_003202713	complete	BLASTp /NCBI nr	<i>M. musculus</i>	4e-43
<i>A. carolinensis</i>	Tetrapoda	AAWZ02027734	complete	tBLASTn/NCBI wsg	<i>G. gallus</i>	2e-24
<i>P. sinensis</i>	Tetrapoda	AGCU01015398	complete	tBLASTn/NCBI wsg	<i>A. carolinensis</i>	6e-26
		AGCU01015399				4e-10

<i>C. mydas</i>	Tetrapoda	AJIM01252458	complete	tBLASTn/NCBI wsg	<i>G. gallus</i>	7e-33
<i>C. picta</i>	Tetrapoda	AHGY01153388	complete	tBLASTn/NCBI wsg	<i>G. gallus</i>	2e-31
<i>P. molurus</i>	Tetrapoda	AEQU010368279	partial	tBLASTn/NCBI wsg	<i>A. carolinensis</i>	1e-29
<i>A. mississippiensis</i>	Tetrapoda	AKHW01109662	complete	tBLASTn/NCBI wsg	<i>A. carolinensis</i>	5e-28
<i>X. tropicalis</i>	Tetrapoda	XP_002939573	complete	BLASTp /NCBI nr	<i>M. musculus</i>	4e-32
<i>L. chalumnea</i>	Coelacanth	BAHO01390606	complete	tBLASTn/NCBI wsg	<i>A. carolinensis</i>	3e-20
<i>D. rerio</i>	Actinopterygii	NP_001129458	complete	BLASTp /NCBI nr	<i>M. musculus</i>	3e-12
<i>O. niloticus</i>	Actinopterygii	XP_003445882	complete	BLASTp /NCBI nr	<i>M. musculus</i>	3e-13
<i>T. nigroviridis</i>	Actinopterygii	CAG10121	partial	BLASTp /NCBI nr	<i>M. musculus</i>	3e-15
<i>O. latipes</i>	Actinopterygii	FS547734	complete	tBLASTn/NCBI est	<i>O. niloticus</i>	4e-34
<i>P. flavescens</i>	Actinopterygii	GO658805	complete	tBLASTn/NCBI est	<i>O. niloticus</i>	2e-33
<i>H. hippoglossus</i>	Actinopterygii	FD698650	complete	tBLASTn/NCBI est	<i>O. niloticus</i>	1e-20
<i>R. rutilus</i>	Actinopterygii	EG545621	complete	tBLASTn/NCBI est	<i>O. niloticus</i>	3e-17
<i>I. punctatus</i>	Actinopterygii	CK419473	complete	tBLASTn/NCBI est	<i>O. niloticus</i>	3e-17

Supplementary Table 7

Origin of SYCP2 homologues			
Species name	Taxonomic rank	Accession Number	Cluster (Classification is based on the phylogenetic analysis)
<i>M. musculus</i>	Tetrapoda	NP_796165.2	SYCP2
<i>R. norvegicus</i>	Tetrapoda	NP_570091.1	SYCP2
<i>H. sapiens</i>	Tetrapoda	Q9BX26	SYCP2
<i>C. griseus</i>	Tetrapoda	XP_003496812.1	SYCP2
<i>M. ochrogaster</i>	Tetrapoda	XP_005362821.1	SYCP2
<i>C. simum</i>	Tetrapoda	XP_004430278.1	SYCP2
<i>I. tridecemlineatus</i>	Tetrapoda	XP_005325353.1	SYCP2
<i>P. abelii</i>	Tetrapoda	XP_002830535.1	SYCP2
<i>G. gorilla</i>	Tetrapoda	XP_004062509.1	SYCP2
<i>P. troglodytes</i>	Tetrapoda	XP_514753.4	SYCP2
<i>P. paniscus</i>	Tetrapoda	XP_003810862.1	SYCP2
<i>A. melanoleuca</i>	Tetrapoda	XP_002915577.1	SYCP2
<i>N. leucogenys</i>	Tetrapoda	XP_003277571.2	SYCP2
<i>E. caballus</i>	Tetrapoda	XP_001915188.2	SYCP2
<i>P. anubis</i>	Tetrapoda	XP_003904590.1	SYCP2
<i>H. glaber</i>	Tetrapoda	XP_004891734.1	SYCP2
<i>C. lanigera</i>	Tetrapoda	XP_005410101.1	SYCP2
<i>M. putoriusfuro</i>	Tetrapoda	XP_004760159.1, XP_004786041.1	SYCP2
<i>M. fascicularis</i>	Tetrapoda	EHH65200.1	SYCP2
<i>C. hircus</i>	Tetrapoda	XP_005688477.1	SYCP2
<i>O. aries</i>	Tetrapoda	XP_004014808.1	SYCP2
<i>C. lupus</i>	Tetrapoda	XP_005635419.1	SYCP2
<i>C. jacchus</i>	Tetrapoda	XP_002747778.1	SYCP2
<i>D. novemcinctus</i>	Tetrapoda	XP_004460192.1	SYCP2
<i>S. boliviensis</i>	Tetrapoda	XP_003932694.1	SYCP2
<i>O. garnettii</i>	Tetrapoda	XP_003787798.1	SYCP2
<i>O. degus</i>	Tetrapoda	XP_004644264.1	SYCP2
<i>T. manatus latirostris</i>	Tetrapoda	XP_004370583.1	SYCP2

<i>O. orca</i>	Tetrapoda	XP_004282440.1	SYCP2
<i>B. taurus</i>	Tetrapoda	DAA23391.1	SYCP2
<i>F. catus</i>	Tetrapoda	XP_003983389.1	SYCP2
<i>M. mulatta</i>	Tetrapoda	XP_002798120.1	SYCP2
<i>C. porcellus</i>	Tetrapoda	XP_005000459.1	SYCP2
<i>O. cuniculus</i>	Tetrapoda	XP_002721859.1	SYCP2
<i>J. jaculus</i>	Tetrapoda	XP_004669500.1	SYCP2
<i>L. africana</i>	Tetrapoda	XP_003422251.1	SYCP2
<i>M. auratus</i>	Tetrapoda	XP_005074640.1	SYCP2
<i>E. telfairi</i>	Tetrapoda	XP_004716146.1	SYCP2
<i>O. princeps</i>	Tetrapoda	XP_004586169.1	SYCP2
<i>S. araneus</i>	Tetrapoda	XP_004620278.1	SYCP2
<i>S. harrisii</i>	Tetrapoda	ENSSHAT00000006344	SYCP2
<i>T. truncatus</i>	Tetrapoda	XP_004325470.1	SYCP2
<i>M. domestica</i>	Tetrapoda	XP_003339740.1	SYCP2
<i>C. cristata</i>	Tetrapoda	XP_004687145.1	SYCP2
<i>F. albicollis</i>	Tetrapoda	XP_005057470.1	SYCP2
<i>M. undulatus</i>	Tetrapoda	XP_005147648.1	SYCP2
<i>G. gallus</i>	Tetrapoda	XP_417396.4	SYCP2
<i>F. cherrug</i>	Tetrapoda	XP_005445089.1	SYCP2
<i>C. picta</i>	Tetrapoda	XP_005302999.1	SYCP2
<i>F. peregrinus</i>	Tetrapoda	XP_005243895.1	SYCP2
<i>G. fortis</i>	Tetrapoda	XP_005423715.1	SYCP2
<i>P. humilis</i>	Tetrapoda	XP_005525012.1	SYCP2
<i>Z. albicollis</i>	Tetrapoda	XP_005489193.1	SYCP2
<i>C. livia</i>	Tetrapoda	XP_005499775.1	SYCP2
<i>S. scrofa</i>	Tetrapoda	XP_005673125.1	SYCP2
<i>X. tropicalis</i>	Tetrapoda	NP_001072339.1	SYCP2
<i>P. alecto</i>	Tetrapoda	ELK04360.1	SYCP2
<i>C. mydas</i>	Tetrapoda	EMP35819.1	SYCP2
<i>A. platyrhynchos</i>	Tetrapoda	ENSAPLT00000014689	SYCP2
<i>M. davidii</i>	Tetrapoda	ELK27576.1	SYCP2
<i>O. anatinus</i>	Tetrapoda	ENSOANT00000014773	SYCP2

<i>A. sinensis</i>	Tetrapoda	XP_006024152.1	SYCP2
<i>A. mississippiensis</i>	Tetrapoda	XP_006271806.1	SYCP2
<i>P. sinensis</i>	Tetrapoda	XP_006126260.1	SYCP2
<i>L. chalumnae</i>	Coelacanth	XP_005993653.1	SYCP2
<i>C. milii</i>	Chondrichthyes	AFO94093	SYCP2
<i>L. oculatus</i>	Actinopterygii	ENSLOCT00000003938	SYCP2
<i>H. burtoni</i>	Actinopterygii	XP_005948370.1	SYCP2
<i>M. zebra</i>	Actinopterygii	XP_004554211.1	SYCP2
<i>O. niloticus</i>	Actinopterygii	XP_005478298.1	SYCP2
<i>D. rerio</i>	Actinopterygii	XP_685048.5	SYCP2
<i>P. nyererei</i>	Actinopterygii	XP_005733119.1	SYCP2
<i>O. latipes</i>	Actinopterygii	XP_004070700.1	SYCP2
<i>M. musculus</i>	Tetrapoda	XP_003085913.1	NO145
<i>R. norvegicus</i>	Tetrapoda	XP_002725278.1	NO145
<i>H. sapiens</i>	Tetrapoda	Q5T4T6	NO145
<i>N. leucogenys</i>	Tetrapoda	XP_003263555.1	NO145
<i>P. troglodytes</i>	Tetrapoda	XP_518236.2	NO145
<i>P. paniscus</i>	Tetrapoda	XP_003827594.1	NO145
<i>P. abelii</i>	Tetrapoda	XP_002816467.2	NO145
<i>G. gallus</i>	Tetrapoda	XP_004939717	NO145
<i>G. gorilla</i>	Tetrapoda	XP_004043318.1	NO145
<i>G. fortis</i>	Tetrapoda	XP_005424991.1	NO145
<i>Z. albicollis</i>	Tetrapoda	XP_005481878.1	NO145
<i>C. simum</i>	Tetrapoda	XP_004432246.1	NO145
<i>C. lupus</i>	Tetrapoda	XP_852239.3	NO145
<i>C. hircus</i>	Tetrapoda	XP_005696946.1	NO145
<i>F. catus</i>	Tetrapoda	XP_003985864.1	NO145
<i>O. rosmarus divergens</i>	Tetrapoda	XP_004403776.1	NO145
<i>M. fascicularis</i>	Tetrapoda	XP_005554098.1	NO145
<i>O. aries</i>	Tetrapoda	XP_004019403.1	NO145
<i>E. caballus</i>	Tetrapoda	XP_005604082.1	NO145
<i>M. ochrogaster</i>	Tetrapoda	XP_005355200.1	NO145
<i>M. domestica</i>	Tetrapoda	XP_003340705.1	NO145

<i>O. garnettii</i>	Tetrapoda	XP_003788414.1	NO145
<i>M. putoriusfuro</i>	Tetrapoda	XP_004753812.1	NO145
<i>M. mulatta</i>	Tetrapoda	XP_001091092.2	NO145
<i>I. tridecemlineatus</i>	Tetrapoda	XP_005327573.1	NO145
<i>O. anatinus</i>	Tetrapoda	XP_001514684.2	NO145
<i>P. anubis</i>	Tetrapoda	XP_003897104.1	NO145
<i>J. jaculus</i>	Tetrapoda	XP_004668026.1	NO145
<i>H. glaber</i>	Tetrapoda	XP_004896871.1	NO145
<i>C. lanigera</i>	Tetrapoda	XP_005399037.1	NO145
<i>B. taurus</i>	Tetrapoda	DAA16073.1	NO145
<i>O. orca</i>	Tetrapoda	XP_004281128.1	NO145
<i>C. jacchus</i>	Tetrapoda	XP_003732639.1	NO145
<i>C. porcellus</i>	Tetrapoda	XP_003468883.1	NO145
<i>D. novemcinctus</i>	Tetrapoda	XP_004477008.1	NO145
<i>T. manatus latirostris</i>	Tetrapoda	XP_004390527.1	NO145
<i>O. cuniculus</i>	Tetrapoda	XP_002714289.1	NO145
<i>T. truncatus</i>	Tetrapoda	XP_004324370.1	NO145
<i>S. boliviensis</i>	Tetrapoda	XP_003927475.1	NO145
<i>O. degus</i>	Tetrapoda	XP_004628497.1	NO145
<i>E. telfairi</i>	Tetrapoda	XP_004712275.1	NO145
<i>A. platyrhynchos</i>	Tetrapoda	ENSAPLT00000002807	NO145
<i>X. laevis</i>	Tetrapoda	AAI61717.1	NO145
<i>F. albicollis</i>	Tetrapoda	XP_005041684.1	NO145
<i>S. harrisii</i>	Tetrapoda	ENSSHAT00000011927	NO145
<i>X. tropicalis</i>	Tetrapoda	XP_004915355.1	NO145
<i>C. ferus</i>	Tetrapoda	EPY83840.1	NO145
<i>M. auratus</i>	Tetrapoda	XP_005066317.1	NO145
<i>C. mydas</i>	Tetrapoda	EMP31654.1	NO145
<i>C. livia</i>	Tetrapoda	XP_005512634.1	NO145
<i>M. davidii</i>	Tetrapoda	ELK25675.1	NO145
<i>T. chinensis</i>	Tetrapoda	XP_006141256.1	NO145
<i>A. sinensis</i>	Tetrapoda	XP_006025489.1	NO145
<i>A. mississippiensis</i>	Tetrapoda	XP_006277528.1	NO145



<i>P. sinensis</i>	Tetrapoda	XP_006138891.1	NO145
<i>O. hannah</i>	Tetrapoda	ETE65392.1	NO145
<i>L. chalumnae</i>	Coelacanth	XP_006006451.1	NO145
<i>C. milii</i>	Chondrichthyes	AFO97946	NO145
<i>L. oculatus</i>	Actinopterygii	ENSLOCT00000016215	NO145
<i>H. burtoni</i>	Actinopterygii	XP_005952425.1	NO145
<i>T. nigroviridis</i>	Actinopterygii	CAF92301.1	NO145
<i>P. nyererei</i>	Actinopterygii	XP_005754689.1	NO145
<i>D. rerio</i>	Actinopterygii	XP_005162635.1	NO145
<i>O. niloticus</i>	Actinopterygii	XP_005465050.1	NO145
<i>M. zebra</i>	Actinopterygii	XP_004570790.1	NO145
<i>O. latipes</i>	Actinopterygii	XP_004086924.1	NO145
<i>B. floridae</i>	Cephalochordata	EEN47795.1	
<i>C. intestinalis</i>	Tunicata	XP_004227200.1	
<i>C. savignyi</i>	Tunicata	ENSCSAVT00000014355	
<i>S. purpuratus</i>	Echinodermata	XP_003730029.1	
<i>A. pompejana</i>	Annelida	GO231057	
<i>L. gigantea</i>	Mollusca	FC677437	
<i>A. californica</i>	Mollusca	XP_005096076.1	
<i>C. gigas</i>	Mollusca	EKC24557.1	
<i>H. microstoma</i>	Platyhelminthes	CDJ07634.1	
<i>E. granulosus</i>	Platyhelminthes	EUB56346	
<i>C. finmarchicus</i>	Crustacea	FK041407.1	
<i>N. vectensis</i>	Cnidaria	FC224810	
<i>H. magnipapillata</i>	Cnidaria	XP_004210390.1	
<i>T. adhaerens</i>	Placozoa	XP_002113953.1 EDV23043.1	

## Erklärung

Hiermit versichere ich an Eides statt,

dass ich die Dissertation eigenständig angefertigt habe und keine anderen als die von mir angegebenen Quellen oder Hilfsmittel benutzt habe,

dass ich die Gelegenheit zur Promotion nicht kommerziell vermittelt bekommen habe und ich keine Person oder Organisation eingeschaltet habe, die gegen Entgelt einen Betreuer bzw. eine Betreuerin für die Anfertigung der Dissertation sucht,

dass ich die Regeln der Universität Würzburg über gute wissenschaftliche Praxis eingehalten habe,

dass die Dissertation weder in gleicher noch ähnlicher Form in einem anderen Prüfungsverfahren vorgelegen hat,

und

dass ich früher keine weiteren akademischen Grade erworben oder zu erwerben versucht habe

---

Ort, Datum

---

Unterschrift

## **Lebenslauf**

## List of scientific publications

### Peer-reviewed articles

**Fraune, J.**, M. Wiesner and R. Benavente, 2014 The synaptonemal complex of the basal metazoan *Hydra*: more similarities to vertebrate than invertebrate meiosis model organism. *J Genet Genomics, in revision*.

**Fraune, J.**, C. Brochier-Armanet, M. Alsheimer and R. Benavente, 2013 Phylogenies of central element proteins reveal the dynamic evolutionary history of the mammalian synaptonemal complex: ancient and recent components. *Genetics* 195: 781-793.

**Fraune, J.**, M. Alsheimer, J. N. Volff, K. Busch, S. Fraune, T. C. G. Bosch, R. Benavente, 2012b *Hydra* meiosis reveals unexpected conservation of structural synaptonemal complex proteins across metazoans. *Proc Natl Acad Sci U S A* 109: 16588-16593.

**Fraune, J.**, S. Schramm, M. Alsheimer and R. Benavente, 2012a The mammalian synaptonemal complex: protein components, assembly and role in meiotic recombination. *Exp Cell Res* 318: 1340-1346.

Schramm, S., **J. Fraune**, R. Naumann, A. Hernandez-Hernandez, C. Hoog, H. J. Cooke, M. Alsheimer, R. Benavente, 2011 A novel mouse synaptonemal complex protein is essential for loading of central element proteins, recombination, and fertility. *PLoS Genet* 7: e1002088.

### Published abstracts

**Fraune, J.**, C. Brochier-Armanet, M. Alsheimer, R. Benavente, Sept. 2013 The evolution of mammalian synaptonemal complex proteins across metazoan. *The EMBO Conference on Meiosis*, Dresden.

**Fraune, J.**, A. Rehm, M. Harmi, A. Klimovich, T.C.G. Bosch, R. Benavente Sept. 2013 The single nuclear lamin of *Hydra*: A role in polyp proliferation and senescence? *International workshop "Unravelling the developmental regulatory networks in early animals"*, Tutzing.

**Fraune, J.**, K. Winkel, M. Alsheimer, R. Benavente, Sept. 2011 *Hydra* meiosis reveals unexpected conservation of structural synaptonemal complex proteins. *The EMBO Conference on Meiosis*, Naples.

**Fraune, J.**, K. Winkel, M. Alsheimer, R. Benavente, Sept. 2011 *Hydra* meiosis reveals unexpected conservation of structural synaptonemal complex proteins. *International workshop "Searching for Eve: Basal metazoans and the evolution of multicellular complexity"*, Tutzing.

